Nonlinear Dynamics of Nd:YAG lasers: Hopf bifurcation, Multistability and Chaotic Synchronization

Parvathi.M.R

International School of Photonics
Cochin University of Science and Technology
Cochin 682 022, India

Thesis submitted to Cochin University of Science and Technology in partial fulfillment of the requirements for the award of the Degree of Doctor of Philosophy

May 2009

Nonlinear Dynamics of Nd:YAG lasers: Hopf bifurcation, Multistability and Chaotic Synchronization

Author:

Parvathi.M.R
Research Fellow
International School of Photonics
Cochin University of Science and Technology
Cochin 682 022, India
E-mail: parvathiabhin@gmail.com

Research Advisor:

Dr: V.M.Nandakumaran
Professor
International School of Photonics
Cochin University of Science and Technology
Cochin 682 022, India
E-mail: nandak@cusat.ac.in

International School of Photonics
Cochin University of Science and Technology
Cochin 682 022, India
www.photonics.cusat.edu

May 2009

To My Parents

CERTIFICATE

This is to certify that the research work presented in the thesis entitled ***Nonlinear Dynamics of Nd:YAG lasers: Hopf bifurcation, Multistability and Chaotic Synchronization*** is based on the original work done by Ms.Parvathi.M.R under my guidance at the International School of Photonics, Cochin University of Science and Technology, Cochin- 682 022 and that no part thereof has been included in any other thesis submitted previously for the award of any Degree.

Kochi
May 30, 2009

Dr.V.M.Nandakumaran
(Supervising Guide)
International School of Photonics
CUSAT

DECLARATION

Certified that the work presented in the thesis entitled ***Nonlinear Dynamics of Nd:YAG lasers: Hopf bifurcation, Multistability and Chaotic Synchronization*** is based on the original work carried out by me under the guidance of Dr.V.M.Nandakumaran, Professor, International School of Photonics, Cochin University of Science and Technology, Cochin -682 022 and that no part of thereof has been included in any other thesis submitted previously for the award of any Degree.

Kochi Parvathi.M.R

May 30, 2009

ACKNOWLEDGEMENTS

I express my deep sense of thankfulness to Prof.V.M.Nandakumaran for his consistent guidance and intellectual support which helped me to complete my research work successfully and submit the thesis in time. I am grateful to Prof.V.P.N.Nampoori, Prof.P.Radhakrishnan, Prof.C.P.Girijavallabhan, Prof.Unnikrishnan Nayar and Mr.M.Kailasnath for their support and encouragement throughout my research career.

Thanks to Dr.Bindu M.Krishna who always boosted my energy levels with her positive thoughts and pleasant behavior whenever I was depressed. I can not forget how she found time to spend with me- however busy she was- to go through my results, correct them and give suggestions for future works.

Thanks to Mr.Manu P.John and Dr.Rajesh S and Mr.Jijo.P.U for their valuable advices and fruitful discussions which always created turning points in my research. I also thank Ms.Chitra R.Nayak for her timely advices.

A word of gratitude to Mr.Prabhathan and Mr.Tamilarasan who sent some important journal papers whenever I was needed.
I thank my friends at ISP for their affection and timely help which made my ISP days unforgettable.

I also thank other staff and students of ISP and CELOS.

With immense pleasure I express my gratitude to Dr.E.D.Jemmis, Director, Indian Institute of Science Education and Research, Thiruvananthapuram for giving me opportunity to work there and utilize the facilities available there.

I am also thankful to the very supportive teachers especially Dr.Ayan Dutta, students and other staff at IISER.

I thank CELOS and UGC for the financial assistance.

Thanks to my parents without whom I would have never been where I am now.

Thanks to Abhin who joined me half way of my research, for his love, support and encouragement which helped a lot for the successful completion of my research.

Parvathi.M.R

PREFACE

The word “chaos” has become very popular nowadays. In electrical circuits, chemical reactions, laser systems every where we can find chaos. There is chaos within our body itself. The biological signals within our body can become chaotic at times. Unpredictability which is the main characteristic feature of chaos is everywhere. In nature the climate changes can become unpredictable. Sometimes spreading of a disease and population growth may go beyond our calculations. Since last century scientists are trying to unravel the mysteries behind chaos. They defined a chaotic system as one whose dynamics is complex and at the same time governed by deterministic evolution equations. The most important characteristic property of a chaotic system is found to be its sensitive dependence on initial conditions. Several roots to chaos are found and various quantitative and qualitative measures of chaos are introduced.

It seems quite amazing that we can make two chaotic systems behave in the same manner or make them synchronize with each other. Synchronization of chaotic lasers has gained great importance as a means to generate high power laser sources. Efficient communication systems are devised based on the synchronization property of chaotic semiconductor lasers. Recently it has been shown that multimode lasers have many advantages over single mode lasers. Therefore novel high quality communication systems have been developed using multimode Nd:YAG lasers.

Another related area which needs special attention is control of chaos. Introduction of a delay feedback is found to be an efficient method for controlling chaos in various laser systems. Semi conductor lasers and Nd:YAG lasers are found to exhibit interesting phenomena like hysteresis

and multistability. Multistability is also found to occur in various biological systems. Availability of good and fast computational tools and easily accessible control parameters make the laser systems good candidates as model systems for studying these phenomena.

Nonlinear dynamics of multimode Nd:YAG lasers is the central theme of this thesis. We discuss the synchronization of chaotic Nd:YAG lasers under various coupling schemes, Hopf bifurcation phenomena exhibited by the laser under the variation of a particular control parameter and also the delay induced multistability in the laser system. The thesis is divided into seven chapters.

Chapter 1 gives an introduction to chaos. Chaos in various dynamical systems is discussed briefly giving special concern to lasers. The characteristic features of a chaotic system are identified. Different tools for measuring chaos, routes to chaos undertaken by dynamical systems are also described. Hopf bifurcation phenomena and period doubling route to chaos are discussed in detail taking Rossler system and van der Pol oscillator as examples. There is also discussion about the origin of chaos in laser systems especially in semiconductor and Nd:YAG lasers.

The concept of synchronization is introduced in **Chapter 2**. There is discussion about various coupling schemes used for achieving synchronization. Different types of synchronization in dynamical systems such as generalized synchronization, phase synchronization, lag synchronization and complete synchronization are explained. We take Rossler oscillator as a model system to study phase and lag synchronization. Synchronization phenomena exhibited by various dynamical systems

especially lasers are discussed. The importance of controlling chaos and various chaos controlling schemes are also described briefly in this chapter.

In **Chapter 3**, there is description of our model system used for numerical studies which is an Nd:YAG laser with intracavity KTP crystal. Origin of chaotic intensity fluctuations in this laser is discussed. There is detailed description of laser dynamics based on a rate equation model. Lasers with two mode and three mode output are studied separately. Time series plots, phase space plots and bifurcation diagrams are used to get a clear picture about the laser dynamics. The reverse period doubling route from chaos to stability exhibited by the laser as the orientation of the YAG rod and KTP crystal is varied is also studied.

In **Chapter 4** we present the results of our numerical studies on synchronization and control of chaos in coupled chaotic multimode Nd:YAG lasers. Effect of unidirectional and bidirectional couplings on the dynamics of Nd:YAG lasers having two mode and three mode output are studied. Lasers are coupled via external electronic coupling in which pumping of each laser is modulated according to the output intensity of the other. Unidirectional and bidirectional coupling schemes are adopted. It is found that bidirectional direct coupling scheme is effective in achieving control of chaos, synchronization and amplification in output intensity for lasers with two mode output. With bidirectional difference coupling the lasers remain chaotic for the entire range of coupling strength without any amplification or synchronization in output intensity. Lasers are found to exhibit phase synchronization under unidirectional direct coupling at higher coupling strengths. Unidirectional difference coupling can only produce amplification in output intensity for the second laser without any synchronization between

them. In the case of lasers having three mode output, bidirectional difference coupling can give synchronization of higher quality as compared to unidirectional difference coupling, only at the cost of higher coupling strength.

In **Chapter 5** we are presenting an analytical and numerical treatment of the dynamics of Nd:YAG laser operating with two modes having parallel polarization. System fixed points are found out analytically. It is found that the system has got nine fixed points out of which only three are having real values. In order to check the stability of these three fixed points, we use Routh-Hurwitz criteria and also the method of eigen values. It is found that one fixed point loses stability at a particular value of the control parameter and evolves as a limit cycle through Hopf bifurcation. The other two fixed points remain unstable throughout the entire region of the control parameter. Change in sign of the Routh Hurwitz coefficients and the real part of eigen values confirm our result. Hopf bifurcation phenomena exhibited by Nd:YAG laser is studied numerically also. Effect of change in control parameter on the energy transfer between the two modes is also investigated.

Chapter 6 deals with the dynamics of Nd:YAG laser under a delay feedback. An optoelectronic delay feedback is given to an Nd:YAG laser operating in the limit cycle region and its dynamics is studied. Both positive and negative feedback cases are studied separately. Laser with positive feedback is found to exhibit rich dynamics as compared to that with negative feedback. We mainly use bifurcation diagrams to study the laser dynamics. Lasers with positive feedback exhibit quasiperiodicity, period doubling and chaos with increase of delay time. We use power spectra and intensity peak series plots to characterize various regions in the output. Existence of chaotic

region is confirmed with a positive Lyapunov exponent and a fractional correlation dimension. Laser is found to exhibit multistability and hysteresis for certain delay times. One interesting result in the delay feedback studies is the coexistence of chaotic and quasiperiodic regions in the laser output at a particular value of the delay under positive feedback. Chaotic windows are found to occur in a regular fashion as the delay is increased. As the feedback fraction is increased the laser output intensity also increases.

With negative feedback, a sudden jump into chaotic region is observed at smaller delays. Chaotic and periodic regions occur alternately as the delay is increased. The frequency with which the chaotic region appears increases as the delay is increased while the peak intensity value of the chaotic regions decreases. At higher feedback fractions also the laser output intensity undergoes a sudden jump into the chaotic region. The output remains chaotic for higher delays.

Summary and conclusions of our work are given in **Chapter 7**. Some possible works in this field are also discussed.

CONTENTS

CHAPTER 1

CHAOS AND LASERS

In this chapter we describe chaos in various dynamical systems, with special reference to lasers. We give the conditions necessary for the occurrence of chaos, different tools for characterizing chaos and various routes to chaos exhibited by dynamical systems. Hopf bifurcation and period doubling route to chaos are also discussed taking Rossler system and van der Pol oscillator as examples.

1.1 WHAT IS CHAOS?

"Chaos is the science of complexity of change"

Chaos is there in the unpredictable weather, in the share price fluctuations in stock market and even in the variation of commodity prices. We can see chaos in ecology, economics, epidemiology, in the beating of the heart and in the electrical signals from the brain. Discovery of chaos changed the world's understanding of the foundations of Physics and led to new findings on the frontiers of lasers, fluid mechanics, chemical reactions, neural networks and biological rhythms. Chaos based studies of EEG and ECG signals lead to new developments in brain research and cardiology. It provided a novel way of thinking meaningfully about many phenomena such as turbulence which otherwise were considered as a matter of utter confusion [1].

The word chaos means a state of disorder. Henri Poincare, a prominent mathematician and theoretical astronomer was the first person to glimpse the possibility of chaos. He developed a powerful geometric approach to various scientific problems. That approach flowered into the modern subject of dynamics with its applications spreading over vast scientific areas [2]. Interest in nonlinear dynamics especially chaos gained pace after 1963, when Lorenz published his pioneering numerical work on a simple convection model and discussed its implications for weather prediction [3].

A physical system whose state changes with time is termed as a dynamical system. The changes occur due to influence of forces that act on the system.

The evolution of physical systems depends on the nature of the forces acting on them and also on their initial condition. If the forces acting on a system are nonlinear we call the system as a nonlinear dynamical system. For certain values of the parameters that control the system, the evolution of many of the nonlinear dynamical systems become unpredictable [4]. A system whose temporal or spatial evolution seems random, but is completely deterministic, i.e obeys some definite evolutionary equation, is called a chaotic system. Its central characteristic is that the system does not repeat its past behavior. For chaotic systems even a small difference in the initial conditions leads to an exponentially growing error and the system dynamics becomes unpredictable after a very short time. This is known as sensitivity to initial conditions. As Poincare said "*…it may happen that small differences in the initial conditions produce very great ones in the final phenomena. A small error in the former will produce an enormous error in the latter. Prediction becomes impossible, and we have the fortuitous phenomenon*" [2]. If the prediction becomes impossible a chaotic system can resemble a stochastic system. But for a chaotic system the irregularity arises from its intrinsic dynamics, not from any unpredictable external influences.

We can define chaos as "aperiodic long-term behavior in a deterministic system that exhibits sensitive dependence on initial conditions." [5]. The most interesting thing about chaos is that in spite of its highly complex nature it happens in systems which are not complex and are even very simple.

1.2 CONDITIONS NECESSARY FOR CHAOS

Dynamical systems can be broadly classified into continuous time dynamical system and discrete time dynamical system. A continuous time dynamical system can be represented by a set of equations of the form

$$\frac{d\vec{X}}{dt} = \vec{F}\left(\vec{X}, \mu\right) \qquad (1.1)$$

where

$\vec{X} = (x_1, x_2, ...x_n)$ and $\vec{F} = (F_1, F_2, ...F_n)$

$(x_1, x_2, ...x_n)$ are the dynamical variables and $(F_1, F_2, ...F_n)$ are the source functions. μ is a set of control parameters that can be varied.

We can write the necessary conditions for the occurrence of chaos in such a system as

1) It must be nonlinear
2) The order or dimension of the system must be greater than or equal to 3.

Discrete time dynamical system can be represented by maps of the form

$$\vec{X}_{n+1} = F_\mu\left(\vec{X}_n\right) \qquad (1.2)$$

where n refers to discrete values of time.

Linear maps do not show chaotic behavior. Nonlinear maps are of two types namely invertible and noninvertible. Invertible maps can exhibit chaos only if the dimension is greater than one. Noninvertible maps can exhibit chaos even if the dimension is one.

1.3 TOOLS FOR THE STUDY OF CHAOS

Three powerful mathematical tools used in the study of dynamical systems are phase space, Poincare section and power spectra. They give a qualitative and global understanding of chaos.

1.3.1 Phase space

The phase space of a dynamical system is a mathematical space having orthogonal coordinate directions which represent each of the variables needed to specify the instantaneous state of the system. The state of a particle moving in one dimension is specified by its position (x) and velocity ($\dot{x}$).Thus its phase space is a plane. For a particle moving in three dimensions the phase space will be six dimensional. The phase space variables need not be mechanical coordinates like position and velocity. They may be concentration of reactants in a chemical reaction or output intensity or gain as in the case of laser etc. The state of a dynamical system is represented by a point in the phase space. As the system evolves in time, it constitutes a trajectory in the phase space [2, 4, 5].

1.3.2 Poincare section

Poincare section provides a means for simplifying the complicated structure of attractors. Generally for an n- dimensional flow, the Poincare section will be an (n-1) dimensional hypersurface transverse to the flow. In order to construct the Poincare section for a three dimensional attractor, choose a

plane transverse to the direction of motion of the trajectories. Put a point on this plane every time the trajectory crosses it. This plane then constitutes the Poincare section for the attractor. It should be noted that while constructing the Poincare section, motion of the trajectories only in one direction has to be considered. The time interval between successive intersections need not be equal. The nonlinear three dimensional differential equations are replaced by nonlinear algebraic two dimensional difference equations that are simple and easier to handle. At the same time it retains the essential qualitative features of the phase flow. This reduction in dimension provides greater simplification. The observation of the distribution of points on a computer-generated Poincare section [2, 4, 5] will be useful for the study of chaos.

1.3.3 Power spectrum

The spectral analysis of a signal is an important tool in the study of the temporal behavior of a system. Power spectrum gives the relative strengths of various frequency components of a time series. It is calculated by taking the Fourier transform of the auto-correlation function of the time series. Auto-correlation function measures the correlation between observations at different distances (times) apart. These functions exhibit the loss of information along the trajectory. The power spectrum is a function in the frequency domain. The power spectrum for a chaotic motion will be of continuous and broad band nature [2, 4].

1.4 QUANTITATIVE MEASURES OF CHAOS

The motion of typical nonlinear systems undergoes characteristic changes as certain control parameters are varied continuously. These changes are

identified by the changes of the system attractors or phase space structures and stability properties. In addition to these we use some quantitative criteria to differentiate between chaotic and regular motions. The most important criteria used for this purpose are

1) Lyapunov exponents

2) Correlation function

3) Attractor dimensions

1.4.1 Lyapunov exponents

Named after A.M.Lyapunov, a Russian mathematician, Lyapunov exponents describe the rate of divergence or convergence of nearby trajectories onto the attractor in different directions in phase space. It gives a measure of the sensitive dependence upon initial conditions which is a characteristic of chaotic system. Consider a system evolving from two slightly different initial conditions x and x+ε. After n iterations the divergence of the two trajectories may be represented as [2, 4, 5]

$$\varepsilon(n) \approx \varepsilon e^{\lambda n} \qquad (1.3)$$

where λ, the Lyapunov exponent gives the average rate of divergence. If λ is negative, the two nearby trajectories converge and the evolution is not chaotic. If λ is positive, nearby trajectories diverge as the evolution is sensitive to initial conditions and hence chaotic. We can similarly define Lyapunov exponents for continuous systems.

Consider an n-dimensional system represented by the equation

$$\dot{X} = F(X) \qquad (1.4)$$

where $\dot{x}_1 = F_1(x_1, x_2, ..., x_n)$

$\dot{x}_2 = F_2(x_1, x_2, ..., x_n)$

.....

.....

$\dot{x}_n = F_n(x_1, x_2, ..., x_n)$

$X(t) = (x_1(t), x_2(t), ..., x_n(t))$ represent the trajectory of the system (1.4). Consider two nearby trajectories in the n-dimensional phase space starting from slightly different initial conditions X_0 and $X_o' = X_0 + \delta X_0$ respectively. Their time evolution will give the vectors $X(t)$ and $X(t) + \delta X(t)$. In order to find the time evolution of δX, we linearize equation (1.4) so as to get

$$\delta \dot{X} = M\left(\dot{X}(t)\right) \bullet \delta(X)$$

where M= $\partial F / \partial X_{X=X_0}$ is the Jacobian matrix of F.

The Lyapunov exponent of the system can be defined as

$$\lambda(X_0, \delta X) = \lim_{t\to\infty} \frac{1}{t} \log\left(\frac{d(X_0, t)}{d(X_0, 0)}\right) \qquad (1.5)$$

where $d(X_0, t)$ is a measure of the distance between the trajectories $X(t)$ and $X'(t)$.

1.4.2 Correlation function

For a map $x_{n+1} = f(x_n)$ the correlation function C(m) is defined as [6]

$$C(m) = \lim_{N\to\infty}\left(1/N\right)\sum_{n=0}^{N} x_n x_{n+m} - \left(\bar{x}\right)^2 \qquad (1.6)$$

where $\bar{x}$ is the mean value of the x_n given by

$$\bar{x} = \lim_{N\to\infty}\left(1/N\right)\sum_{n=0}^{N} x_n \qquad (1.7)$$

Correlation function gives a measure of the extent to which iterates m steps apart are correlated in their evolution. Decaying correlation is a characteristic of the chaotic motion. Or we can say that correlation function measures the degree of randomness of a chaotic system.

1.4.3 Attractor dimensions

An attractor is a certain subspace of the full phase space into which all the trajectories settle down eventually. For regular nonchaotic systems attractor could be a point (of zero dimension) or a curve- a limit cycle- (of dimension one) or a torus (of dimension two). But when it comes to a chaotic system the task of finding dimension becomes tedious. A number of dimensions can be used to describe the characteristic features of a chaotic attractor. Most important of them are discussed below.

i) Fractal dimension or Capacity dimension or Hausdorff dimension (D_F) [4,5]

Consider a straight line of length L. Suppose this line can be covered by N(ε) one-dimensional boxes of side ε, then we can write

$$N(\varepsilon) = L\left(1/\varepsilon\right)$$

Similarly for a two-dimensional square of side L, the number of boxes required are

$$N(\varepsilon) = L^2\left(1/\varepsilon\right)^2$$

For a three-dimensional cube the exponent is 3.

Generally for a d-dimensional figure we can write

$$N(\varepsilon) = L^d\left(1/\varepsilon\right)^d \qquad (1.8)$$

Taking logarithms on both sides

$$d = \frac{\log N(\varepsilon)}{\log L + \log\left(1/\varepsilon\right)} \qquad (1.9)$$

In the limit of small ε, we can write

$$D_F = \lim_{\varepsilon \to 0} \frac{\log N(\varepsilon)}{\log\left(1/\varepsilon\right)} \qquad (1.10)$$

which is the capacity dimension or fractal dimension. There are attractors, called strange attractors for which the dimension will be noninteger. However when the phase space dimension becomes greater than two, the task of computing D_F becomes very difficult.

ii) Correlation dimension (D_C) [4,5]

The Correlation dimension is defined by

$$D_C = \lim_{r \to 0} \frac{\log C(r)}{\log r} \qquad (1.11)$$

where $C(r)$ is the correlation function discussed earlier.

Correlation dimension can be calculated using a well known algorithm developed by Grassberger and Procaccia. As correlation dimension takes into account the density of data points on the attractor, its estimation requires a large number of data points. For a point attractor D_C=0 and for a limit cycle attractor D_C=1. A chaotic attractor is characterized by a noninteger D_C value.

Based on the above discussions we can summarize the important characteristic features of a chaotic system as

1) At least one positive Lyapunov exponent.
2) Continuous broad band power spectrum.
3) Decaying autocorrelation function.
4) A noninteger fractal and correlation dimension.

1.5 ROUTES TO CHAOS

For every dynamical system there will be a set of control parameters whose variation can produce sudden changes in the system dynamics. These sudden qualitative changes which occur at a critical value of the control parameter are called bifurcations. Bifurcations may lead the system to chaos. Often

there will be some intermediate states through which the system evolves before coming to the chaotic state. Usually one type of motion losses stability at a particular value of the control parameter at the same time giving rise to a new type of stable motion. This process continues further to give new and often more complicated type of motions. We can identify various routes to chaos taken by dynamical systems. The most common are

i) The period doubling route

ii) The quasiperiodic route

iii) Intermittency route.

1.5.1 Period doubling route

In period doubling route, the period of the oscillation doubles as the control parameter is varied [1, 4, 7]. After a sequence of such period doublings the system becomes aperiodic or chaotic. Logistic map is a simple model system where we can see this period doubling route to chaos.

Logistic map is a discrete dynamical system represented by the equation

$$X_{n+1} = \lambda X_n (1 - X_n) \qquad (1.12)$$

where $0 \leq \lambda \leq 4$ and $0 \leq X \leq 1$

Bifurcation diagram for a logistic map showing period doubling phenomena is given below [1, 4]

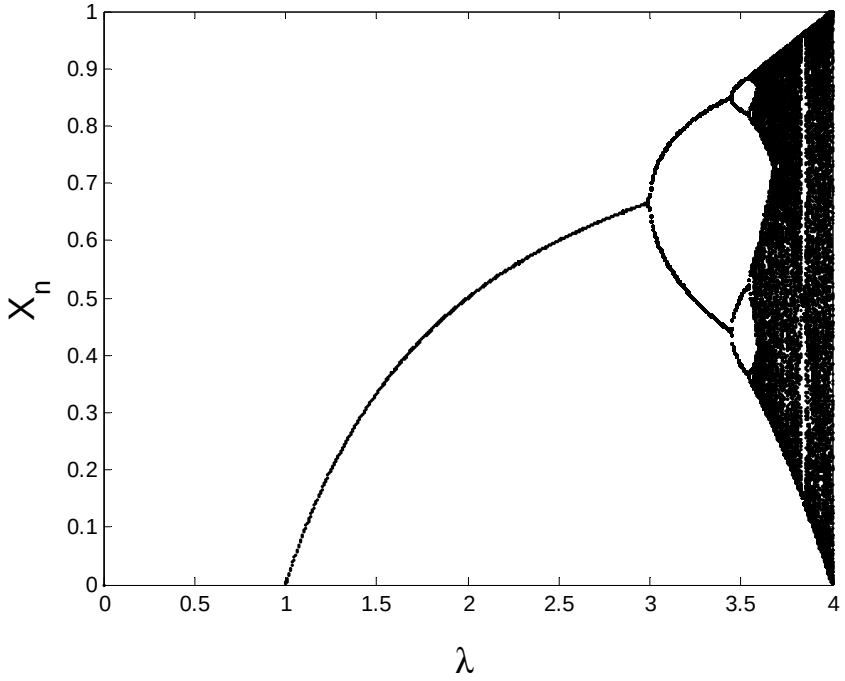

Figure 1.1: Bifurcation diagram of the logistic equation

1.5.2 Quasiperiodic route

The quasiperiodic route to chaos is also termed as Ruelle- Newhouse - Takens scenario. The basic mechanism taking place here is the phenomenon called Hopf bifurcation. In Hopf bifurcation a stable fixed point loses stability at a particular value of the control parameter and evolves into a limit cycle. The system undergoes one more Hopf bifurcation as the control parameter is varied further to form a two frequency periodic orbit. If the two frequencies of this orbit are not commensurate we call it as a quasiperiodic orbit. This quasiperiodic orbit then bifurcates into chaotic motion as the

control parameter is varied. Quasiperiodic route to chaos is observed in maps and in continuous time dynamical systems [4].

1.5.3 Intermittency route

This route is also known as Pomeau-Manneville scenario. Time series appears as nearly periodic interrupted by occasional irregular bursts. The time between bursts is statistically distributed like a random variable even though the system is completely deterministic. As the control parameter is varied the bursts become more and more frequent and finally the system becomes fully chaotic at a particular value of the control parameter. This intermittent behavior was first observed by Pomeau and Manneville in Lorenz equations [4, 5].

1.6 TWO SIMPLE MODEL SYSTEMS

In this section we describe two simple model systems namely the Rossler system and the van der Pol oscillator.

1.6.1 CHAOS IN A ROSSLER SYSTEM

The Rossler system is represented by the following set of equations [8, 9]

$$\begin{aligned} \dot{x} &= -y - z \\ \dot{y} &= x + ay \\ \dot{z} &= b + z(x - c) \end{aligned} \qquad (1.13)$$

where a,b,c are parameters. The parameter c is treated as the control parameter.

This system has only one quadratic nonlinearity xz. These equations represent a continuous time dynamical system that exhibits chaotic dynamics as the control parameter is varied. The famous simply folded band attractor for the Rossler system is shown in figure 1.2. An orbit within the attractor follows an outward spiral close to the X-Y plane around an unstable fixed point. Once the graph spirals out enough, it shows a rise and twist in the z dimension because of the influence of a second fixed point. Even though each variable is oscillating within a fixed range of values, the oscillations are found to be chaotic.

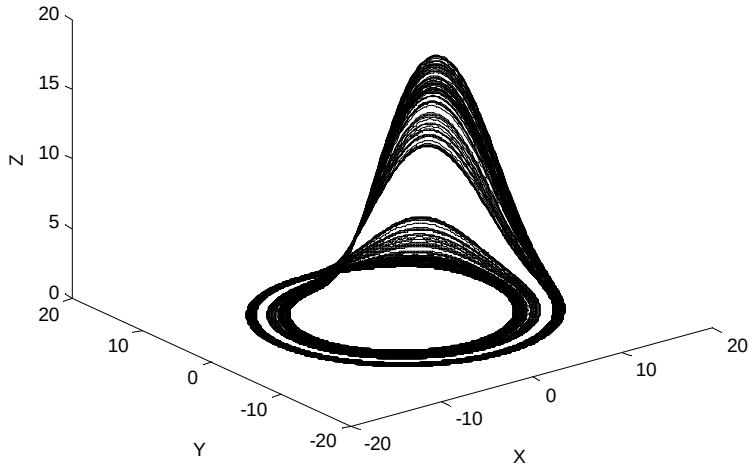

Figure 1.2: Simply folded band attractor of the Rossler system

To study the dynamics of the Rossler system we fix the parameters a=b=0.1 and vary c. The attractors corresponding to various c values are given in figure 1.3.

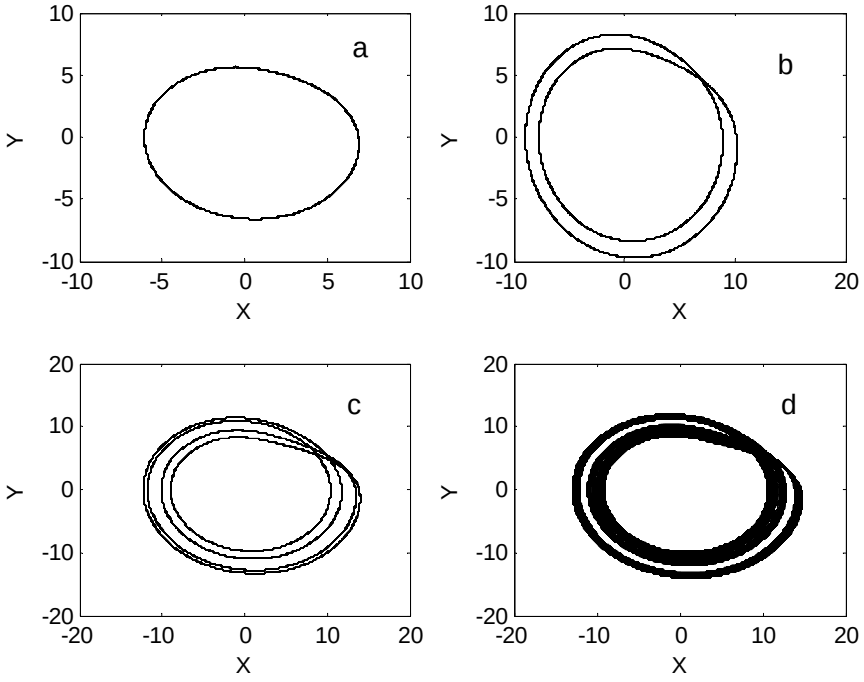

Figure 1.3: Attractors of the Rossler system for various c values .a) c=4; b) c=6; c) c=8.5; d) c=9

We can see the structure of attractor changing as the c value is varied. The attractor is a single loop periodic orbit at low c value. It suddenly undergoes period doubling at a bifurcation value of c changing into a double loop. The period doubling continues infinitely at higher c values and at last there is chaos. The route taken by the Rossler system is called the period doubling route to chaos. Figure 1.4 is the bifurcation diagram where the local maxima of the x- variable are plotted against the bifurcation parameter c. Similar

period doubling route to chaos is exhibited by semiconductor laser [10] and Nd:YAG laser [11]. Also Rossler system is a very good candidate for studying different types of synchronization such as phase and lag [12].

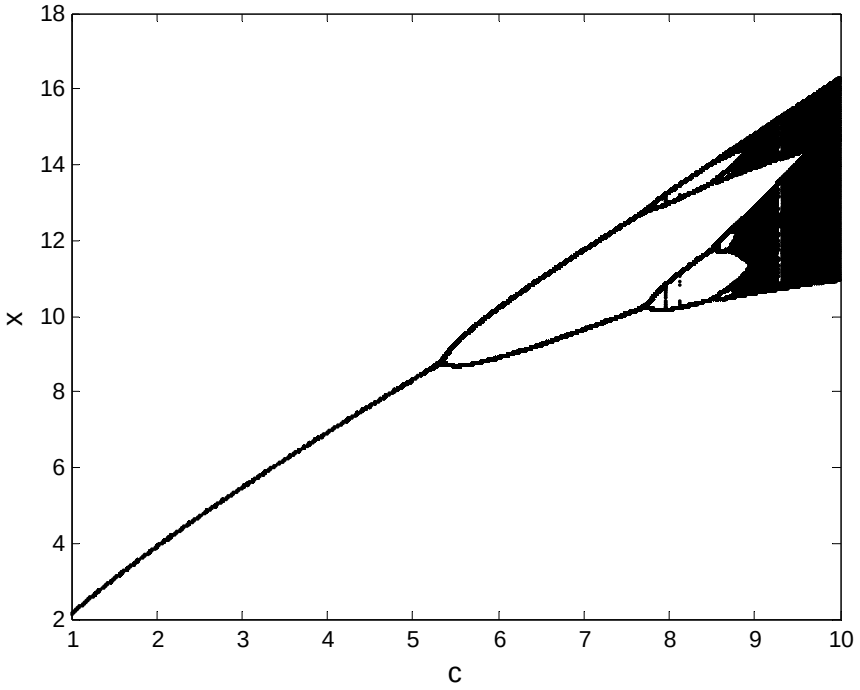

Figure 1.4: Bifurcation diagram for the Rossler system

1.6.2 THE VAN DER POL OSCILLATOR

It is a type of non conservative oscillator with a nonlinear damping. It evolves in time according to the pairs of first order differential equations [4-6]

$$\begin{aligned} \dot{x} &= y \\ \dot{y} &= b\left(1-x^2\right)y - x \end{aligned} \qquad (1.14)$$

where b is the damping coefficient.

Origin is found to be the equilibrium point for this system. Eigen values of the system are given by

$$\lambda_{\pm} = \frac{1}{2}\left[b \pm \sqrt{b^2 - 4}\right] \qquad (1.15)$$

Corresponding to different regions of the parameter b we can have different types of equilibrium states which are given in table 1.1.

Range of b	Nature of eigenvalues	Type of attractor/repellor
$-\infty<b<-2$	$\lambda_{\pm}<0$, $\lambda_{+} \neq \lambda_{-}$	Stable node
$b=-2$	$\lambda_{+} = \lambda_{-} <0$	Stable star
$-2<b<0$	$\lambda_{\pm} = \alpha \pm i\beta$, $\alpha<0$	Stable focus
$b=0$	$\lambda_{\pm} = \pm i\beta$	Center
$0<b<2$	$\lambda_{\pm} = \alpha \pm i\beta$, $\alpha>0$	Unstable focus
$b=2$	$\lambda_{+} = \lambda_{-} >0$	Unstable star
$2<b<\infty$	$\lambda_{\pm}>0$, $\lambda_{+} \neq \lambda_{-}$	Unstable node

Table 1.1: Dynamics of the van der Pol oscillator for different b values.

The attractor is an unstable equilibrium point for $0<b<\infty$. At b=0, the real parts of the eigen values $\lambda_{\pm}$ changes from negative to positive values as the parameter b is increased through zero. This causes a bifurcation from a stable focus to a stable limit cycle. A limit cycle is an isolated closed stable orbit that can exist in two dimensional dynamical systems. Every trajectory beginning sufficiently near a limit cycle approaches it either for $t\rightarrow \infty$ or $t\rightarrow -\infty$. A limit cycle is said to be stable if all the nearby trajectories approach it as $t\rightarrow \infty$. If the trajectories deviate from it as $t\rightarrow \infty$ (or approach it as $t\rightarrow -\infty$),

the limit cycle is said to be unstable. A stable limit cycle is a period T attractor or a periodic attractor. Such a bifurcation is called a Hopf bifurcation. i.e as a control parameter is varied a stable equilibrium point losses stability at a critical value and evolves into a limit cycle. It is characterized by a change of the real part of a pair of complex conjugate eigen values from negative to positive. In the van der Pol oscillator the limit cycle attractor is found to occur due to the dynamical balance between the positive and the negative damping. Figure 1.5 shows the limit cycle attractor for the van der Pol oscillator.

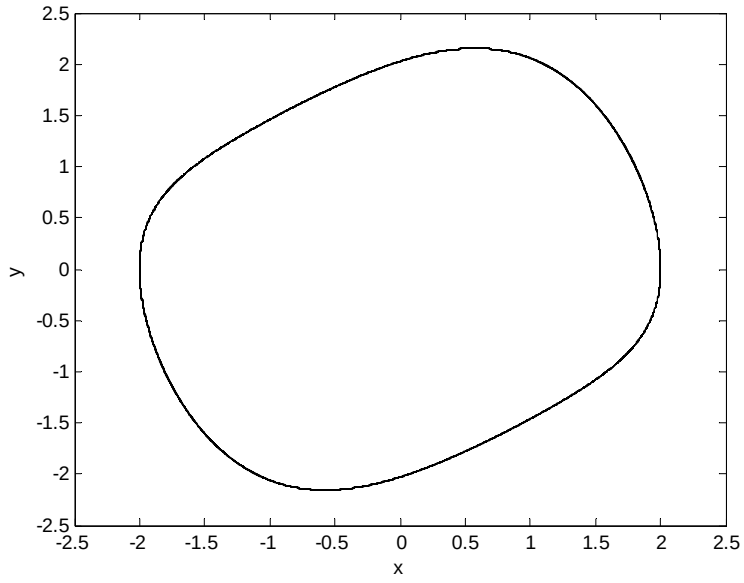

Figure 1.5: Phase portrait of the van der Pol oscillator for b=0.4 exhibiting limit cycle motion.

When driven by an external periodic forcing the oscillator exhibits interesting dynamical behaviors. A driven van der Pol oscillator is represented by the equation [4]

$$\dot{x} = y$$
$$\dot{y} = b\left(1 - x^2\right)y - x + f\cos\omega t \qquad (1.16)$$

Here b is the damping coefficient, f is amplitude of the driving force and ω is the frequency of the external periodic forcing.

Depending on the values of ω we can see mode locking, quasiperiodicity and chaos in the oscillator output. The oscillator dynamics can be summarized as in the following table.

f	Range of ω	Output dynamics
1.0	0-1.5	Mode locking and quasiperiodicity
2.5	0-6	Mode locking, large periodic oscillations and quasiperiodicity
5	2.424-2.502	Periodic windows,period doubling bifurcations and chaos

Table 1.2: Dynamics of the driven van der Pol oscillator for various ranges of f and ω

Bifurcation diagram for the driven van der Pol oscillator showing the period doubling route to chaos is given in figure 1.6.

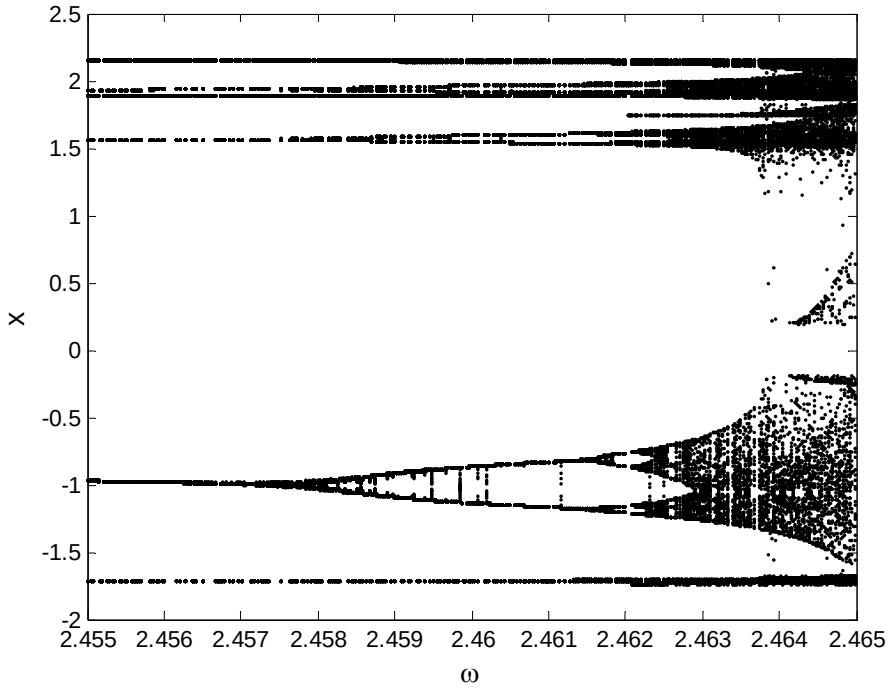

Figure 1.6: Period doubling route to chaos in driven van der Pol oscillator

1.7 LASERS

Lasers are devices that generate, or amplify coherent radiation at frequencies in the infrared, visible or ultraviolet regions of the electromagnetic spectrum. Invention of Ruby laser by Maiman in 1960 had a great impact on the scientific community. Processes such as signal generation, amplification, transmission and detection at much higher frequencies are made possible. Unique properties of lasers such as ultrashort pulsewidth, high power and short wavelength helped scientists and engineers to perform a wide variety of new and unexpected functions [13].

A laser consists of a gain medium placed inside a highly reflective optical cavity and a source to supply energy to the gain medium. The gain medium is a material which can amplify light by stimulated emission. The optical cavity consists of two mirrors. They are arranged such that the light bounces back and forth between the mirrors each time passing through the gain medium. One of the two mirrors –the output coupler- is made partially transparent so as to couple out the laser beam. Light of a specific wavelength is amplified through stimulated emission as it passes thorough the gain medium. Part of the light that is between the mirrors, after sufficient amplification comes out as laser beam through the output coupler. The process of supplying energy required for amplification is called pumping. Usually electric discharge or flash lamp is used as pumping sources. The output of laser may be of two types- continuous constant amplitude output and pulsed output [14].

1.8 DIFFERENT TYPES OF LASERS

1.8.1 Gas lasers

The Helium-Neon laser was the first gas laser to be operated successfully. It was fabricated by Ali Javan and his co-workers [15]. It emits at a variety of wavelengths with the well-known red light at 6328 Å. It is commonly used for educational purposes because of its low cost. Carbon dioxide lasers can emit hundreds of kilowatts at 9.6 μm and 10.6 μm and are often used in industry for cutting and welding. Argon-ion lasers have emission at wavelengths 351nm- 528.7 nm. Metal ion lasers are gas lasers that can generate light at deep ultraviolet wavelengths. Helium-Silver (HeAg) and Neon-Copper (NeCu) lasers come under this category. These lasers have

found applications in fluorescence suppressed Raman spectroscopy because of their narrow oscillation linewidth.

1.8.2 Chemical lasers

Chemical lasers obtain their energy from chemical reactions. They can produce power in the megawatt level and are used in industry for cutting and drilling and also for military purposes. Examples are Hydrogen fluoride laser and Deuterium fluoride laser.

1.8.3 Excimer laser

Excimer lasers are powered by chemical reaction involving excimer (excited dimer) which is a short lived dimeric or heterodimeric molecule formed from two atoms one of which is in an excited electronic state. They produce ultraviolet light and are used in semiconductor photolithography and in eye surgery.

1.8.4 Solid state lasers

Solid state laser materials have a crystalline host doped with ions that provide the required energy states. Neodymium is a common dopant in various solid state laser crystals which include yttrium orthovanadate ($Nd:YVO_4$), yttrium lithium fluoride (Nd:YLF) and yttrium aluminium garnet (Nd:YAG). These lasers can produce high powers in the infrared region. They find applications in cutting, welding, marking of metals, in spectroscopy and for pumping dye lasers. They can be frequency doubled, tripled or quadrupled to produce light at desired wavelengths. Solid state lasers where light is guided due to total internal reflection in an optical fiber are called fiber lasers.

1.8.5 Semiconductor lasers

Stimulated emission in a semiconductor pn junction is the basis of semiconductor lasers. The laser emission is not as monochromatic as that from a gas laser as it occurs between two bands of energies. Because of the direct conversion of electric current to light energy, semiconductor laser is very efficient. External cavity semiconductor lasers can generate high power outputs with good beam quality, narrow linewidth radiation with tunable wavelength and ultra short laser pulses.

1.8.6 Dye lasers

Dye lasers use organic dye as the lasing medium. They are highly tunable and capable of producing very short-duration pulses in the femtosecond range. Dye lasers are used dermatologically to make skin tone more even.

1.9 CHAOS IN LASERS

Instabilities in laser action were apparent since early days of laser technology. Semi classical model of the laser known as the Maxwell-Bloch equations [2] describe the time dependence of the electric field E, the mean polarization P of the atoms and the amount of population inversion D.

$$\begin{aligned} \frac{dE}{dt} &= -\kappa E + \kappa P \\ \frac{dP}{dt} &= \gamma_1 ED - \gamma_1 P \\ \frac{dD}{dt} &= \gamma_2(\lambda + 1) - \gamma_2 D - \gamma_2 \lambda EP \end{aligned} \qquad (1.17)$$

where κ is the decay rate in the laser cavity due to beam transition, γ_1 is the decay rate of the atomic polarization, γ_2 is the decay rate of the population inversion and λ is a pumping energy parameter.

Even though numerical simulation of Maxwell-Bloch equations may exhibit chaos, many conventional lasers do not operate within a parameter range where chaos occurs. In them the polarization and population inversion decay quickly to their steady state values which in turn reduces the dimension of the system to one. This will make the system out of the chaotic behavior. But the chaotic behavior can be induced by modifying the laser configurations i.e by tuning the cavity length, varying the laser gain, tilting the mirrors or by adding feedback from external cavity [16]. Lasers in which the frequency is broadened by the characteristics of the laser medium exhibit both periodic and chaotic behavior.

A detailed study of Maxwell- Bloch equations was carried out by Herman Haken [17] who reported that the instabilities seen in the Lorenz model [3] in fluids are identical with that of a single mode laser. This discovery was so important that it paved the way to a lot of research in the area of laser chaos. It started with Arecchi who reported the experimental observation of subharmonic bifurcations, generalized multistability, and chaotic behavior in a Q-switched CO_2 laser. They also presented a theoretical model which is found to be in good agreement with the experimental results [18]. In 1983 Gioggia and Abraham found instabilities in a single mode, inhomogeneously broadened Xenon laser exhibiting complicated periodic behavior ultimately reaching a deterministic chaotic behavior. Period doubling, two frequency quasiperiodic and intermittency route to chaos have also been found [19]. Chaos in a solid state laser with periodically modulated pump was reported

by Klische et.al [20]. A comparison of theoretical and experimental studies of unidirectional, single mode, inhomogeneously broadened ring laser was carried out by Tarroja et.al [21].

Semiconductor lasers are of special importance because of their potential applications in areas such as secure communication. Some of the pioneering works in this area include those of Min Tang, Shyh Wang and Kawaguchi [22, 23]. In 1986, studies by Winful and Liu revealed a quasiperiodicity route to chaos for a directly modulated self-pulsating semiconductor laser [24]. Kao et.al investigated a period doubling route to chaos in modulated semiconductor laser [25]. Effect of nonlinear gain on period doubling and chaos in a semiconductor laser was studied by G.P.Agrawal and it was shown that chaos occurred at modulation frequency around 1 GHz, which is of much importance in optical communication system [10]. Synchronization of chaotic lasers is widely studied [26] as it can enhance privacy and security of communication systems [27]. Semiconductor laser with feedback is an excellent model of nonlinear optical system which shows chaotic dynamics. The feedback induced instabilities, chaos and their applications have been widely studied [28-34].

Chaos in solid state lasers is also an area of much interest. Nd:YAG laser with intracavity KTP crystal serves as a good model system for this purpose. An early prediction of instabilities in this laser was made by Arecchi and Ricca [35]. Baer reported chaotic intensity fluctuations in this laser system and analyzed it using a rate equation model [36]. Significant contributions include those of Wu, Mandel, Oka and Kubota, Bracikowski and Rajarshi Roy [37-40]. A reverse period doubling route from chaos to stability in a two mode intracavity doubled Nd:YAG laser was reported in 1999 [11].

Dynamics of Nd:YAG laser with three modes has also been studied [41]. Recently it has been shown that multimode lasers have many advantages over single mode lasers which make them suitable for communication purposes [42-44].

REFERENCES

[1] Deterministic Chaos. N.Kumar, Univ.Press (1996).

[2] Chaotic Dynamics- An Introduction, G.L.Baker & J.P.Gollub. Cambridge Univ.Press II Ed (1996)

[3] E.N.Lorenz. J.Atmos.Sci, **20** (1963) 130

[4] Nonlinear Dynamics- Integrability, Chaos and Patterns, M.Lakshmanan and S.Rajasekar, Springer International Edition (2005)

[5] Nonlinear dynamics and chaos with applications to Physics,Biology, Chemistry and Engineering, Steven H.Strogatz, Perseus Books (1994)

[6] Chaos in Laser Matter Interactions, Peter W.Milloni, Mei-Li Shih and J.R.Ackerhalt, World Scientific Publishing Co Pvt Ltd (1987)

[7] Chaos in Dynamical Systems, Edward Ott, Cambridge Uni.Press (1993)

[8] Nonlinear Dynamics and Chaos, J.M.T.Thompson & H.B.Stewart, II Ed (2001)

[9] Chaos- An Introduction to Dynamical Systems. Kathleen T.Alligood, Tim D.Sauer and James A.Yorke, Springer International Edition (1996)

[10] G.P.Agrawal, Appl.Phys.Lett. **49** (1986) 1013

[11] Thomas Kuruvilla and V.M.Nandakumaran, CHAOS **9** (1999) 208

[12] Michael G.Rosenblum, Arkady S.Pikovsky and Jurgen Kurths, Phys.Rev.Lett. **78** (1997) 4193

[13] Lasers, A.E.Seigman, Published by University Science Books (1986)

[14] Lasers –Theory and Applications, K.Thyagarajan and A.K.Ghataka, Plenum Publishing Corporation, New York (1981)

[15] A.Javan, W.R.Bennett.Jr and D.R.Herriott, Phys.Rev.Lett. **6** (1961) 106

[16] Fischer I, Hess O , ElsaBer and Gobel, Phys.Rev.Lett. **73** (1994) 2188

[17] H.Haken, Phys.Lett.A. **53** (1975) 77

[18] F.T.Arecchi, R.Meucci , G.Piccioni and J.Tredicce, Phys.Rev.Lett. **49** (1982) 1217

[19] R.S.Gioggia and N.B.Abraham, Phys.Rev.Lett. **51** (1983) 650

[20] W.Klische, H.R.Telle and C.O.Weiss, Opt.Lett. **9** (1984) 561

[21] M.F.H.Tarroja, N.B.Abraham, D.K.Bandy and L.M.Narducci, Phys.Rev.A. **34** (1986) 3148

[22] H.Kawaguchi, Appl.Phys.Lett. **45** (1984) 1264

[23] M.Tang and S.Wang, Appl.Phys.Lett. **48** (1986) 900

[24] H.G.Winful, Y.C.Chen and J.M.Liu, Appl.Phys.Lett. **48** (1986) 616

[25] Y.H.Kao and H.T.Lin, IEEE J.Quan.Elec. **29** (1993) 1617

[26] V.Bindu and V.M.Nandakumaran, Phys.Lett.A. **277** (2000) 345

[27] V.Bindu and V.M.Nandakumaran, J.Opt.A.Pure & Appl.Opt. **4** (2002) 115

[28] Joachim Sacher, Wolfgang Elsasser and Ernst.O.Gobel, Phys.Rev.Lett. **63** (1989) 2224

[29] Mork Jesper, Tromborg Bjarne and Mark Jannik, IEEE J.Quan.Elec. **28** (1992) 93

[30] Otsubo Junji, Proceedings of Meeting of Japan Society for Laser Microscopy, **22** (1998) 25

[31] S.Tang and J.M.Liu, IEEE J.Quan.Elec. **37** (2001) 329

[32] Fan-yi and Jia-Ming Liu, IEEE J.Quan.Elec **39** (2003) 562

[33] S.Rajesh and V.M.Nandakumaran , Phys.Lett.A. **319** (2003) 340

[34] S.Rajesh and V.M.Nandakumaran, Physica D. **213** (2006) 113

[35] F.T.Arecchi and A.M.Ricca, *Coherence and Quantum Optics IV*, edited by L.Mandel and E.Wolf (Plenum, New York, 1978) 975

[36] T.Baer, J.Opt.Soc.Am.B. **3** (1986) 1175

[37] P.Mandel and X.G.Wu, J.Opt.Soc.Am.B. **3** (1986) 940

[38] X.G.Wu and P.Mandel, J.Opt.Soc.Am.B. **4** (1987)1870

[39] M.Oka and S.Kubota, Opt.Lett. **13** (1988) 805

[40] C.Bracikowski and Rajrshi Roy, CHAOS **1**(1991) 49

[41] Thomas Kuruvilla and V.M.Nandakumaran , Pramana **54** (1999) 393

[42] Zhou Yun, Wu Liang and Zhu Shi-Qun, Chinese Phys. **14** (2005) 2196

[43] R.M.Lopez-Gutierrez, C.Cruz-Hernadez, C.Posadas- Castillo, E.E.Garcia-Guerrero, PROCEEDINGS OF WORLD ACADEMY OF SCIENCE, ENGINERING AND TECHNOLOGY, **30** (2008) 1032

[44] Liang Wu, Shiqun Zhu, Phys.Lett.A. **308** (2003) 157

CHAPTER 2

SYNCHRONIZATION AND CONTROL OF CHAOS

The phenomenon of synchronization – its fundamental concepts, different methods for achieving synchronization, important types of synchronization- is presented in this chapter. Chaotic synchronization in various laser systems is also discussed. Special mention is made about the importance of chaos control and various methods employed for chaos control.

2.1 INTRODUCTION

The word ‘synchronization’ which means “ sharing the common time” or “ occurring in the same time” has its origin from the Greek words ‘chronos’(means time) and ‘syn’ (means the same, common) . We use ‘synchronization’ to describe processes that occur at the same time. Various man made devices such as pendulum clocks, musical instruments, lasers exhibit this phenomenon. Synchronization comes into play within human body also. Synchronous variation of cell nuclei, synchronous firing of neurons and adjustment of heart rate with respiration are a few to name. We can see several oscillating objects around us such as violins in an orchestra, fireflies emitting sequences of light pulses, crickets producing chirps and birds flapping their wings. These objects are not isolated from their environment, but interact with other objects. Even though this interaction can be very weak at times, an object adjusts its rhythm with that of others. As a result violinists play in unison, birds in a flock flap their wings simultaneously or insects in a population produce acoustic or light pulses at a common rate. As said in [1], “this adjustment of rhythms due to an interaction is the essence of synchronization”.

Dutch researcher Christian Huygens is the first scientist to observe and describe the synchronization phenomena in seventeenth century. He made an interesting discovery that a couple of pendulum clocks hanging from a common support are synchronized which means their oscillations coincided perfectly and the pendula move always in opposite directions. In his own words “*It is quite worth noting that when we suspended two clocks so constructed from two hooks imbedded in the same wooden beam, the motions of each pendulum in opposite swings were so much in agreement that they*

never receded the least bit from each other and the sound of each was always heard simultaneously. Further if this agreement was disturbed by some interference, it reestablished itself in a short time. For a long time I was amazed at this unexpected result, but after a careful examination finally found that the cause of this is due to the motion of the beam, even though this is hardly perceptible. The cause is that the oscillations of the pendula, in proportion to their weight, communicate some motion to the clocks. This motion, impressed onto the beam, necessarily has the effect of making the pendula come to a state of exactly contrary swings if it happened that they moved otherwise at first and from this finally the motion of the beam completely ceases. But this cause is not sufficiently powerful unless the opposite motions of the clocks are exactly equal and uniform". [1]

It is also possible to make two chaotic systems get synchronized. Because of the sensitive dependence of initial conditions, it is very difficult to predict the present position of the system on the attractor. If there are two identical chaotic systems starting with slightly different initial conditions, we can make them follow same path on the attractor – making them synchronized- through some coupling. Applications of this chaotic synchronization will be discussed later.

2.2 METHODS OF SYNCHRONIZATION

According to Huygens the conformity of the rhythms of two clocks is due to an imperceptible motion of the beam. It can be the vibration or a slight movement from right to left. The motion of each pendulum is transmitted to the other pendulum through this common beam. Thus their motion gets influenced by each other. This means that the beam provides some coupling

between the clocks which resulted in their synchronized anti-phase motion. Synchronization can be achieved between two oscillators only if there is some kind of coupling between them. Degree of synchronization may vary with the strength of coupling. The coupling strategies must be chosen as per the system properties and the particular application for which the synchronization is sought for. The synchronization strategies can be broadly classified into drive-response scheme and coupling scheme.

2.2.1 DRIVE-RESPONSE SCHEME

There will be a driving system which is chaotic and a response system which is a subsystem of the driving system. Both the systems are coupled unidirectionally i.e the dynamics of the response system is influenced by that of the driving system, but not in the opposite direction [2, 3]. The system can be schematically represented as shown below.

Figure 2.1: Drive – Response scheme

In a simple synchronization circuit, there will be only one response system driven by the drive system. We can also construct cascaded drive –response system [4] where there is more than one response subsystem driven by a common drive system. The response subsystems will synchronize with the drive and with each other provided that each response system is stable.

2.2.2 COUPLING SCHEME

In this scheme there are two chaotic systems which are identical but starting from slightly different initial conditions [5, 6]. The two systems can be coupled unidirectionally or bidirectionally. Figure 2.2 is a schematic representation of this coupling scheme.

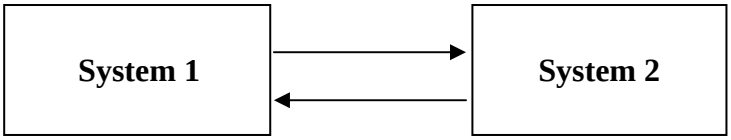

Figure 2.2: General coupling scheme

2.2.2.1 Occasional Coupling

It is a subclass of the drive-response scheme. Here the drive signal is sent only occasionally to the response system and at those times the response variables are updated. In between the updates the drive and response evolve independently. The time interval during which the response system gets influenced by the driving system is called the synchronization phase. The two systems get synchronized during this phase. On the other hand during autonomous phase there will be no coupling between the two systems and they evolve independently [4].

2.2.2.2 Variable feedback

In variable feedback scheme, there is a master system and slave systems. A fraction of the difference between the outputs of the master and the slave is

fed back to the input of the slave system [7]. Figure 2.3 gives a schematic representation of this coupling scheme.

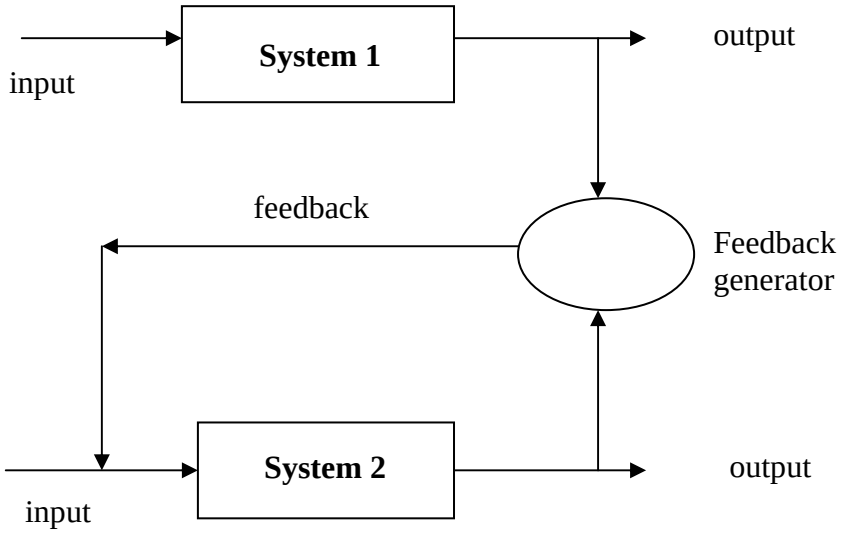

Figure 2.3: Variable feedback scheme

2.3 TYPES OF SYNCHRONIZATION

Depending on the degree of correlation between the interacting systems, there exist different types of synchronization such as generalized synchronization, phase synchronization, lag synchronization and complete synchronization.

2.3.1 COMPLETE SYNCHRONIZATION

Complete synchronization is the strongest among all types in the degree of correlation. It is identified as the coincidence of states of interacting systems i.e $x_1(t) = x_2(t)$ and it appears only when the interacting systems are identical.

Complete synchronization is a threshold phenomenon. It occurs only when the coupling exceeds some critical value. Below the threshold, even though the states of two chaotic systems are different, they will be close to one another. When the threshold is exceeded, the two systems become identical in time still remaining chaotic [1].

2.3.2 GENERALIZED SYNCHRONIZATION

Generalized synchronization has been introduced for drive-response system and is identified as the presence of some functional relation between the states of the drive and the response. i.e $x_2(t) = \psi(x_1(t))$. The state of the driven system is completely determined by the state of the driving system [1, 8]

2.3.3 PHASE SYNCHRONIZATION

There have always been complex and obscure ideas about the phase of a chaotic system. However phase synchronization of two chaotic systems can be defined as the entrainment between the phases of interacting systems while their amplitude remains chaotic and uncorrelated [9]. It occurs between systems with a slight parameter mismatch. Phase of a chaotic time series can be calculated using the method of Hilbert transform [10]. Phase synchronization is weaker than generalized synchronization and may occur in cases where generalized synchronization is not observed. But in some cases depending on parameter mismatches, phase synchronization appears after generalized synchronization with increase in coupling strength [1, 11].

2.3.4 LAG SYNCHRONIZATION

Lag synchronization is also observed in coupled systems with parameter mismatches. It appears as coincidence of states of the interacting systems shifted in time i.e $x_2(t) = x_1(t+\tau_0)$ .As the coupling strength is increased the time shift τ_0 decreases, leading to complete synchronization. Usually the lag synchronization is characterized by the quantity called similarity function, which is the time averaged difference between the variables x_1 and x_2 taken with time shift τ [11-13].

$$S(\tau) = \sqrt{\frac{\left\langle [x_2(t+\tau) - x_1(t)]^2 \right\rangle}{\left[\left\langle x_1^{\,2}(t) \right\rangle \left\langle x_2^{\,2}(t) \right\rangle \right]^{1/2}}} \qquad (2.1)$$

If the signals x_1 and x_2 are independent, $S(\tau) \approx \sqrt{2}$ for all τ. If $x_1(t) = x_2(t)$, as for complete synchronization $S(\tau)$ has its minimum equal to zero for $\tau=0$. If a time lag exists between the two signals, $S(\tau)$ has a minimum for nonzero τ.

Usually for a system of two coupled non identical oscillators, there is a transition from non synchronization to phase synchronization then to lag synchronization and finally to complete synchronization with increase in coupling strength.

To describe phase and lag synchronization we take Rossler system whose dynamics are given in detail in the chapter 1 as an example [11]
Consider a system of two coupled chaotic Rossler oscillators

$$\begin{aligned}
\dot{x}_{1,2} &= -\omega_{1,2} y_{1,2} - z_{1,2} + \varepsilon\left(x_{2,1} - x_{1,2}\right) \\
\dot{y}_{1,2} &= \omega_{1,2} x_{1,2} + a y_{1,2} \\
\dot{z}_{1,2} &= b + z_{1,2}\left(x_{1,2} - c\right)
\end{aligned} \tag{2.2}$$

where a=0.165, b=0.2 and c=10. The parameters $\omega_{1,2} = \omega_0 \pm \Delta$ and ε determine the parameter mismatch and coupling strength respectively. The mismatch is produced by choosing ω_0 =0.86 and Δ=0.02. Figure 2.4 shows the projections of the attractor of the coupled Rossler system on the plane ($x_1(t)$, $x_2(t)$) and the delayed coordinate plots $x_2(t+\tau)$ vs $x_1(t)$ for various coupling strengths.

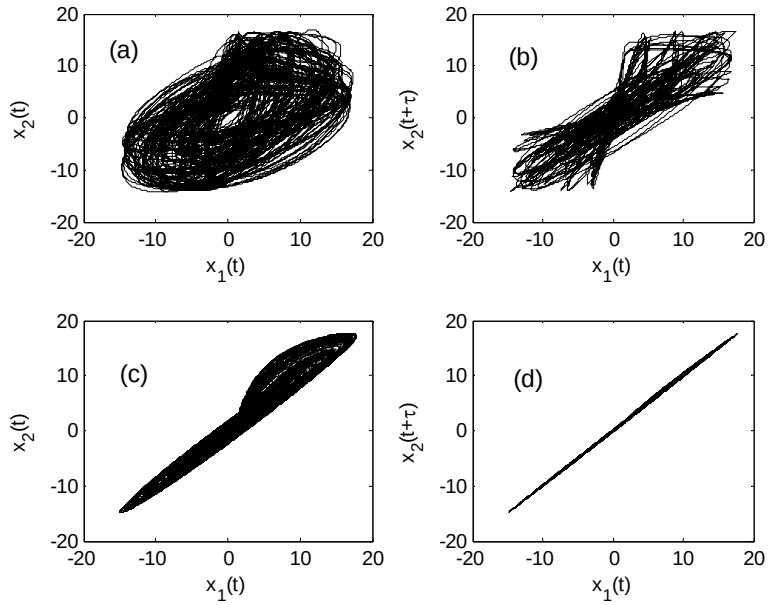

Figure 2.4: (a) and (b) corresponds to ε=0.04 and time shift τ_0 =0.9 a region with phase synchronization. (c) and (d) corresponds to ε=0.28 and time shift τ_0 =0.15 a region with lag synchronization

2.4 CONCEPT OF CHAOTIC SYNCHRONIZATION WITH SPECIAL REFERENCE TO LASER SYSTEMS

It is possible to make two or more coupled systems to follow closely related orbits even when their motions are chaotic. Synchronization of coupled chaotic systems has been widely studied for the past few decades. This phenomenon has found numerous applications in areas such as laser dynamics [14-17], electronic circuits [18, 19], chemical and biological systems [20, 21], and secure communication [22, 23]. Synchronization is also found to occur in coupled maps [24-26], coupled semiconductor lasers [27] and in coupled Josephson junction arrays [28].

The main motivation behind the development of coupled lasers was the requirement of high power laser sources. Also synchronization of chaotic lasers has found to play vital role in secure communication. Semiconductor lasers with emission in the long wavelength (1.3-1.5μm) region are very useful in optical communication systems. Semiconductor lasers and erbium doped fiber lasers are the most efficient sources in present day communication systems [23]. Nd:YAG laser with intracavity KTP crystal is a system of special interest because of its high nonlinearity and multimode operation. The development of high power laser diode arrays which provide a long lived, highly efficient pump source for the Nd YAG laser, and the availability of doubling crystals with large non linear coefficients have permitted the development of cw visible sources with electrical efficiencies approaching 1%. These systems are one of the most efficient sources of cw coherent light in this portion of the visible spectrum [29]. Chaotic Nd:YAG lasers are proved to be ideal candidates for multichannel communication purposes. Chaotic synchronization of multimode Nd: YAG lasers can be

used in digital communication of two-dimensional messages and in encrypted audio transmission [30, 31]. In a multimode laser chaotic synchronization between corresponding cavity modes will be different from that between different cavity modes. Thus each pair of corresponding cavity modes can be used as a channel in optical communication [32].

2.5 CONTROL OF CHAOS IN LASER SYSTEMS

Even though chaotic lasers are important from the point of view of communication, there are situations where we have to control chaos such as in experiments where a stable laser output is desired. Control of chaos in semiconductor lasers is very much important so as to improve the quality of optical communication systems. In 1988 it was Pettini who made the discovery that introduction of some suitable time dependant variations to certain parameters of the system can control chaos [33]. It was shown that application of periodic perturbations to the accessible control parameters of multimode solid state lasers can eliminate chaos in the output [34]. Later Ott, Grebogi and York developed a method for chaos control by stabilizing the unstable periodic orbits embedded in the chaotic attractor of the system [35]. In a method devised by Murali and Lakshmanan introduction of a second periodic signal generator in series with the original produces a quasiperiodic driving which in turn suppresses chaos [36]. Bidirectional coupling with another laser is found to be an efficient method for controlling chaos in directly modulated semiconductor laser [14, 37]. Recently a much novel and efficient method for controlling chaos in directly modulated semiconductor laser was introduced in which a delayed optoelectronic feedback was given to suppress chaos [38]. This time delay feedback control scheme introduced by Pyragas is known as Time Delay Auto Synchronization (TDAS) and has

been used for chaos control in various dynamical systems [39]. In TDAS method the Unstable Periodic Orbits of the chaotic system is stabilized by applying a self-adjusting feedback with a delay time that is equal to the period of the corresponding cycle. But in the delay feedback control scheme discussed in [38], a simple positive feedback of very small delay compared with the period of the 1 cycle is applied. Roy et al used the method of occasional proportional feedback to control chaos in Nd:YAG lasers [40].

REFERENCES

[1] Synchronization -A universal concept in nonlinear sciences, Arkady Pikovski, Michael Rosenblum and Jurgen Kurths, Cambridge University Press, Cambridge (2001)

[2] L.M.Pecorra and T.L.Carroll, Phys.Rev.Lett. **64** (1990) 821

[3] L.M.Pecorra and T.L.Carroll , Phys.Rev.A. **44** (1991) 2374

[4] Louis M.Pecora, Thomas M.Carroll , Greg A.Johnson , Douglas J.Mar and James F.Heagy, CHAOS **7** (1997) 520

[5] H.Fujisaka and T.Yamada, Prog.Theor.Phys. **69** (1983) 32

[6] N.F.Rulkov, A.R.Volkovski, A.Rodriguez-Lozano, E.Del Rio and M.G.Velarge Int J.Bifurc.Chaos. **2** (1992) 669

[7] O.Morgul, Phys.Lett A. **247** (1998) 391

[8] Zhigang Zheng and Gang Hu, Phys. Rev. E. **62** (2000) 7882

[9] Grogory V.Osipov, Arkady S.Pikovsky, Mochael G.Rosenblum and Jurgen Kurths, Phys. Rev. E. **55** (1997) 2353

[10] Tolga Yasinkaya and Ying- Cheng Lai, Phys.Rev.Lett. **79** (1997) 3885

[11] Michael G.Rosenblum, Arkady S.Pikovsky and Jurgen Kurths, Phys.Rev.Lett. **78** (1997) 4193

[12] Saeed Taherion and Ying –Cheng Lai, Phys. Rev.E. **59** (1999) 6247

13] Meng Zhan, G.W.Wei and C.H.Lai, Phys. Rev.E. **65** (2002) 036202

[14] V.Bindu and V.M.Nandakumaran, Phys.Lett.A. **277** (2000) 345

[15] Thomas Kuruvilla and V.M.Nandakumaran, Pramana **54** (2000) 393

[16] L.Fabiny, P.Colet and R.Roy, Phys.Rev.A. **47** (1993) 4287

[17] R.Roy and K.S.Thornburg Jr., Phys.Rev.Lett.**72** (1994) 2009

[18] V.S. Anischenko et al., Int.J.Bifurcation Chaos Appl. Sci.Eng. **2**

(1992) 633

[19] J.F. Heagy, T.L. Carroll and L.M.Pecora, Phys.Rev.E. **50** (1994) 1874

[20] I.Schreiber and M.Marek, Physica D. **5** (1982) 2582

[21] S.K.Han, C.Kurrer and K.Kuramoto, Phys.Rev.Lett. **75** (1995) 3190

[22] L.Kocarev and U.Parlitz, Phys.Rev.Lett. **74** (1983) 5028

[23] V.Bindu and V.M.Nandakumaran, J. Opt. A. Pure& Appl. Opt. **4** (2002) 115

[24] S.Sinha, Phys.Rev. E. **57** (1998) 4041

[25] R.E.Amritkar, P.M Gade, A.D Gangal and V.M. Nandakumaran, Phys.Rev.A . **44** (1991) 3407

[26] K. Kaneko, Prog.Theor.Phys.**74** (1985) 1033

[27] S. Dasgupta and D.R.Anderson, J.Opt.Soc.Am.B. **11** (1994) 290

[28] S.Watanbe, S.H. Strogatz, H.S.J. Vander Zant and T.P.Orlando, Phys.Rev.Lett. **74** (1995) 379

[29] T.Baer, J.Opt.Soc.Am.B. **3** (1986) 1175

[30] Zhou Yun, Wu Liang and Zhu Shi-Qun, Chinese Phys. **14** (2005) 2196

[31] R.M.Lopez-Gutierrez, C.Cruz-Hernadez, C.Posadas- Castillo, and E.E.Garcia- Guerrero, PROCEEDINGS OF WORLD ACADEMY OF SCIENCE, ENGINERING AND TECHNOLOGY **30** (2008) 1032

[32] Liang Wu and Shiqun Zhu, Phys.Lett.A. **308** (2003) 157

[33] Controlling Chaos Through Parametric Excitations, Dynamics and Stochastic Processes. M.Pettini. Eds.R.Lima, L.Streit, M.Pettini and R.V.Mendes (Springer-Verlag, New York) (1988) 242

[34] Pere Colet and Y.Braiman, Phy.Rev.E. **53** (1996) 200

[35] E.Ott, C.Grebogi and J.A.Yorke, Phys.Rev.Lett. **64** (1990) 1196

[36] K.Murali and M.Lakshmanan, J.Circ.Sys.Comp. **3** (1993) 125

[37] T.Kuruvilla and V.M.Nandakumaran, Phys.Lett.A. **254** (1999) 39

[38] S.Rajesh and V.M.Nandakumaran, Phys.Lett.A. **319** (2003) 340

[39] K.Pyragas, Phys.Lett.A. **170** (1992) 421

[40] R.Roy, T.W.Murphy, T.D. Maier, Z.Gills and E.R. Hunt, Phys.Rev.Lett. **68** (1992) 1259.

CHAPTER 3

LASER MODEL AND ITS DYNAMICAL PROPERTIES

In this chapter we describe the laser model used for our numerical studies. The dynamics of two mode and three mode Nd: YAG lasers with intracavity KTP crystal is discussed using rate equations. Phase portraits and bifurcation diagrams are used to get a clear picture of laser dynamics.

3.1 LASER MODEL

Nd:YAG laser, one of the most commonly used solid state lasers possesses a number of unique properties favorable for laser operation. The YAG (yttrium aluminium garnet) host is hard and has good optical quality and high thermal conductivity. Because of the cubic structure of YAG, the laser has a narrow fluorescent linewidth which again results in high gain and low threshold for the laser operation. Nd:YAG host also possesses many physical, chemical and mechanical properties. The YAG structure is stable from the lowest temperatures up to the melting point. Even though the strength and hardness of YAG are lower than ruby it is high enough to not produce any serious breakage problems during fabrication [1-3].

Usually Nd:YAG lasers are optically pumped using flash lamp or laser diode. The lasing medium is the colorless isotropic crystal $Y_3Al_5O_{12}$ (YAG) with nearly 1% of yttrium replaced by neodymium. The energy levels of the Nd^{3+} ion are responsible for the fluorescent properties in the amplification process. The energy level diagram of neodymium ions is shown in figure 3.1. Neodymium ions are excited to high energy levels using an optical pumping mechanism. These ions deexcite to the level marked M which is the metastable state having a life time of about 0.25 ms. Laser action is obtained between the levels M and L at a wavelength of about 1.06 μm. Nd:YAG lasers find applications in ophthalmology, dentistry, cosmetic medicine, manufacturing and fluid dynamics [4,5,6].

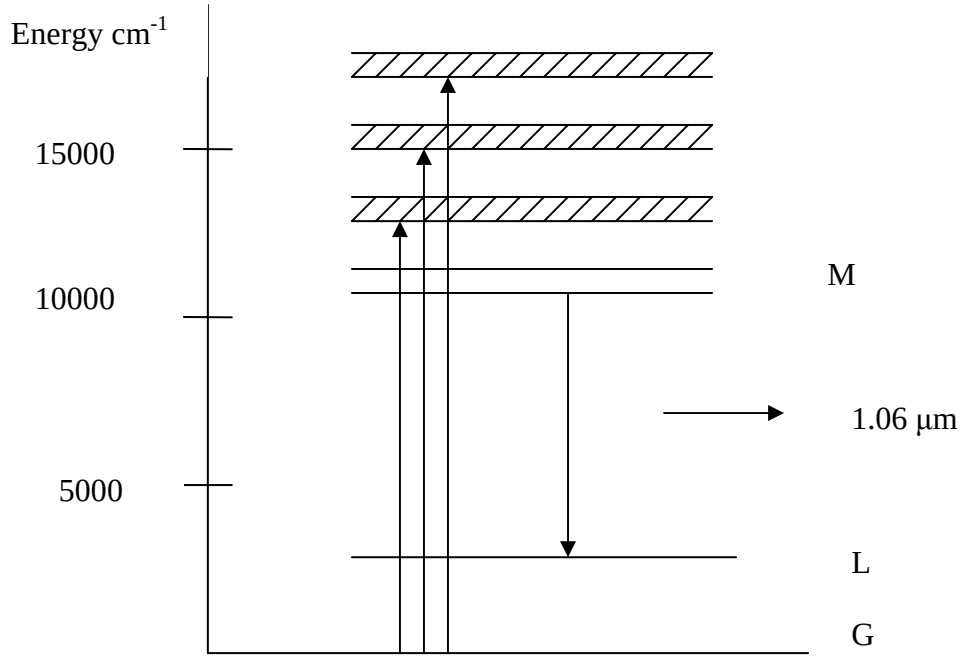

Figure 3.1: Energy level diagram of neodymium ions.

Our model system is a diode-pumped Nd:YAG laser with intracavity KTP (potassium titanyl phosphate) crystal. Nd:YAG laser has the fundamental wavelength at 1064 nm in the infrared region. The laser output is stable without the intracavity doubling crystal. When the nonlinear KTP crystal in inserted into the laser cavity some of the infrared fundamentals are converted into green light (532 nm)by the process of second harmonic and sum frequency generation. Different longitudinal modes get coupled due to this sum frequency generation, which again produces deterministic intensity fluctuations in the laser output. Therefore with the crystal inserted into the laser cavity, output intensity exhibits periodic and chaotic fluctuations [7].

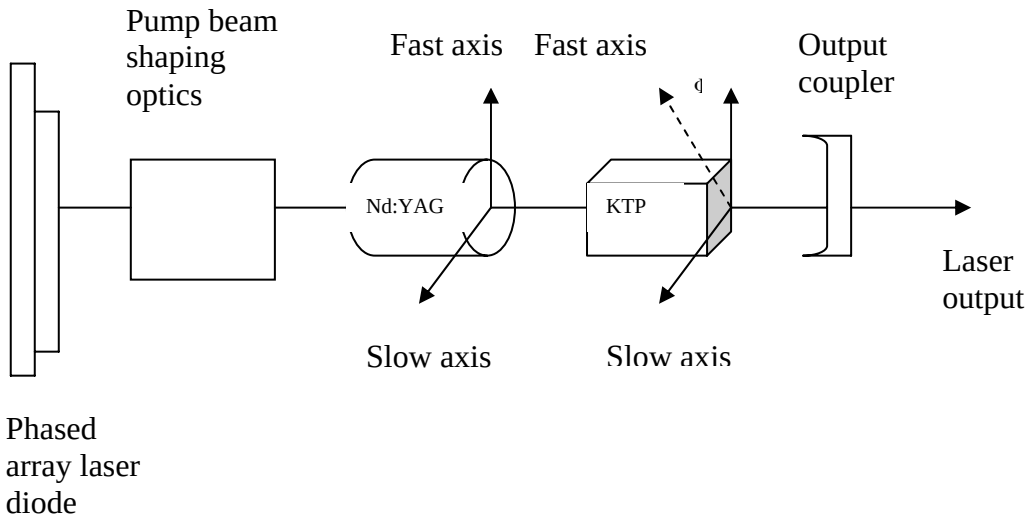

Figure 3.2: Schematic of the laser model used for numerical studies

Figure 3.2 is a schematic of the laser model used in our numerical studies [8]. The nonlinear KTP crystal which serves as the frequency doubling element is placed inside the Nd:YAG laser cavity. The intensity at the fundamental wavelength is maximum within the laser cavity. The intensity of green light produced by the KTP crystal is found to be proportional to the square of the fundamental intensity. Therefore the KTP crystal is placed inside the laser cavity to get maximum green light. The YAG rod and KTP crystal have the property called birefringence. A birefringent material possesses two orthogonal directions along which the material has different indices of refraction. Therefore light polarized along one axis travels faster than the light polarized along the other orthogonal axis. Accordingly one of

the axes is termed as “fast” axis and the other is called “slow” axis. Undoped YAG is isotropic and homogeneous and exhibits no birefringence. When YAG crystal is doped with neodymium ion Nd^{3+}, it introduces some stress induced birefringence in the Nd:YAG rod. There are only two orthogonal polarization directions for the laser and the laser output is usually polarized in either one or both of these orthogonal polarization directions. The number of modes can vary from one to ten.

Green light is produced in the KTP crystal by second harmonic generation and by sum frequency generation [8]. In second harmonic generation two photons from the same cavity mode of fundamental frequency ω combine to generate one photon of green at frequency 2 ω. In sum frequency generation one photon from a cavity mode at frequency ω_1 combine with one photon from another mode at frequency ω_2 to produce one photon of green at frequency (ω_1+ ω_2). The amount of green light produced by sum frequency generation depends on the orientation of the contributing laser cavity modes i.e whether they are polarized parallel or perpendicular to each other.

Baer developed a deterministic rate equation model to describe the laser dynamics. The differential equations describing the time dependence of the laser intensity (I_1) and gain (G_1) for single mode operation are [7]

$$\tau_c \frac{dI_1}{dt} = (G_1 - \alpha_1 - \varepsilon I_1) I_1 \qquad (3.1a)$$

$$\tau_f \frac{dG_1}{dt} = (\beta I_1 + 1) G_1 + G_1^0 \qquad (3.1b)$$

where τ_c is the cavity round trip time, τ_f is the fluorescence life time (of Nd^{3+} ion), α_1 is the mode 1 losses, ε is the nonlinear coefficient which is related to the KTP crystal properties and describes the conversion efficiency of the fundamental intensity into green light, β is the saturation parameter and G_1^0 is the small signal gain related to the pump rate. Values of the parameters are given in table below.

τ_c	0.5 ns
τ_f	240μs
α_1	0.015
ε	$5\times10^{-5}\,W^{-1}$
β	$1W^{-1}$
G_1^0	0.12

Table 3.1: Parameter values used in Eqs.3.1 (a) and 3.1(b)

This model can be extended to the case of two oscillating longitudinal modes where each longitudinal mode is represented by a pair of equations similar to Eqs. 3.1(a) and 3.1(b) [7].

$$\tau_c \frac{dI_1}{dt} = \left(G_1 - \alpha_1 - \varepsilon I_1 - 2\varepsilon I_2\right) I_1 \qquad (3.2a)$$

$$\tau_f \frac{dG_1}{dt} = -\left(\beta I_1 + \beta_{12} I_2 + 1\right) G_1 + G_1^0 \qquad (3.2b)$$

$$\tau_c \frac{dI_2}{dt} = \left(G_2 - \alpha_2 - \varepsilon I_2 - 2\varepsilon I_1\right) I_2 \qquad (3.3a)$$

$$\tau_f \frac{dG_2}{dt} = -\left(\beta I_2 + \beta_{21} I_1 + 1\right) G_2 + G_2^0 \qquad (3.3b)$$

where $\beta_{12} = \beta_{21}$ (0.666 W^{-1}) is the cross- saturation parameter for modes 1 and 2 .

The losses in the fundamental intensity which arises due to the intracavity doubling and the sum-frequency generation are represented by the last two terms in Eqs. (3.2a) and (3.3a) respectively. The cross-saturation effects due to the partial inhomogeneous broadening in the laser cavity are incorporated in the rate equation by the second terms in Eqs. (3.2b) and (3.3b) where intensity of one mode is coupled to the gain of the other mode.

The above model can be extended so as to include more oscillating longitudinal modes. If there are N oscillating modes we can write [7]

$$\tau_c \frac{dI_i}{dt} = \left(G_i - \alpha_i - \varepsilon I_i - 2\sum_{j \neq i}^{N} \varepsilon I_j \right) I_i \qquad (3.4a)$$

$$\tau_f \frac{dG_i}{dt} = -\left(\beta I_i + \sum_{j \neq i}^{N} \beta_{ij} I_j + 1 \right) G_i + G_i^0 \qquad (3.4b)$$

i=1, 2…N

β_{ij} is the cross- saturation of modes i and j.

Later Bracokowski and Rajarshi Roy [8, 9] reported that the chaotic intensity fluctuations in the laser output can be eliminated by proper orientation of the YAG rod and the KTP crystal. They also modified the Baer model by incorporating a geometric factor (represented as g in Eqn.3.5a) which is a measure of the relative orientation of the YAG and KTP fast axes.

Each cavity mode can be polarized in either one of the two orthogonal polarization directions. The modified rate equations for the fundamental

intensities I_k and gains G_k associated with the k^{th} longitudinal mode are given by

$$\tau_c \frac{dI_k}{dt} = \left(G_k - \alpha - g\varepsilon I_k - 2\varepsilon \sum_{j \neq k} \mu_{jk} I_j \right) I_k \qquad (3.5a)$$

$$\tau_f \frac{dG_k}{dt} = \gamma - \left(1 + I_k + \beta \sum_{j \neq k} I_j \right) G_k \qquad (3.5b)$$

k=1, 2, 3….are the mode numbers.

Here γ is the small signal gain which is related to the pump rate.

The parameter values are same as in table 3.1

For modes having same polarization as the k^{th} mode, μ_{jk} =g, and for modes having orthogonal polarization, μ_{jk} = (1-g) .This difference arises due to the different amounts of sum frequency generated green light produced by pairs of parallel polarized modes or by pairs of orthogonally polarized modes.

Numerical simulations of the rate equations for a two mode Nd: YAG laser with intracavity KTP crystal show a reverse period doubling route from chaos to stability as the control parameter is varied [10]. The modes chosen are orthogonally polarized and termed as j and k. The control parameter is ‘g’. The rate equations are

$$\tau_c \frac{dI_j}{dt} = \left(G_j - \alpha - g\varepsilon I_j - 2\varepsilon(1-g)I_k\right)I_j$$
$$\tau_f \frac{dG_j}{dt} = \gamma - \left(1 + I_j + \beta I_k\right)G_j$$
$$\tau_c \frac{dI_k}{dt} = \left(G_k - \alpha - g\varepsilon I_k - 2\varepsilon(1-g)I_j\right)I_k \qquad (3.6)$$
$$\tau_f \frac{dG_k}{dt} = \gamma - \left(1 + I_k + \beta I_j\right)G_k$$

As the control parameter, which is the orientation of YAG and KTP fast axes, is changed from 0 to 1 the output intensity undergoes a reverse period doubling sequence from chaos to stable behavior [10]. The phase portraits where the total output intensity is plotted against total gain for different g values showing the reverse period doubling route is given in figure 3.3.

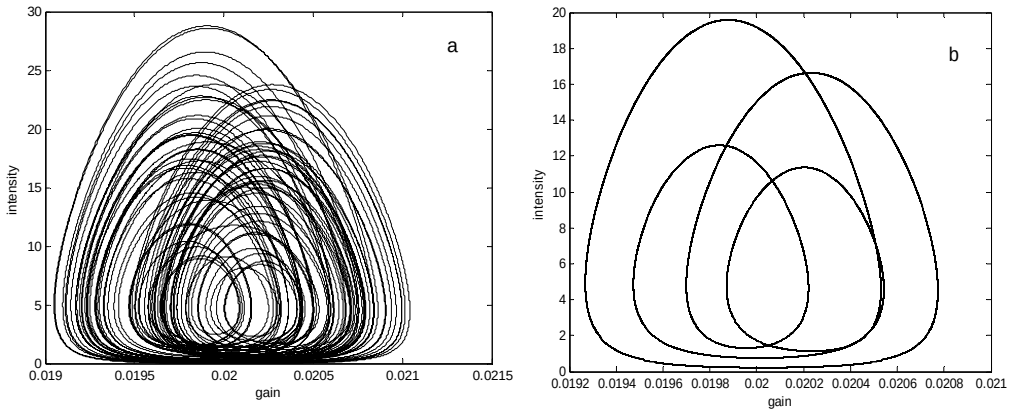

Figure 3.3: Phase portrait for two mode laser with a) g=0.002 b) g=0.1

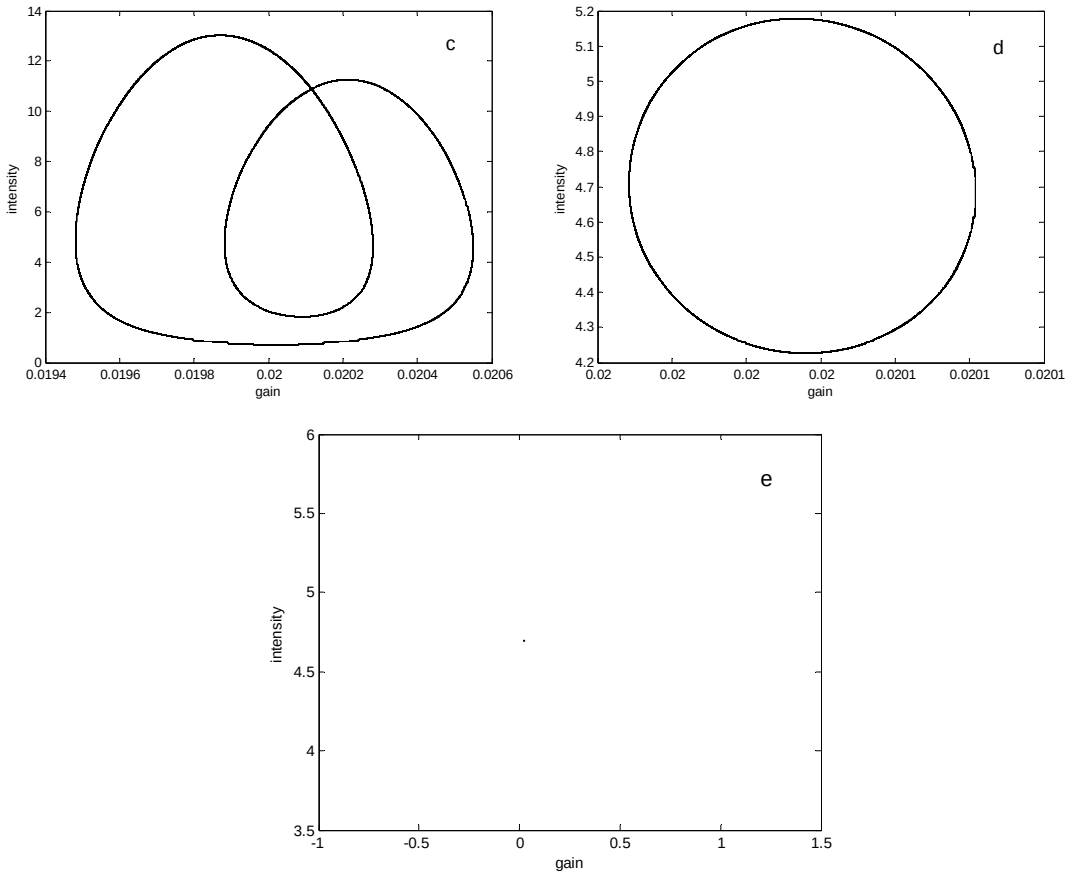

Figure 3.3: Phase portrait for two mode laser with c) g=0.2 d) g=0.5 e) g=0.65

A bifurcation diagram is drawn taking the control parameter g along x axis and maxima of the intensity along y axis.The reverse period doubling route is clear from the bifurcation diagram shown below.

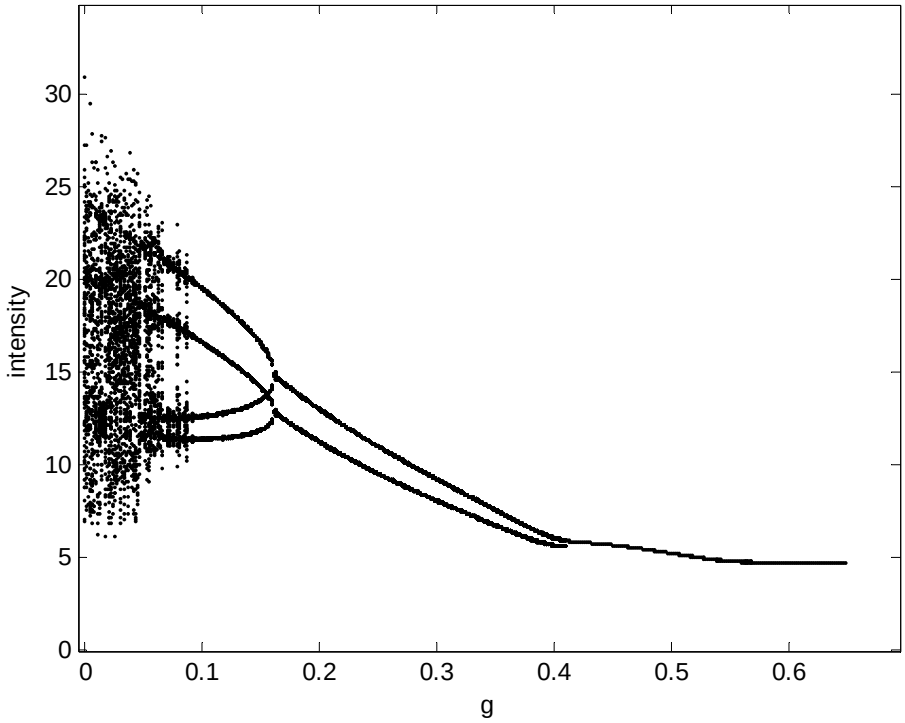

Figure 3.4: Bifurcation diagram for the laser showing the reverse period doubling route

The laser intensity is found to be stable for higher g values [11]. It has been proved analytically that there was no sumfrequency generation at g=1. So there is no mode coupling at this g value and hence the output intensity is stable.

Effect of varying g value on the energy transfer between the modes is also studied [10]. For this intensity in the x -polarized mode is plotted against that in the y -polarized mode for various g values. For g=0.002, there is a complex pattern indicating that the energy exchange between the modes take

place in a chaotic manner.As the g value is increased, we can see a closed loop which means that energy tranfer has a pariodic nature. Finally coming to the stable region it is a single spot showing that there is no exchange of energy between the modes. The various plots are given in figure 3.5.

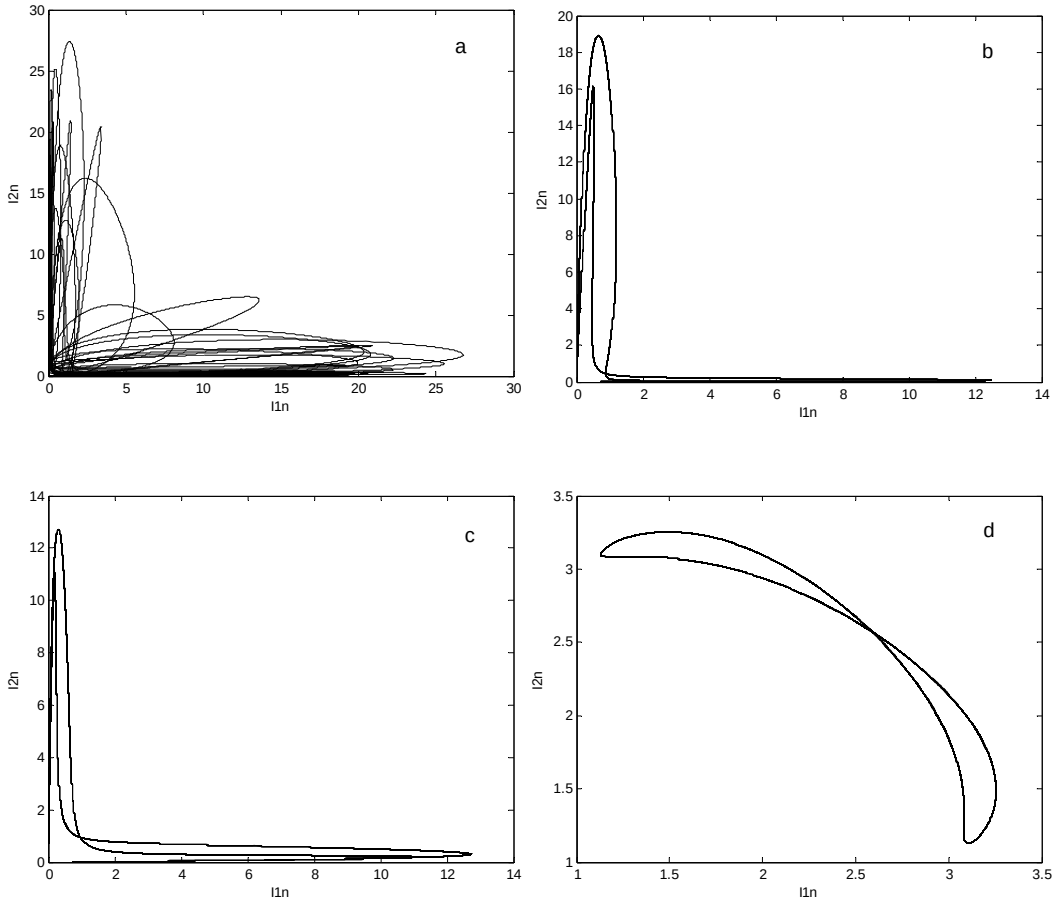

Figure 3.5: Intensity in the x -polarized mode plotted against that in the y-polarized mode for a) g=0.002 b) g=0.1 c) g=0.2 d) g=0.5

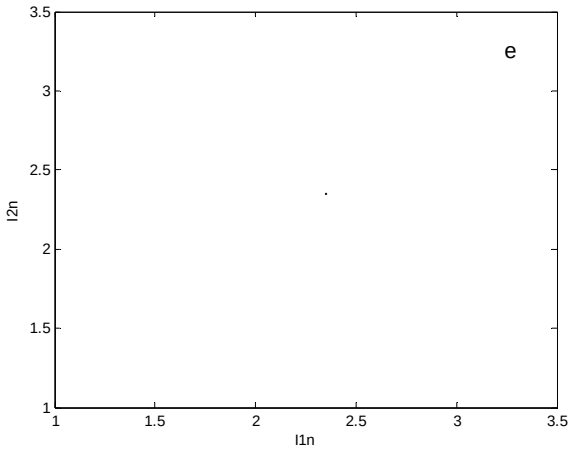

Figure 3.5: Intensity in the x- polarized mode plotted against that in the y- polarized mode for e) g=0.65

Numerical studies for a three mode laser reveals almost similar behavior, although the reverse period doubling route is absent. We assume that the laser is operating with three coexisting longitudinal modes with two modes polarized parallel to each other and the third mode polarized orthogonal. The corresponding rate equations are [12].

$$
\begin{aligned}
\tau_c \frac{dI_j}{dt} &= \left(G_j - \alpha - g\varepsilon I_j - 2\varepsilon\left((1-g)I_k + (1-g)I_l\right)\right)I_j \\
\tau_f \frac{dG_j}{dt} &= \gamma - \left(1 + I_j + \beta\left(I_k + I_l\right)\right)G_j \\
\tau_c \frac{dI_k}{dt} &= \left(G_k - \alpha - g\varepsilon I_k - 2\varepsilon\left((1-g)I_j + gI_l\right)\right)I_k \\
\tau_f \frac{dG_k}{dt} &= \gamma - \left(1 + I_k + \beta\left(I_j + I_l\right)\right)G_k \\
\tau_c \frac{dI_l}{dt} &= \left(G_l - \alpha - g\varepsilon I_l - 2\varepsilon\left((1-g)I_j + gI_k\right)\right)I_l \\
\tau_f \frac{dG_l}{dt} &= \gamma - \left(1 + I_l + \beta\left(I_j + I_k\right)\right)G_l
\end{aligned}
\tag{3.7}
$$

The laser is found to be chaotic upto g=0.4, after which it becomes periodic. When g=0.43, we can see period three oscillations in the output . Figure 3.6 shows the intensity time series plots corresponding to the chaotic and periodic regions. Figure 3.7 shows corresponding phase space plots.

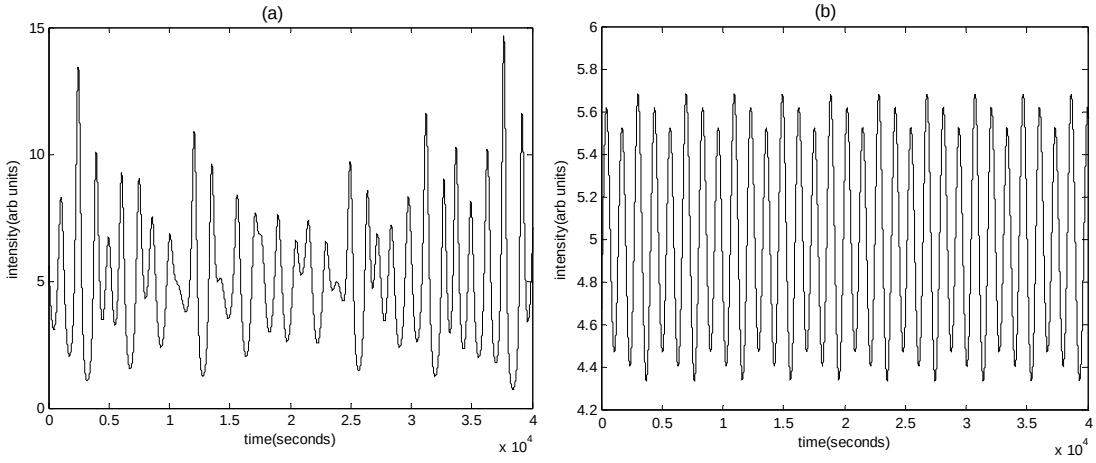

Figure 3.6: Intensity time series plots for three mode laser with a) g=0.12 b) g=0.43

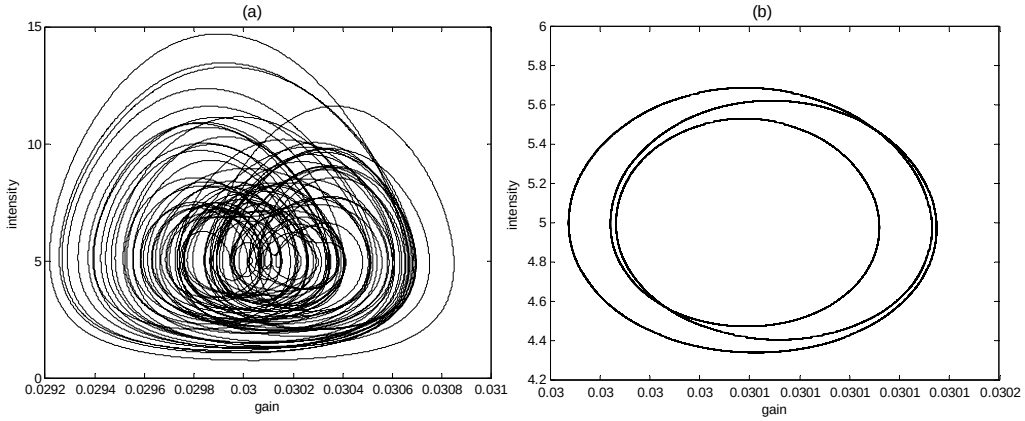

Figure 3.7: Phase space plots for three mode laser with a) g=0.12 b) g=0.43

The numerical studies reveal that for two mode and three mode lasers, an increase in the control parameter- orientation of the YAG and KTP fast axes- causes a transition from chaotic to stable behavior . The route taken in each case is different and the orientation of the laser cavity modes play an important role in determining the dynamics. Also the nature of energy transfer between the modes is affected by the orientation of YAG rod and KTP crystal.

REFERENCES

[1] Solid- state laser engineering, Walter Koechner, 3rd edition, New York, Springer Verlag (1992)

[2] Physics of Solid State Lasers, V.V.Antsiferov and G.I.Smoirnov, Cambridge International Science Publishing (2005)

[3] Introduction to laser diode pumped solid state lasers, Richard Scheps, Washington:Spie Press (2002)

[4] Lasers-Theory and Applications, K.Thyagarajan and A.K.Ghatak, Plenum Publishing Corporation, New York (1981).

[5] Lasers and Electro-optics: Fundamentals and Engineering, Christopher C.Davis, Cambridge University Press (1996)

[6] Atomic Physics of Lasers, Derek A.Eastham, Taylor & Francis Publishers (1986)

[7] T.Baer, J.Opt.Soc.Am.B. **3** (1986) 1175

[8] C.Bracikowski and Rajarshi Roy, CHAOS **1** (1991) 49

[9] C.Bracikowski and Rajarshi Roy, Phys.Rev.A. **43** (1991) 6455

[10] Thomas Kuruvilla and V.M.Nandakumaran, CHAOS **9** (1999) 208

[11] G.E.James, E.M.Harrel and R.Roy, Phys.Rev.A. **41** (1990) 2778

[12] Thomas Kuruvilla and V.M.Nandakumaran, Pramana **54** (2000) 393

CHAPTER 4

SYNCHRONIZATION AND CONTROL OF CHAOS IN COUPLED CHAOTIC MULTIMODE Nd: YAG LASERS

In this chapter we numerically investigate the dynamics of a system of two coupled chaotic multimode Nd: YAG lasers with two mode and three mode outputs. Unidirectional and bidirectional coupling schemes are adopted; intensity time series plots, phase space plots and synchronization plots are used for studying the dynamics. Quality of synchronization is measured using correlation index plots. It is found that for lasers with two mode output, bidirectional direct coupling scheme is found to be effective in achieving complete synchronization, control of chaos and amplification in output intensity. For lasers with three mode output, bidirectional difference coupling scheme gives much better chaotic synchronization as compared to unidirectional difference coupling but at the cost of higher coupling strength. We also conclude that the coupling scheme and system properties play an important role in determining the type of synchronization exhibited by the system.

4.1 INTRODUCTION

Study of coupled chaotic systems, especially their synchronization properties has been an area of intense research for the last few decades. This phenomenon has found many applications in laser dynamics [1-4], electronic circuits [5, 6], chemical and biological systems [7, 8] and secure communication [9, 10]. Dynamics of an array of coupled systems has also been studied for coupled maps [11-13], coupled semi conductor lasers [14], neural networks [15] and in the Josephson junction [16]. Many studies of coupled lasers have been motivated by the requirement of high power coherent sources. Intracavity doubled continuous wave infrared lasers have been identified as efficient source of coherent visible light. The development of high power laser diode arrays which provide a long lived, highly efficient pump source for the Nd: YAG laser and the availability of doubling crystals with large non linear coefficients have permitted the development of cw visible sources with electrical efficiencies approaching 1%. These systems are one of the most efficient sources of cw coherent light in this portion of the visible spectrum [17]

Nd: YAG laser with intracavity KTP crystal is a system of special interest as the crystal can introduce periodic as well as chaotic fluctuations in the laser output. Baer developed a deterministic rate equation model and explained the fluctuations as the manifestation of deterministic chaos [17]. It has been shown that the laser output can be stabilized through a sequence of reverse period doubling bifurcation by varying the orientation of KTP crystal and the laser cavity [18].

Several investigations have been carried out to understand the dynamics of coupled Nd: YAG lasers. Roy and Thornburg studied the coupling of two

chaotic Nd: YAG lasers experimentally [4]. In their experiment the coupling of lasers was achieved by generating two laser beams on the same crystal so that the intracavity laser fields overlap. They have also studied the chaotic behavior of two coupled single mode Nd: YAG lasers [19]. Coupled dynamics of two chaotic Nd: YAG lasers operating in three longitudinal modes were studied to show that the system goes from chaotic state to periodic and then to steady state as the coupling strength is increased [2].

Synchronization of chaotic systems has been widely studied because of its potential applications in the area of secure communication. Chaos based communication using Lorentz oscillators, Rossler systems and electronic circuits are possible at bandwidths of several tens of kilohertz [20-30]. By using the synchronization of optical chaos the available bandwidth can be extended up to hundreds of megahertz. Information encoding and decoding was studied in semiconductor lasers [31, 32], solid state lasers [33], fiber-ring lasers [34] and in microchip lasers [35]. Quality of message encoding and decoding also depends on the choice of coupling scheme between the transmitter and the receiver laser systems. Proper selection of coupling schemes can enhance the privacy and security of communication.

Only single mode laser systems have been considered for single channel communication for the past several years. Recent studies reveal that multimode lasers can be used effectively for multichannel communication. Chaotic Nd: YAG lasers are ideal candidates for this purpose because of their inherent nonlinearity and multimode operation. Chaotic synchronization of multimode Nd:YAG lasers can be used to achieve high quality digital communication of two dimensional messages and encrypted audio transmission [36,37]. Each pair of corresponding cavity modes in a system of

coupled chaotic multimode Nd:YAG lasers can be used as a channel in optical communication [38]. To the best of our knowledge the effect of various coupling schemes on the dynamics of multimode Nd: YAG lasers and their synchronization properties have not yet been discussed in detail.

In this chapter we present the results of our numerical studies on the effect of external electronic coupling on the dynamics of two mode and three mode lasers. Direct and difference couplings are investigated separately for unidirectional and bidirectional schemes.

4.2 LASER MODEL

The model system consists of two identical Nd:YAG lasers operating in the chaotic region and starting from slightly different initial conditions. The dynamics of individual lasers are described in the previous chapter. The lasers are coupled via external electronic coupling scheme whereby the pumping of each laser is modulated according to the output intensity of the other. The rate equations for the coupled system are given by [2]

$$\begin{aligned}\tau_c \frac{dI_{k1}}{dt} &= \left(G_{k1} - \alpha - g\varepsilon I_{k1} - 2\varepsilon \sum_{j1\neq k1} \mu_{j1k1} I_{j1} \right) I_{k1} \\ \tau_f \frac{dG_{k1}}{dt} &= \gamma_1 - \left(1 + I_{k1} + \beta \sum_{j1\neq k1} I_{j1} \right) G_{k1}\end{aligned} \tag{4.1}$$

$$\begin{aligned}\tau_c \frac{dI_{k2}}{dt} &= \left(G_{k2} - \alpha - g\varepsilon I_{k2} - 2\varepsilon \sum_{j2\neq k2} \mu_{j2k2} I_{j2} \right) I_{k2} \\ \tau_f \frac{dG_{k2}}{dt} &= \gamma_2 - \left(1 + I_{k2} + \beta \sum_{j2\neq k2} I_{j2} \right) G_{k2}\end{aligned} \tag{4.2}$$

A schematic diagram of the coupled system is shown in figure 4.1.

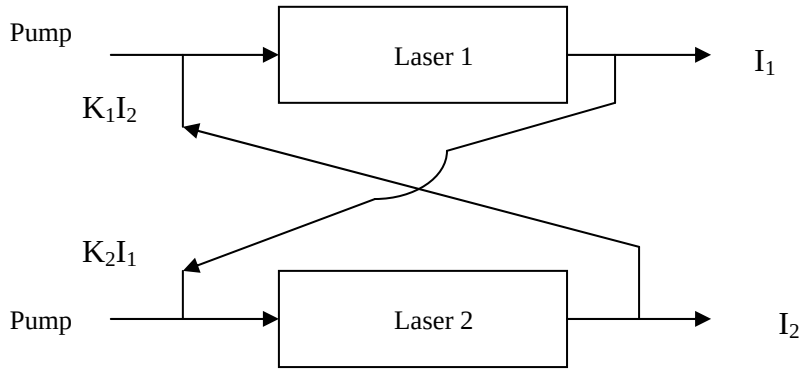

Figure 4.1: Schematic of the coupled laser system

The coupling is done by modifying the parameter γ. We have considered two types of couplings, namely direct coupling and difference coupling schemes. In the direct coupling scheme, the parameter γ of laser 2 is modulated according to the total intensity of laser 1 and vice versa.

$$\gamma_1 = \gamma_b + K_1 \sum_{k2} I_{k2}$$
$$\gamma_2 = \gamma_b + K_2 \sum_{k1} I_{k1} \qquad (4.3)$$

On the other hand, in the difference coupling scheme the parameter is modulated according to the difference in intensities of the two lasers 1 and 2.

$$\gamma_1 = \gamma_b + K_1 \sum \left(I_{k2} - I_{k1}\right)$$
$$\gamma_2 = \gamma_b + K_2 \sum \left(I_{k1} - I_{k2}\right) \qquad (4.4)$$

Here γ_b is the small signal gain (which is related to the pump rate)for the individual lasers, γ_1 and γ_2 are the pump parameters for laser 1 and laser 2 respectively, K_1 and K_2 are the coupling constants, $\sum I_{k1}$ and $\sum I_{k2}$ are the total output intensities in all the modes for laser 1 and laser 2 respectively.

4.3 NUMERICAL RESULTS AND DISCUSSION

The rate equations (4.1) and (4.2) are numerically integrated using Runge-Kutta fourth order method with a nanosecond step size. Intensity time series plots, phase space plots and synchronization plots are used for studying the dynamics. Quality of synchronization is measured using correlation index plots.

4.3.1 DYNAMICS OF THE SYSTEM UNDER UNIDIRECTIONAL COUPLING

Here the coupling constants are set as $K_1=0$ and $K_2=K$ such that laser 1 is coupled to laser 2 and there is no backward coupling. We have investigated the system dynamics under direct and difference coupling schemes for lasers with two mode and three mode output.

4.3.1.1 TWO MODE CASE WITH UNIDIRECTIONAL COUPLING

In this section we present the dynamics of two coupled Nd: YAG lasers each operating in two orthogonal longitudinal modes with unidirectional coupling between them. First we investigate the dynamics of the system under direct coupling scheme. Figure 4.2a shows the time series for the total intensities for the lasers 1 and 2 for the coupling strength K=0.002. It is seen that there is amplification in the output intensity of laser 2 as the coupling strength is

increased. Figure 4.2b shows the time series for the total intensities for the lasers 1 and 2 for K=0.8. Figure 4.3a and 4.3b show the corresponding synchronization plots.

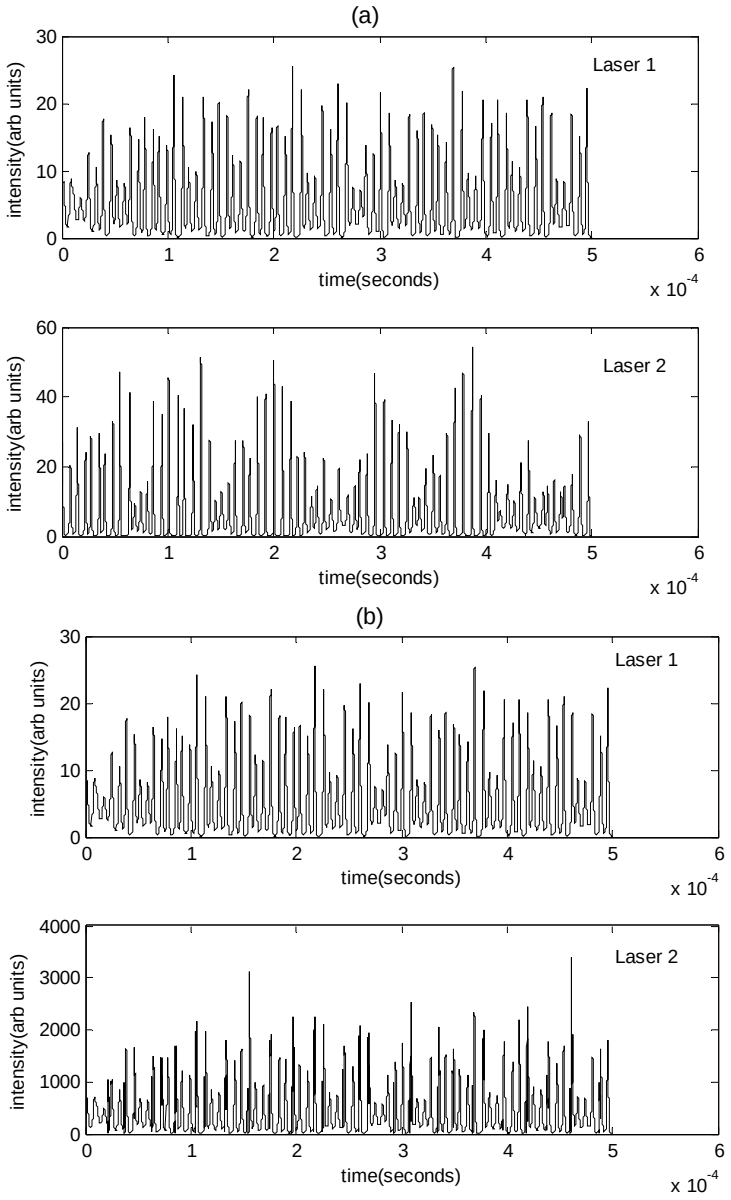

Figure 4.2: Intensity time series plots for laser 1 and 2 for a) K=0.002 b) K=0.8

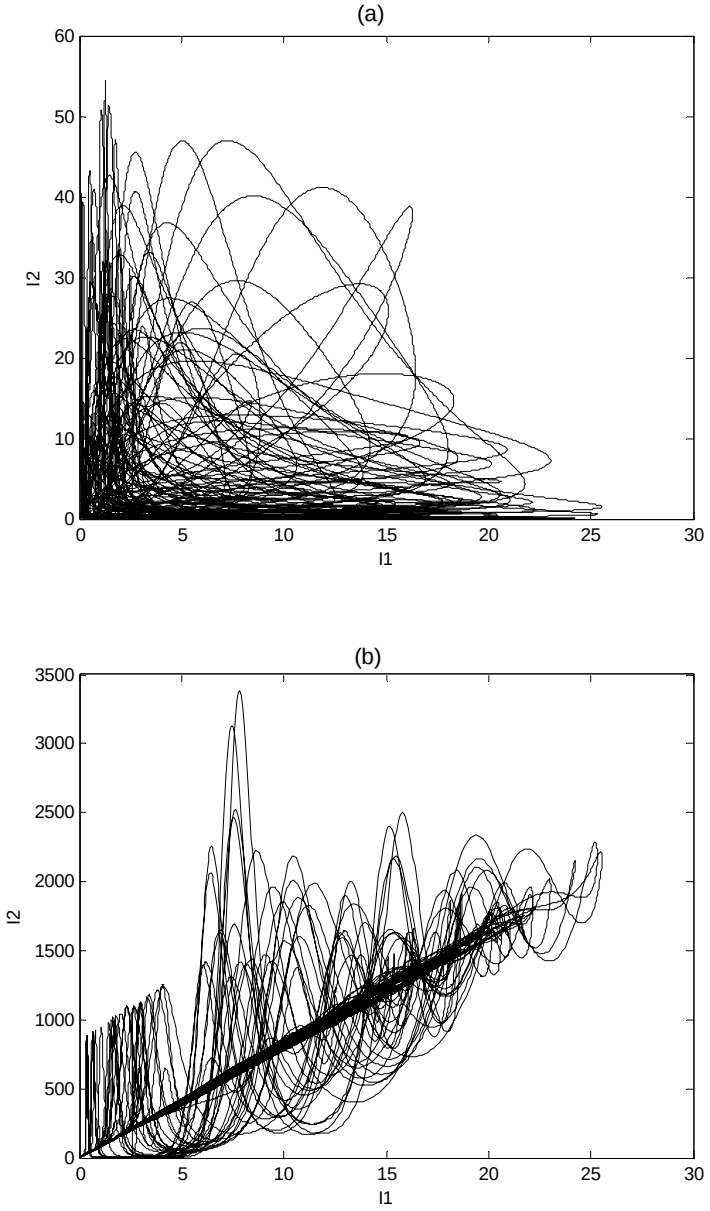

Figure 4.3: Synchronization plots for laser 1 and 2 for a) K=0.002 b) K=0.8

At higher coupling strength (K=1) the two lasers achieve phase synchronization. The intensity time series plot and synchronization plot

corresponding to this coupling strength is given in figure 4.4 and figure 4.5 respectively.

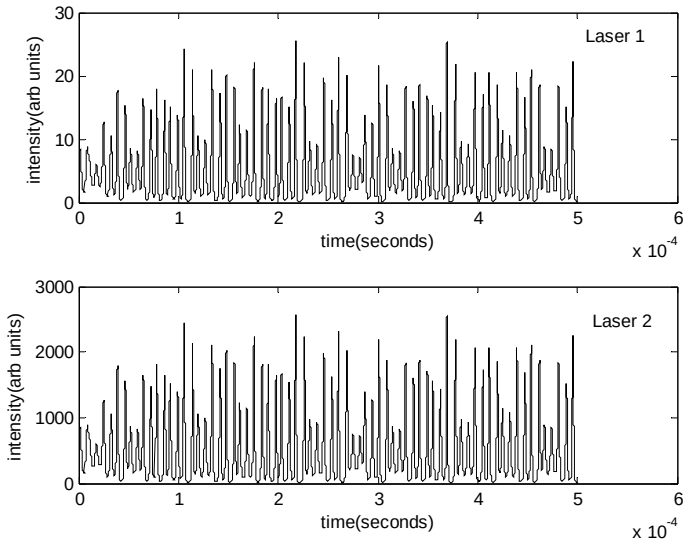

Figure 4.4: Intensity time series plot for the lasers 1 and 2 for K=1

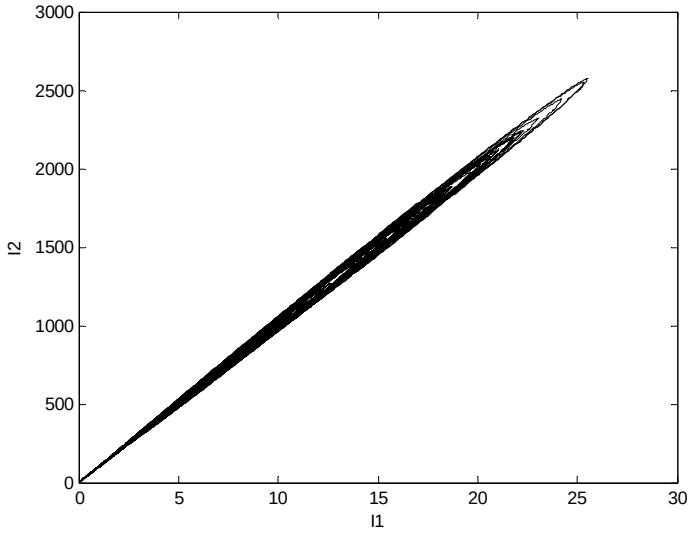

Figure 4.5: Synchronization plot for lasers 1 and 2 for K=1

The phase of the chaotic time series is calculated using the method of Hilbert Transform [40]. In order to estimate the phase function φ (t) corresponding to a time series z (t) we take Hilbert transform of z (t) to obtain

$$\tilde{z}(t) = P.V\left[\frac{1}{\Pi}\int_{-\infty}^{+\infty}\frac{z(t')}{t-t'}dt'\right] \qquad (4.5)$$

where P.V. is the Cauchy principal value for the integral. Now an analytical signal is constructed to yield an amplitude function A (t) and a phase function φ (t) which is given by

$$\psi(t) = z(t) + i\tilde{z}(t) = A(t)e^{i\varphi(t)} \qquad (4.6)$$

In order to show the phase synchronization we calculate the similarity function defined by [41]

$$S(\tau) = \sqrt{\frac{\left\langle [x_2(t+\tau) - x_1(t)]^2 \right\rangle}{\left[\left\langle x_1^{\,2}(t)\right\rangle \left\langle x_2^{\,2}(t)\right\rangle\right]^{1/2}}} \qquad (4.7)$$

where x (t) could either be the phase or intensity of the laser output

For values of the coupling increasing from zero in small steps the similarity function for both phase and intensity are determined. Figure 4.6 shows the variation of similarity function for intensity and phase with respect to increase in coupling strength. It is seen from the figure that for a large range

of values of the coupling strengths the similarity function for the phase show very low values indicating the existence of phase synchronization in the system. The synchronization of intensities is not so pronounced for lower coupling strengths.

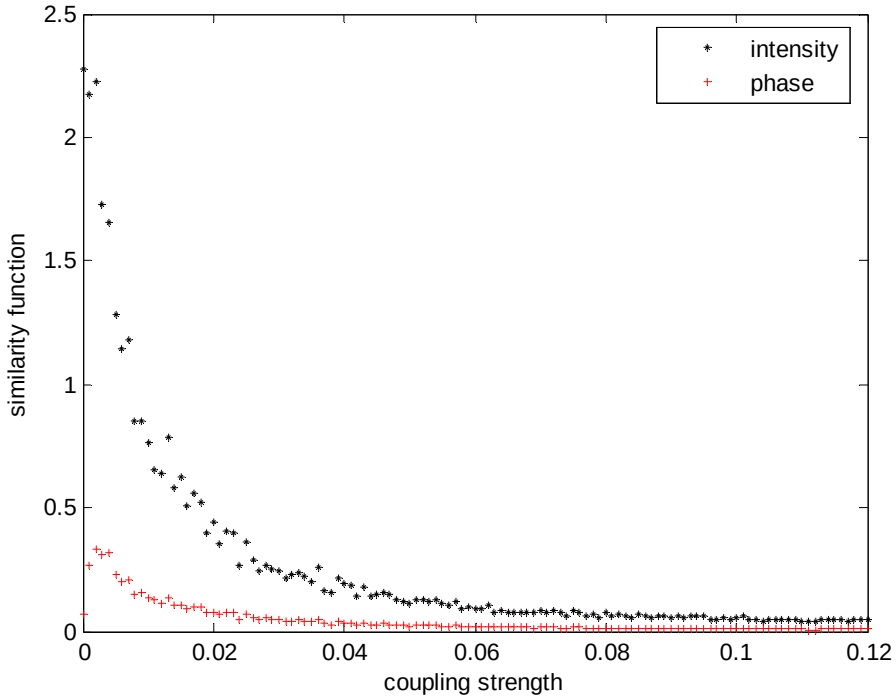

Figure 4.6: Similarity function Vs coupling strength for both phase and intensity under unidirectional direct coupling scheme.

In the case of difference coupling there is no synchronization. However, amplification of the signal is present in this case also. Figure 4.7a shows the intensity time series plots of laser 1 and 2 for the coupling strength K=0.002. Amplification present is clear from the time series plots in Figure 4.7b for the coupling strength K=0.006.

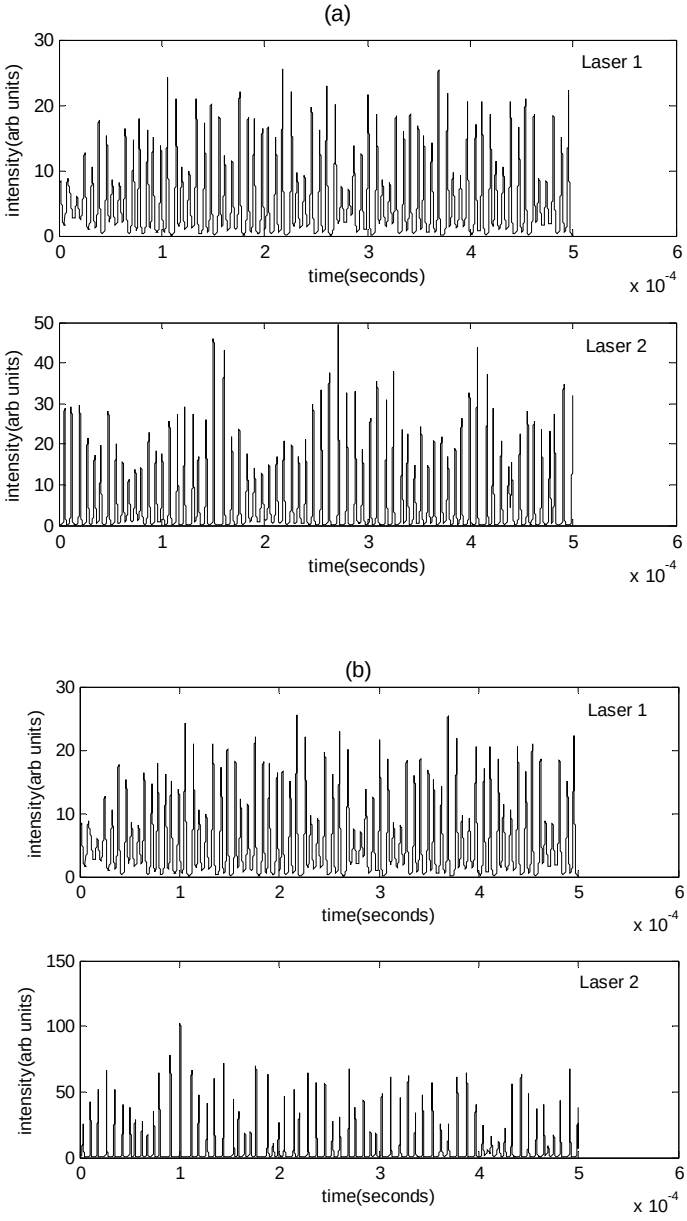

Figure 4.7: Intensity time series plots for lasers 1 and 2 for a) K=0.002 b) K=0.006

Corresponding synchronization plots are given in figure 4.8. Inspite of the high coupling strength the lasers remain unsynchronized.

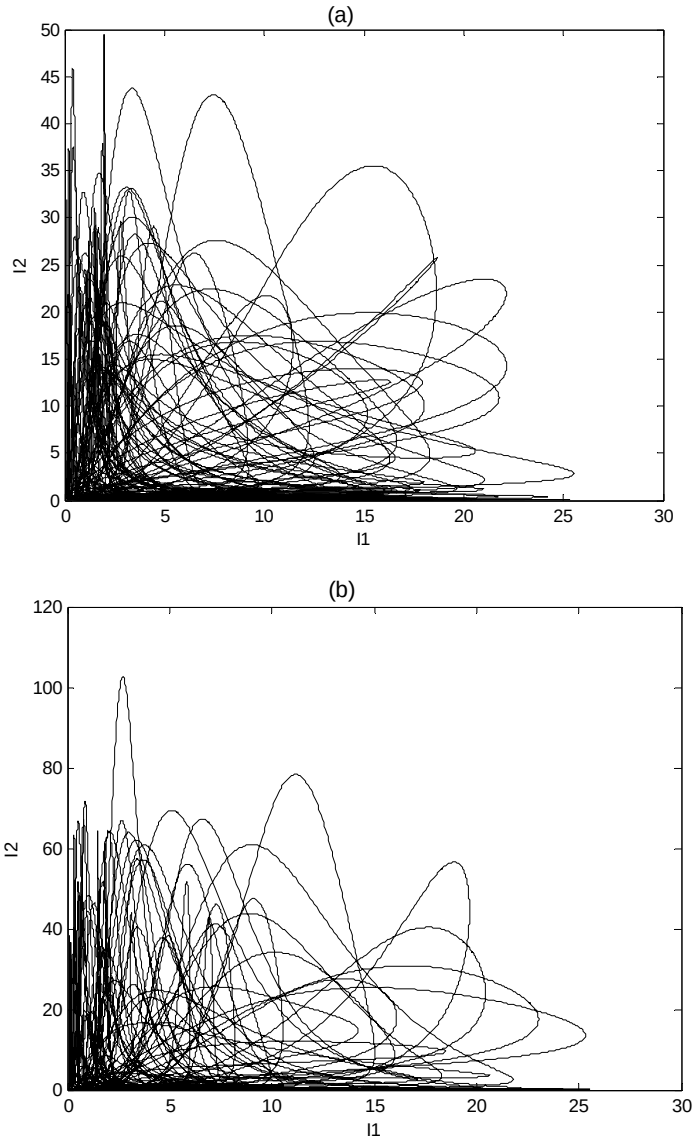

Figure 4.8: Synchronization plots for lasers 1 and 2 for a) K=0.002 b) K=0.006

4.3.1.2 THREE MODE CASE WITH UNIDIRECTINAL COUPLING

Here we consider two coupled Nd: YAG lasers each operating in three longitudinal modes, two of which are polarized parallel to each other while the third mode is polarized in the orthogonal direction. When direct coupling is employed, the system shows amplification of the output intensity of the second laser as in the two mode case, but does not show any tendency to get synchronized. However, when the difference coupling scheme is used, the system shows a tendency towards synchronization. Figure 4.9 show the synchronization plots for various coupling strengths.

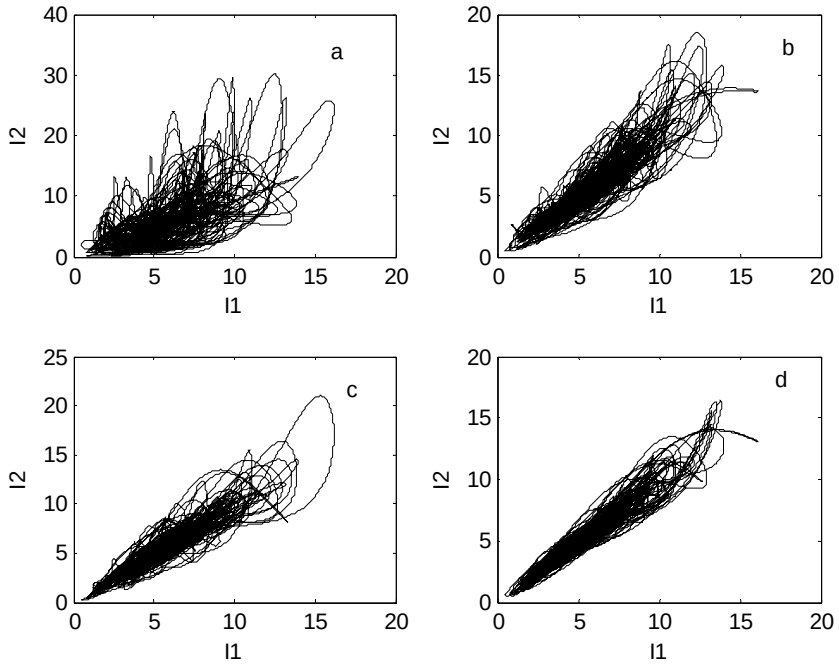

Figure 4.9: Synchronization plots for the coupled lasers for various coupling strengths a) K= 0.02 b) K=0.04 c) K=0.05 d) K=0.055

The quality of synchronization is determined by the correlation index defined by [42]

$$\rho = \frac{\left\langle \left[x(t) - \langle x(t) \rangle \right] \left[y(t) - \langle y(t) \rangle \right] \right\rangle}{\sqrt{\left\langle \left| x(t) - \langle x(t) \rangle \right|^2 \right\rangle} \sqrt{\left\langle \left| y(t) - \langle y(t) \rangle \right|^2 \right\rangle}} \qquad (4.8)$$

where x (t) could either be the phase or intensity of the laser output.

In Figure 4.10 we plot correlation index, as a function of coupling strength. The maximum value of ρ obtained is 0.9710 corresponding to a coupling strength of 0.055.

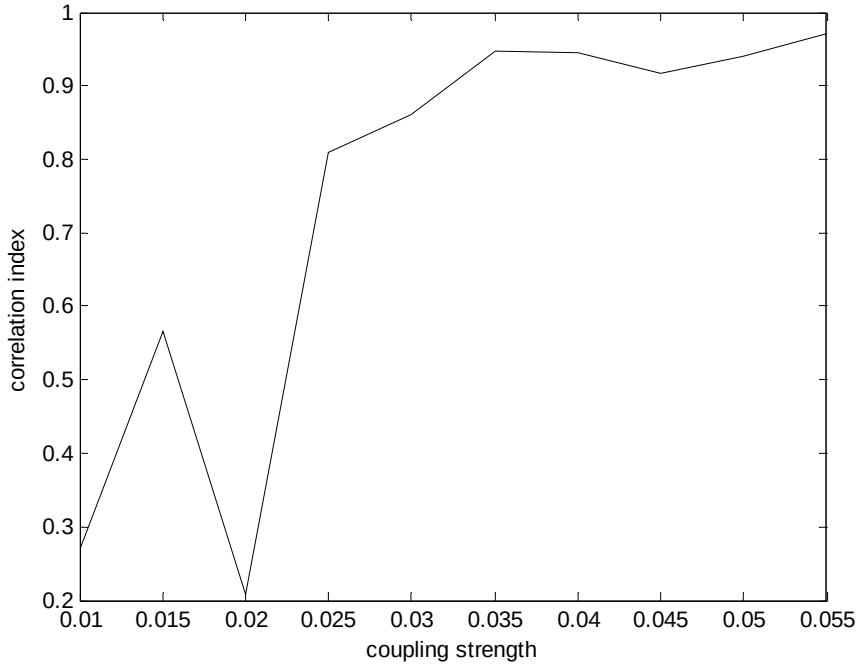

Figure 4.10: Correlation index Vs coupling strength under unidirectional difference coupling scheme

4.3.2 DYNAMICS OF THE SYSTEM UNDER BIDIRECTIONAL COUPLING

The coupling constants are set as $K_1=K_2=K$ so that laser 1 is coupled to laser 2 and vice versa. Here also we give the results of both direct and difference coupling schemes for lasers with two mode and three mode output.

4.3.2.1 TWO MODE CASE WITH BIDIRECTIONAL COUPLING

Dynamics of two coupled Nd: YAG lasers each operating in two orthogonal longitudinal modes with bidirectional coupling between them is studied. Under direct coupling scheme the two lasers remain chaotic up to K=0.0072 after which they begin to be periodic. The two lasers exhibit period 1 oscillations in their output at K=0.008. Even though the lasers exhibit periodic behavior above 0.0072, they are not synchronized. The two lasers get synchronized only at K=0.008. We can also see an amplification in output intensity of both the lasers at K=0.008. After K=0.008, even though synchronization is lost for some values of coupling strength, for higher values of coupling strength they again get synchronized. Figure 4.11 show the intensity time series plots for the lasers for various coupling strengths. The corresponding phase space plots are given in figure 4.12.

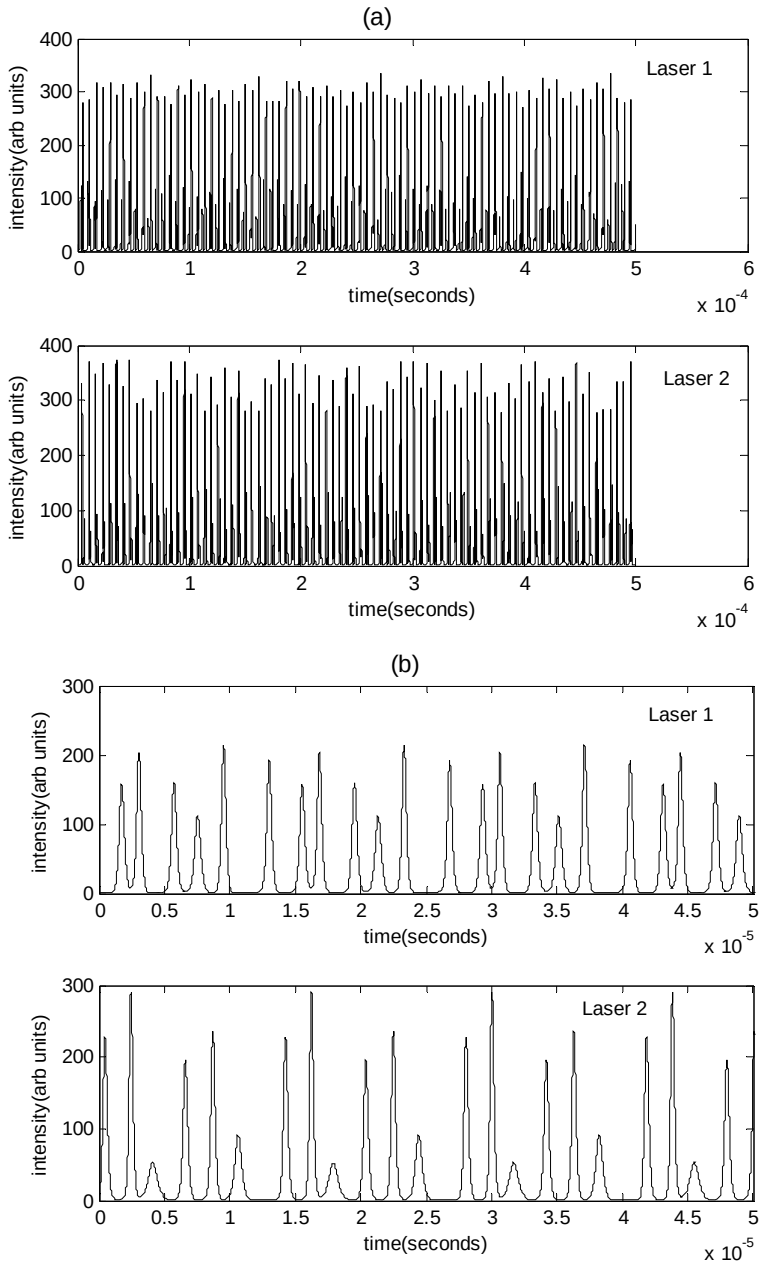

Figure 4.11: Intensity time series plots for lasers 1 and 2 for a) K=0.0072 b) K=0.0075

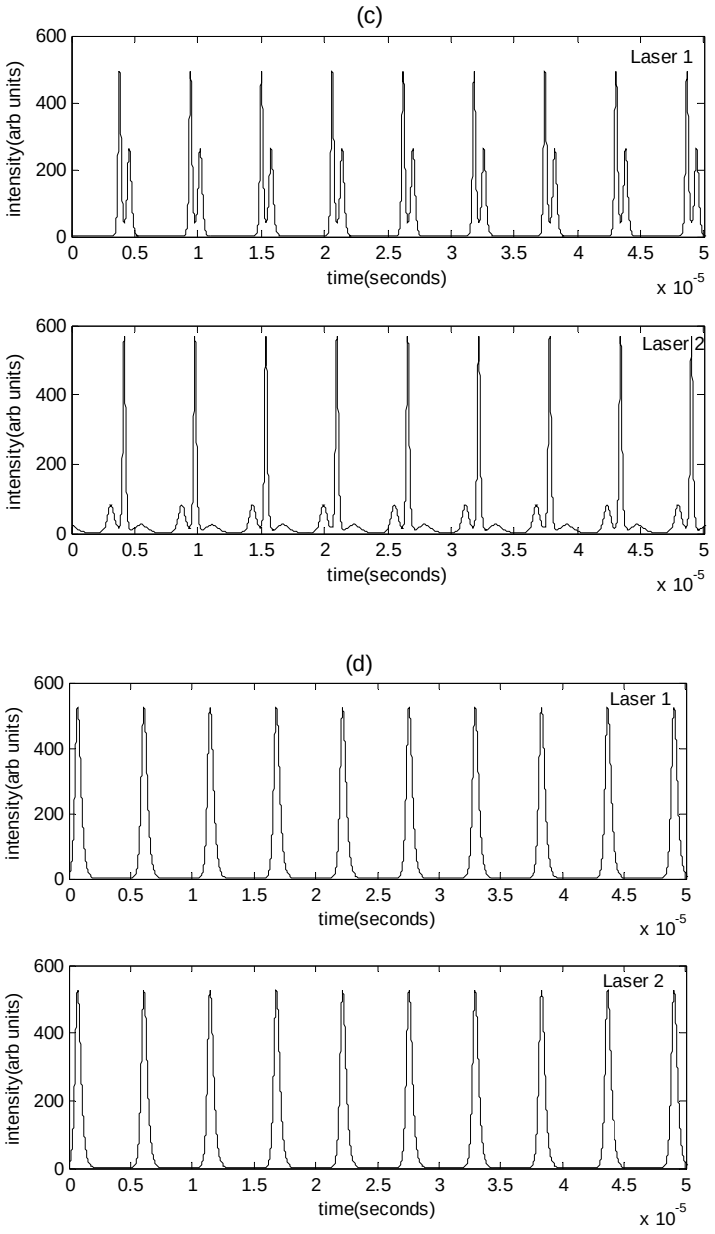

Figure 4.11: Intensity time series plots for lasers 1 and 2 for c) K=0.0077 d) K=0.008

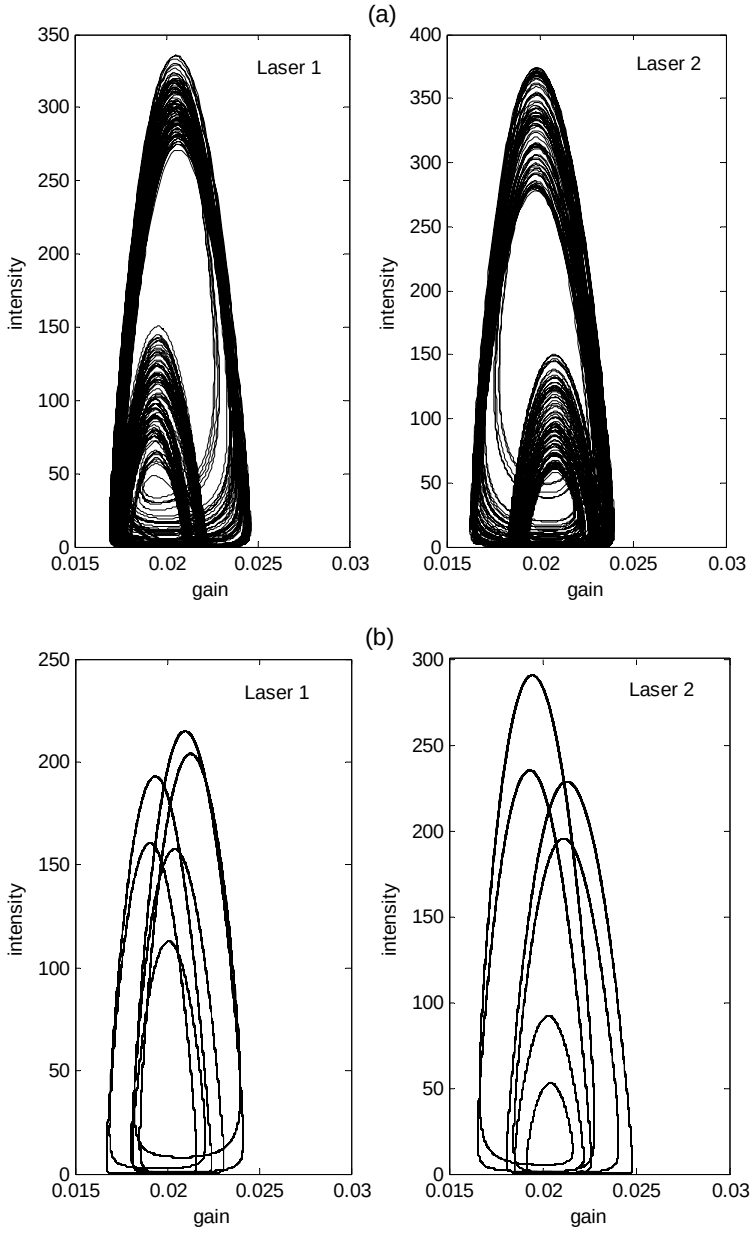

Figure 4.12: Phase space plots for lasers 1 and 2 for a) K=0.0072 b) K=0.0075

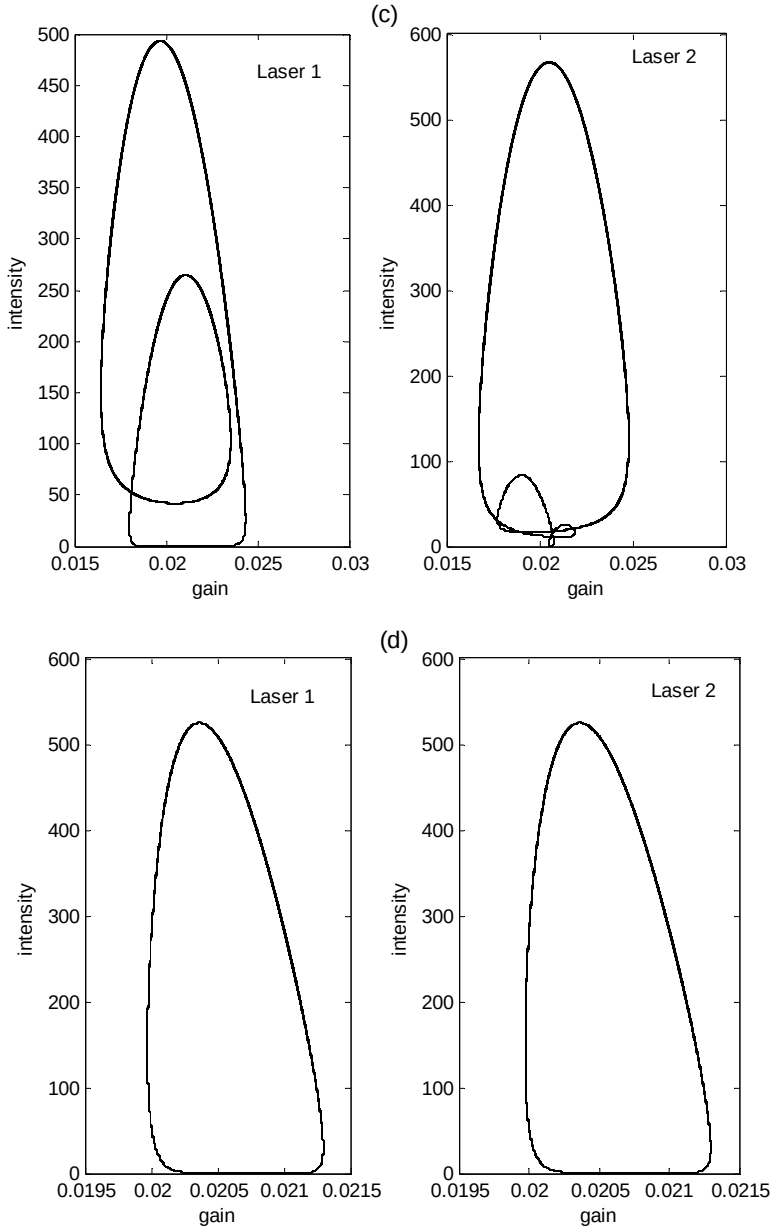

Figure 4.12: Phase space plots for lasers 1 and 2 for c) K=0.0077 d) K=0.008

The synchronization plot corresponding to K=0.008 is given in figure 4.13.

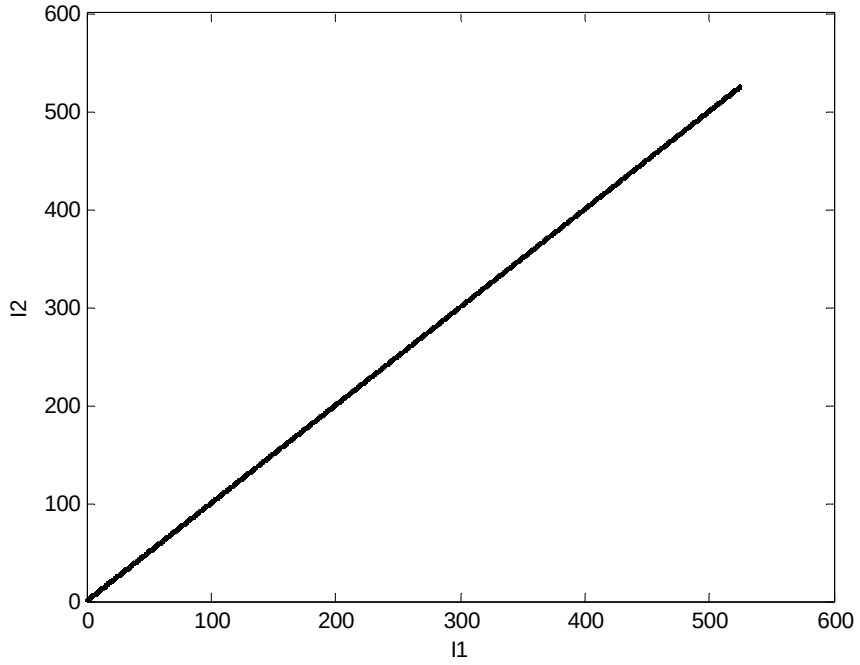

Figure 4.13: Synchronization plot for lasers 1 and 2 for K=0.008

In figure 4.14 we plot the correlation index ρ as a function of coupling strength. ρ is close to 1 for coupling strengths between 0.008 and 0.01.

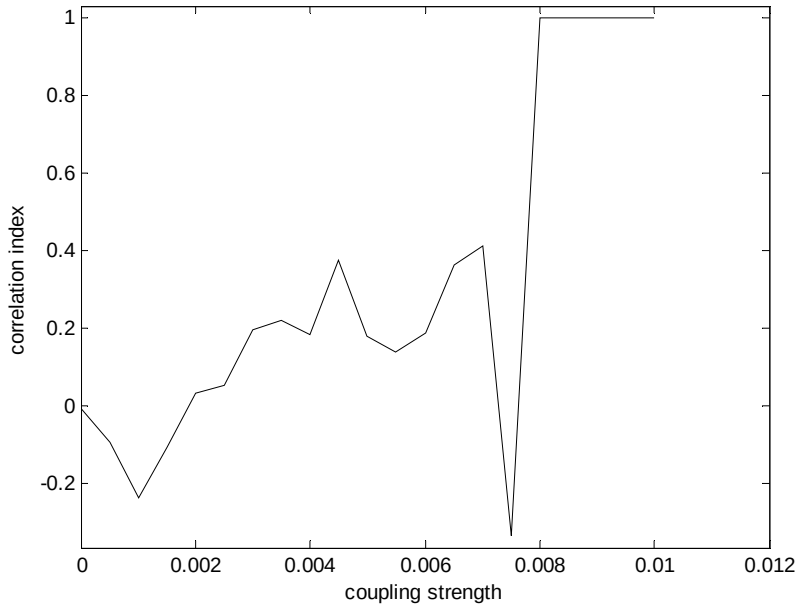

Figure 4.14: Correlation index Vs coupling strength under bidirectional direct coupling

However when we use difference coupling the outputs are neither stabilized nor synchronized.

4.3.2.2 THREE MODE CASE WITH BIDIRECTIONAL COUPLING

Here we consider two Nd: YAG lasers each operating in three longitudinal modes, two of which are polarized parallel to each other while the third mode is polarized in the orthogonal direction. It has been proved earlier that the lasers can be stabilized through direct coupling scheme and thus control chaos [2]. When the difference coupling scheme is used, it is seen that both the lasers remain chaotic throughout the entire range of coupling strengths. Though we can not control chaos using this scheme it is found to be effective in synchronizing the lasers. The quality of synchronization is better as

compared to unidirectional scheme. The synchronization plots for various coupling strengths are shown in figure 4.15.

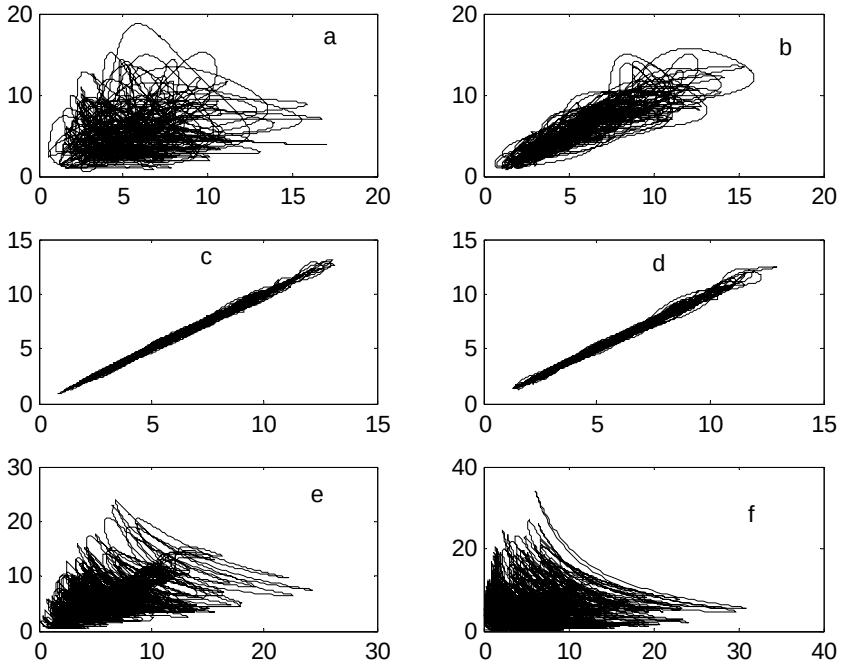

Figure 4.15: Synchronization plots of two, coupled three mode chaotic lasers for various coupling strengths under bidirectional difference coupling scheme.a) K=0.004 b) K=0.02 c) K=0.085 d) K=0.101 e) K=0.102 f) K=0.105

Here also the correlation index is calculated for various values of coupling strength and is plotted in figure 4.16. Correlation index increases with the coupling strength initially, reaches a maximum at the coupling strength 0.101 and decreases steeply for higher values of couplings. Maximum value of the correlation index obtained is 0.9987 corresponding to the coupling strength

0.101. The sharp decrease in correlation index for higher values of couplings indicates the loss of synchronization in that region.

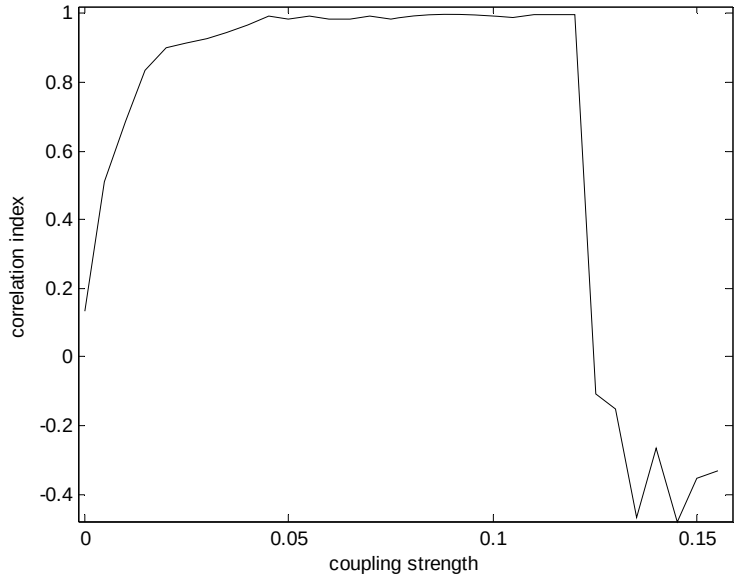

Figure 4.16: Correlation index Vs coupling strength under bidirectional difference coupling

4.4 CONCLUSIONS

Dynamics of a system of two coupled chaotic multimode Nd: YAG lasers having two mode and three mode outputs was studied numerically. The lasers were coupled using external electronic coupling in which the pumping of each laser is modulated according to the output intensity of the other. Both bidirectional and unidirectional coupling strategies are employed. Intensity time series plots, phase space plots and synchronization plots are used to study the individual dynamics and synchronization properties [44].

We have found that for a system of coupled Nd: YAG lasers operating in two modes, complete synchronization between the lasers can be achieved using bidirectional direct coupling only. With this coupling scheme, we can control chaos and get amplification in output intensity of both the lasers. With bidirectional difference coupling, the lasers remain chaotic for the entire region of coupling strength. We can not observe any amplification or synchronization under this scheme. With unidirectional direct coupling, phase synchronization between the lasers can be observed at higher coupling strengths. Amplification in output intensity of second laser is also observed in this region. Unidirectional difference coupling can give the same results except that it does not lead to any type of synchronization.

For systems operating in three mode, both unidirectional and bidirectional difference coupling schemes are effective in inducing complete chaotic synchronization between the lasers. Much better synchronization is obtained with bidirectional difference coupling, but at the cost of higher coupling strength. With bidirectional direct coupling we can control chaos [2] while unidirectional direct coupling is not efficient in controlling chaos or synchronizing the lasers.

To conclude, our results corroborate the findings that the coupling strategies and system properties play an important role in determining the dynamics and synchronization phenomena exhibited [43]. Thus a deep knowledge about the system helps us in choosing the appropriate coupling scheme that gives the desirable output.

REFERENCES

[1] V.Bindu and V.M.Nandakumaran, Phys.Lett.A. **277** (2000) 345

[2] Thomas Kuruvilla and V.M.Nandakumaran, Pramana **54** (2000) 393

[3] L.Fabiny, P.Colet and R.Roy, Phys.Rev.A. **47** (1993) 4287

[4] R.Roy and K.S.Thornburg Jr., Phys.Rev.Lett.**72** (1994) 2009

[5] V.S. Anischenko et al., Int.J.Bifurcation Chaos Appl. Sci.Eng. **2** (1992) 633

[6] J.F. Heagy, T.L. Carroll and L.M.Pecora, Phys.Rev.E. **50** (1994) 1874

[7] I.Schreiber and M.Marek, Physica D. **5** (1982) 2582

[8] S.K.Han, C.Kurrer and K.Kuramoto, Phys.Rev.Lett. **75** (1995) 3190

[9] L.Kocarev and U.Parlitz, Phys.Rev.Lett. **74** (1983) 5028

[10] V.Bindu and V.M.Nandakumaran. J. Opt. A. Pure& Appl. Opt. **4** (2002) 115

[11] S.Sinha, Phys.Rev. E. **57** (1998) 4041

[12] R.E.Amritkar, P.M Gade, A.D Gangal and V.M. Nandakumaran, Phys.Rev.A. 44 (1991) 3407

[13] K. Kaneko, Prog.Theor.Phys.**74** (1985) 1033

[14] S. Dasgupta and D.R.Anderson, J.Opt.Soc.Am.B. **11** (1994) 290

[15] M.Kavato and R.Suzuk, J.Theor.Biol. **86** (1980) 547

[16] S.Watanbe, S.H. Strogatz, H.S.J. Vander Zant and T.P.Orlando, Phys.Rev.Lett. **74** (1995) 379

[17] T.Baer, J.Opt.Soc.Am.B. **3** (1986) 1175

[18] Thomas Kuruvilla and V.M.Nandakumaran, CHAOS **9** (1999) 208

[19] K.S. Thornburg, Jr., M.Moller, Rajarshi Roy, T.W. Carr, R.D.Li, and T.Erneux, Phys.Rev. E. **55** (1997) 3865

[20] L.M.Pecora and T.L.Carroll, Phys.Rev.A. **44** (1991) 2374

[21] K.M.Cuomo and A.V. Oppenheim, Phys.Rev.Lett.**71** (1993) 65

[22] K.Murali and M.Lakshmanan, Phys.Rev.E. **48** (1993) R1624

[23] S.Hayes, C.Grebogi and E.Ott, Phys.Rev.Lett.**70** (1993) 3031

[24] G.Perez and H.A.Cerdeira, Phys.Rev.Lett. **74** (1995) 1970

[25] L.Kocarev and U. Parlitz, Phys.Rev.Lett. **74** (1995) 5028

[26] U. Parlitz, L.Kocarev, T.Stojanovski and H.Preckel, Phys.Rev.E. **53** (1996) 4351

[27] B.Mensour and A.Longtin, Phys.Lett.A. **244** (1998) 59

[28] Y.Zhang, M.Dai, Y.Hua, W.Ni and G.Du, Phys.Rev.E. **58** (1998) 3022

[29] J.M. Gonzalez- Miranda, Phys.Lett.A. **251** (1999)115

[30] O.Morgul and M.Feki, Phys.Lett.A. **251** (1999) 169

[31] C.R. Mirasso, P.Colet and P.Gracia-Fernandez, Phot.Tech.Lett. **8** (1996) 99

[32] A.Sanchez-Diaz, C.Mirasso, P.Colet and P.Gracia-Fernandez, IEEE J.Quan.Elec. **35** (1999) 292

[33] P.Colet and R.Roy, Opt.Lett. **19** (1994) 2056

[34] G.D.Van Wiggeren and R.Roy, Science **279** (1998) 1198

[35] A.Uchida, M.Shinozuka, T.Ogawa and F.Kannari, Opt.Lett. **24** (1999) 890

[36] Zhou Yun, Wu Liang and Zhu Shi-Qun, Chinese Phys. **14** (2005) 2196

[37] R.M.Lopez-Gutierrez, C.Cruz-Hernadez, C.Posadas- Castillo and E.E.Garcia- Guerrero, PROCEEDINGS OF WORLD ACADEMY OF SCIENCE, ENGINERING AND TECHNOLOGY, **30** (2008) 1032

[38] Liang Wu and Shiqun Zhu, Phys.Lett.A. **308** (2003) 157

[39] C.Bracikowski and Rajarshi Roy, CHAOS **1** (1991) 49

[40] Tolga Yalcinkaya and Ying- Cheng Lai, Phys.Rev.Lett. **79** (1997) 3885

[41] Michael G.Rosenblum, Arkady S.Pikovsky and Jurgen Kurths, Phys.Rev.Lett. **78** (1997) 4193

[42] S.Tang, H.F.Chen, S.K.Hwang and J.M.Liu, IEEE.Trans.Circuits Syst. **49** (2002) 163

[43] Shuguang Guan, Kun Li and C.H. Lai, CHAOS **16** (2006) 023107

[44] M.R.Parvathi,Bindu M.Krishna, S.Rajesh, M.P.John and V.M.Nandakumaran, Phys.Lett.A. **373** (2008) 96

CHAPTER 5

HOPF BIFURCATION IN PARALLEL POLARIZED Nd: YAG LASER

In this chapter we investigate analytically and numerically the dynamics of Nd: YAG laser with intracavity KTP crystal operating in two parallel polarized modes. System equilibrium points were found out and the stability of each of them was checked using Routh Hurwitz criteria and also by calculating the eigen values of the Jacobian. It is found that the system possesses three equilibrium points for (I_j, G_j) where j=1, 2.One of these equilibrium points undergoes Hopf bifurcation in output dynamics as the control parameter is increased. The other two remain unstable throughout the entire region of the parameter space. Our numerical analysis of the Hopf bifurcation phenomena is found to be in good agreement with the analytical results. Nature of energy transfer between the two modes is also studied numerically.

5.1 INTRODUCTION

Laser systems have been studied extensively over the last several years because of the rich variety of dynamics they exhibit. A lot of research has been carried out to study the chaotic fluctuations in the output dynamics of laser systems. Among them instabilities in multimode solid state lasers were of special interest. Intracavity doubled continuous wave infrared lasers are efficient sources of coherent visible light. Nd: YAG lasers can be developed as cw visible sources using high power laser diode arrays for pumping and also doubling crystals with large nonlinear gain coefficient. Baer [1] first reported large amplitude fluctuations in this laser system. He observed that large amplitude fluctuations and longitudinal mode instabilities arise in the output of diode pumped Nd: YAG laser in the presence of an intracavity doubling crystal. Coupling of various longitudinal modes of the laser by sum frequency generation was found to be the origin of these instabilities. He developed a deterministic rate equation model to explain these fluctuations. Using this model he was able to predict the dependence of these fluctuations on the pump level, the nonlinear coupling constant and the number of oscillating modes.

A detailed analysis of the periodic and the chaotic fluctuations in the output intensity of multimode solid state laser was carried out by Bracikowski and Rajarshi Roy [2, 3]. They studied the Nd: YAG laser with intracavity KTP crystal and obtained several interesting results. It is possible to eliminate the chaotic fluctuations in this laser and also obtain complex periodic waveforms such as antiphase states by varying the relative orientation of the YAG and

KTP crystals. They have also made a statistical study of these chaotic fluctuations.

Studies by Oka and Kubota have shown that the laser dynamics is strongly influenced by the polarizations of the cavity modes [4]. This dependence is due to the fact that the amount of green light produced by sum frequency generation depends on whether the contributing fundamental modes are polarized parallel or orthogonal to each other. It has been shown that when the laser is operating with two orthogonally polarized modes the chaotic fluctuations in the output intensity can be stabilized through a reverse period doubling bifurcation by varying a particular control parameter (relative orientation of YAG and KTP crystal). The detailed dynamics of such a laser system is given in chapter 3 [5]. Recently Czeranowsky et al studied the influence of orthogonally polarized modes on the output stability of an intracavity doubled Nd:YAG laser [6]. They reported that a high pump power or high conversion efficiency causes the laser output to become unstable through Hopf bifurcation. In this chapter we study the dynamics of Nd: YAG laser with intracavity KTP crystal operating in two parallel polarized modes analytically and numerically. It is found that the laser output exhibits Hopf bifurcation as the control parameter is varied [7]. A detailed stability analysis of the bifurcation phenomena is carried out by using Routh -Hurwitz criteria and also by calculating the eigen values of the Jacobian. Effect of change in orientation of YAG and KTP crystal on the energy transfer between the two laser cavity modes is also studied.

5.2 LASER MODEL

For numerical work we consider Nd: YAG laser with intracavity KTP crystal operating with two longitudinal modes. The modes chosen are having the same polarization states. A detailed description of the laser model is given in the previous chapter. The system can be modeled by the rate equations for the intensity I_k and gain G_k for the k^{th} longitudinal mode [2]. The parameter values are chosen as in table 3.1 given in chapter 3.

$$\tau_c \frac{dI_k}{dt} = \left(G_k - \alpha - g\varepsilon I_k - 2\varepsilon \sum_{j \neq k} \mu_{jk} I_j \right) I_k \qquad (5.1)$$

$$\tau_f \frac{dG_k}{dt} = \gamma - \left(1 + I_k + \beta \sum_{j \neq k} I_j \right) G_k \qquad (5.2)$$

As modes are having same polarization states, we choose $\mu_{jk} = g$.

5.3 RESULTS

It was proved earlier that for Nd:YAG laser operating in two orthogonally polarized modes the output intensity fluctuations change from chaotic to stable behavior through a reverse period doubling bifurcation sequence as the system control parameter (g) is continuously varied. Since there is a strong dependence of the output dynamics on the polarizations of the laser cavity modes, an entirely different dynamical behavior is expected for a laser operating in two parallel polarized modes.

The rate equations for intensity and gain (equations 5.1 and 5.2) are solved using Matlab to get analytical expressions for the solutions in terms of the control parameter g. The system fixed points are obtained by substituting different g values in these expressions. Table 5.1 gives the solutions corresponding to g=0.4.

I_1	G_1	I_2	G_2
0	0.5×10^{-1}	0	0.5×10^{-1}
0	-0.142×10^{-4}	-5004.99	-0.999×10^{-5}
0	0.131×10^{-1}	3.996	0.1×10^{-1}
-5004.99	-0.999×10^{-5}	0	-0.14×10^{-4}
3.996	0.1×10^{-1}	0	0.131×10^{-1}
12491.07	0.784×10^{-5}	-8743.57	0.424×10^{-1}
-8743.57	0.424×10^{-1}	12491.07	0.784×10^{-5}
-1669.60	0.176×10^{-4}	-1669.60	$-.176\times10^{-4}$
2.348	0.1001×10^{-1}	2.348	0.1001×10^{-1}

Table 5.1: Solutions for the laser rate equations (5.1) and (5.2) for g=0.4

It is found that the laser system has got nine fixed points as there are nine sets of solutions for (I_j, G_j) where j=1,2. Out of them only three sets are having real valued solutions:

Set I: Solution with equal values for I_1 and I_2

Set II: Solution with I_1=0

Set III: Solution with I_2=0

5.3.1 ROUTH HURWITZ STABILITY CRITERION

Routh-Hurwitz stability criterion enables [8-11] us to find the existence of positive roots in a polynomial equation without solving the equation. This criterion can be applied to polynomials with only a finite number of terms. By applying the criterion to a control system information about the absolute stability can be obtained directly from the coefficients of the characteristic equation. However Routh-Hurwitz stability criterion has limited use in linear control system analysis as it does not suggest how to improve relative stability or how to stabilize an unstable system. But it is possible to determine the effects of changing one or two parameters of a system by examining the values that cause instability.

Consider a dynamical system in drive response scheme represented by the equations

$$\begin{aligned} \dot{x} &= f(x) \\ \dot{y} &= f(y) + c(y)[h(x) - h(y)] \end{aligned} \qquad (5.3)$$

Here x and y are the state variables of the drive and response respectively. c is the coupling parameter. h(x) and h(y) are the transmitted signals. The coupling parameter is adjusted according to y so that the drive and response get synchronized asymptotically. The synchronization manifold (SM) is the subspace defined by x=y. To check the stability of the SM, we first construct the Jacobian matrix A of the dynamical system.

The characteristic polynomial of an n×n matrix A can be generally written as

$$\Gamma_A(\lambda) = \lambda^n + a_{n-1}\lambda^{n-1} + a_{n-2}\lambda^{n-2} + ... + a_0 \qquad (5.4)$$

One possible form of Hurwitz criterion states that all roots of the characteristic equation $\Gamma_A(\lambda) = 0$ have negative real part when all the north-westerly principal minors $D_1, D_2, \ldots, D_n$ of the $n \times n$ matrix D are positive, where D is given by

$$D = \begin{bmatrix} a_{n-1} & a_n & 0 & . & . & 0 \\ a_{n-3} & a_{n-2} & a_{n-1} & a_n & 0 & . \\ a_{n-5} & a_{n-4} & a_{n-3} & . & . & . \\ . & . & . & . & . & . \\ . & . & . & . & . & . \\ 0 & 0 & 0 & 0 & 0 & a_0 \end{bmatrix} \qquad (5.5)$$

For 4×4 matrix D can be written as

$$D = \begin{bmatrix} a_3 & a_4 & 0 & 0 \\ a_1 & a_2 & a_3 & a_4 \\ 0 & a_0 & a_1 & 0 \\ 0 & 0 & 0 & a_0 \end{bmatrix} \qquad (5.6)$$

The Routh Hurwitz stability conditions are

$$D_1 = a_3 > 0$$

$$D_2 = \begin{bmatrix} a_3 & a_4 \\ a_1 & a_2 \end{bmatrix} = (a_2 a_3 - a_1 a_4) > 0$$

$$D_3 = \begin{bmatrix} a_3 & a_4 & 0 \\ a_1 & a_2 & a_3 \\ 0 & a_0 & a_1 \end{bmatrix} = (a_1 a_2 a_3 - a_1^2 a_4 - a_0 a_3^2) > 0 \qquad (5.7)$$

$$D_4 = a_0(D_3) > 0$$

5.3.2 STABILITY ANALYSIS

To determine the stability of fixed points, equations 5.1 and 5.2 are linearized around the fixed points. Then we get the equation governing the evolution of any small perturbation $(\delta I_1,\ \delta G_1,\ \delta I_2,\ \delta G_2)$ around the steady state $(I_1^*,\ G_1^*,\ I_2^*,\ G_2^*)$

$$\begin{pmatrix} \dot{\delta I_1} \\ \dot{\delta G_1} \\ \dot{\delta I_2} \\ \dot{\delta G_2} \end{pmatrix} = \begin{pmatrix} A_1 & B_1 & C_1 & 0 \\ D_1 & E_1 & F_1 & 0 \\ C_2 & 0 & A_2 & B_2 \\ F_2 & 0 & D_2 & E_2 \end{pmatrix} \begin{pmatrix} \delta I_1 \\ \delta G_1 \\ \delta I_2 \\ \delta G_2 \end{pmatrix} \qquad (5.8)$$

Where

$$A_1 = \frac{G_1 - \alpha - 2\times g\times \varepsilon \times I_1 - 2\times g\times \varepsilon \times I_2}{\tau_c}$$

$$B_1 = \frac{I_1}{\tau_c}$$

$$C_1 = \frac{-2\times g\times \varepsilon \times I_1}{\tau_c}$$

$$D_1 = \frac{-G_1}{\tau_f}$$

$$E_1 = \frac{-1 - I_1 - \beta \times I_2}{\tau_f}$$

$$F_1 = \frac{-\beta \times G_1}{\tau_f}$$

$$A_2 = \frac{G_2 - \alpha - 2 \times g \times \varepsilon \times I_2 - 2 \times g \times \varepsilon \times I_1}{\tau_c}$$

$$B_2 = \frac{I_2}{\tau_c}$$

$$C_2 = \frac{-2 \times g \times \varepsilon \times I_2}{\tau_c}$$

$$D_2 = \frac{-G_2}{\tau_f}$$

$$E_2 = \frac{-1 - I_2 - \beta \times I_1}{\tau_f}$$

$$F_2 = \frac{-\beta \times G_2}{\tau_f}$$

Hence the Jacobian of the system at the steady state $\left(I_1^*, \quad G_1^*, \quad I_2^*, \quad G_2^*\right)$ is given by

$$J = \begin{pmatrix} A_1 & B_1 & C_1 & 0 \\ D_1 & E_1 & F_1 & 0 \\ C_2 & 0 & A_2 & B_2 \\ F_2 & 0 & D_2 & E_2 \end{pmatrix} \qquad (5.9)$$

The characteristic equation of the system is given as

$$\begin{vmatrix} A_1-\lambda & B_1 & C_1 & 0 \\ D_1 & E_1-\lambda & F_1 & 0 \\ C_2 & 0 & A_2-\lambda & B_2 \\ F_2 & 0 & D_2 & E_2-\lambda \end{vmatrix} = 0 \qquad (5.10)$$

where λ is the eigen value of J

Eqn (5.10) can be rewritten as

$$a_4\lambda^4 + a_3\lambda^3 + a_2\lambda^2 + a_1\lambda + a_0 = 0 \qquad (5.11)$$

where

$$a_4 = 1$$
$$a_3 = -A_1 - E_1 - E_2 - A_2$$
$$a_2 = A_1E_1 + (A_1 + E_1)(A_2 + E_2) + (A_2E_2 - B_2D_2) - B_1D_1 - C_1C_2$$
$$a_1 = C_1C_2E_1 - B_1F_1C_2 - B_2F_2C_1 + C_1C_2E_2 + (A_2 + E_2)(B_1D_1 - A_1E_1) - (A_2E_2 - B_2D_2)(A_1 + E_1)$$
$$a_0 = (A_1E_1 - B_1D_1)(A_2E_2 - B_2D_2) - B_1B_2F_1F_2 + B_1F_1C_2E_2 + C_1E_1B_2F_2 - C_1C_2E_1E_2$$

Routh Hurwitz stability conditions for our system becomes

$$a_3 > 0$$
$$(a_2a_3 - a_1) > 0$$
$$(a_1a_2a_3 - a_1^2 - a_0a_3^2) > 0 \qquad (5.12)$$
$$a_0 > 0$$

We have checked the stability of all the three sets of solutions based on this criterion.

1) Solution Set I.

The control parameter is increased and the stability conditions are checked for each case. It is found that the attractor is a stable fixed point for small g values. All the stability conditions are satisfied in this region.

At g=0.28, $\left(a_1a_2a_3 - a_1^2a_4 - a_0a_3^2\right) < 0$ which is a clear indication of the loss of stability of the fixed point. Thus the fixed point loses stability at g=0.28 and becomes a limit cycle which remains stable for higher g values. In Table 5.2 we give the value of the Routh-Hurwitz coefficients with increasing g value.

g	a_3	$(a_2a_3 - a_1) \times 10^{16}$	$(a_1a_2a_3 - a_1^2a_4 - a_0a_3^2) \times 10^{32}$	$a_0 \times 10^{23}$
0.04	65186	3.5265	4.9188	1.2271
0.08	65176	3.8485	4.6044	1.2264
0.12	65166	4.1703	4.0791	1.2256
0.16	65156	4.4918	3.3479	1.2249
0.20	65146	4.8132	2.4053	1.2241
0.24	65136	5.1314	1.2547	1.2233
0.28	65126	5.4550	-0.1052	1.2226
0.32	65116	5.7754	-1.6730	1.2218
0.36	65106	6.0956	-3.4498	1.2211
0.40	65096	6.4155	-5.4341	1.2203
0.44	65086	6.7352	-7.6271	1.2196
0.48	65076	7.0547	-10.0272	1.2188
0.52	65066	7.3738	-12.6350	1.2180

Table 5.2: Routh- Hurwitz coefficients for various g values

From the table we can see that one of the coefficients, $(a_1a_2a_3 - a_1^2a_4 - a_0a_3^2)$ changes sign at g=0.28 while all others remain positive for the entire range of g values. Figure 5.1 shows the variation of the coefficient $(a_1a_2a_3 - a_1^2a_4 - a_0a_3^2)$ with g value.

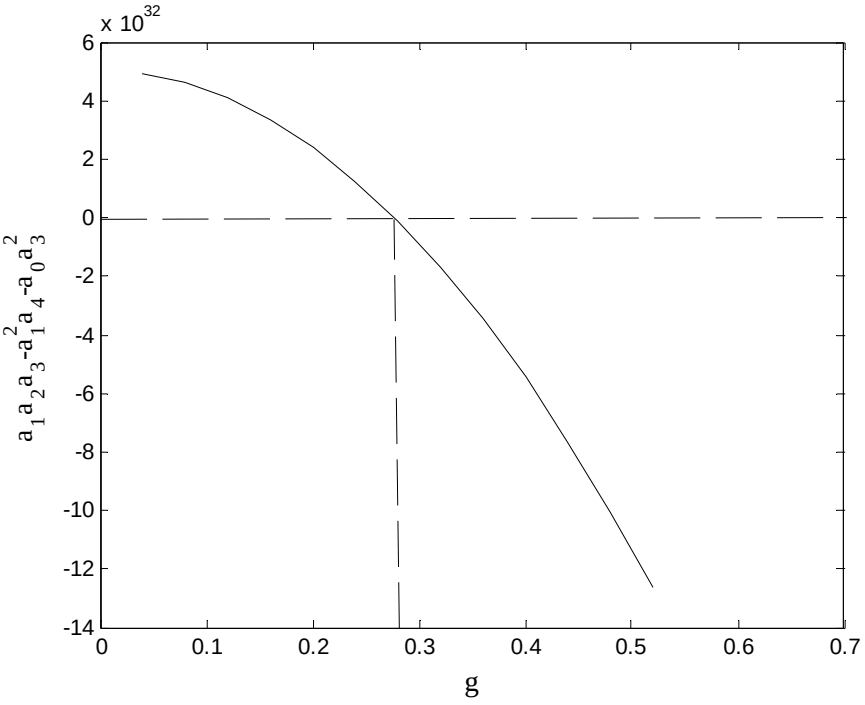

Figure 5.1: Graph showing the variation of the coefficient $(a_1a_2a_3 - a_1^2a_4 - a_0a_3^2)$ with g

We have also calculated the eigen values for the characteristic polynomial for each of the g values.

g	Real part of eigen value
0.04	-0.1394
0.08	-0.1159
0.12	-0.0924
0.16	-0.0688
0.20	-0.0453
0.24	-0.0218
0.28	0.0017
0.32	0.0252
0.36	0.0487
0.40	0.0722
0.44	0.0957
0.48	0.1192
0.52	0.1428

Table 5.3: Change in real part of eigen values with increasing g

At g=0.28 real part of two eigen values become positive which again confirms the loss of stability of the fixed point. Variation in the real part of eigen value is plotted as a function of g in figure 5.2.

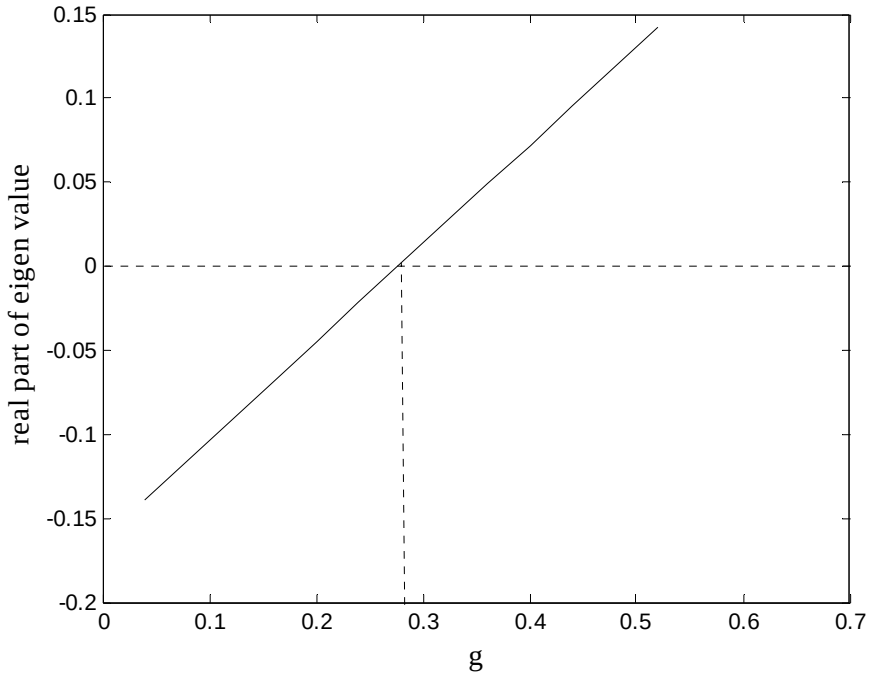

Figure 5.2: Graph showing the variation of real part of eigen value with g

This phenomenon where fixed point losses stability at a particular value of the control parameter and changes into a limit cycle is called Hopf bifurcation.

2) Solution Set II & III

Stability analysis of these fixed points is also carried out as in previous case. It is found that the two fixed points remain unstable for the

entire range of g values. Table 5.4 shows the variation of the Routh Hurwitz coefficients with g values.

g	$a_3 \times 10^7$	$(a_2 a_3 - a_1) \times 10^{19}$	$(a_1 a_2 a_3 - a_1^2 a_4 - a_0 a_3^2) \times 10^{37}$	$a_0 \times 10^{23}$
0.04	-1.5746	1.0124	-8.1486	-2.0829
0.08	-1.5715	1.1147	-9.4168	-2.0794
0.12	-1.5731	1.2105	-10.7640	-2.0821
0.16	-1.5724	1.3092	-12.0670	-2.0817
0.20	-1.5717	2.0813	-13.3650	-2.0813
0.24	-1.5718	1.5075	-14.6850	-2.0820
0.28	-1.5703	1.6042	-15.9590	-2.0805
0.32	-1.5720	1.7074	-17.3300	-2.0833
0.36	-1.5689	1.8002	-18.5440	-2.0797
0.40	-1.5681	1.8979	-19.8320	-2.0793
0.44	-1.5722	2.0077	-21.3150	-2.0852
0.48	-1.5723	2.1078	-22.6460	-2.0859
0.52	-1.5660	2.1902	-23.6870	-2.0781

Table 5.4: Routh- Hurwitz coefficients for various g values

From the table it is clear that only one coefficient remains positive while the other three remain negative for the entire range of g values which indicates the unstable nature of the solutions.

Figure 5.3 is a plot showing the variation of coefficient $(a_1 a_2 a_3 - a_1^2 a_4 - a_0 a_3^2)$ with g value for these solutions. The coefficient remains negative for the entire range of g value.

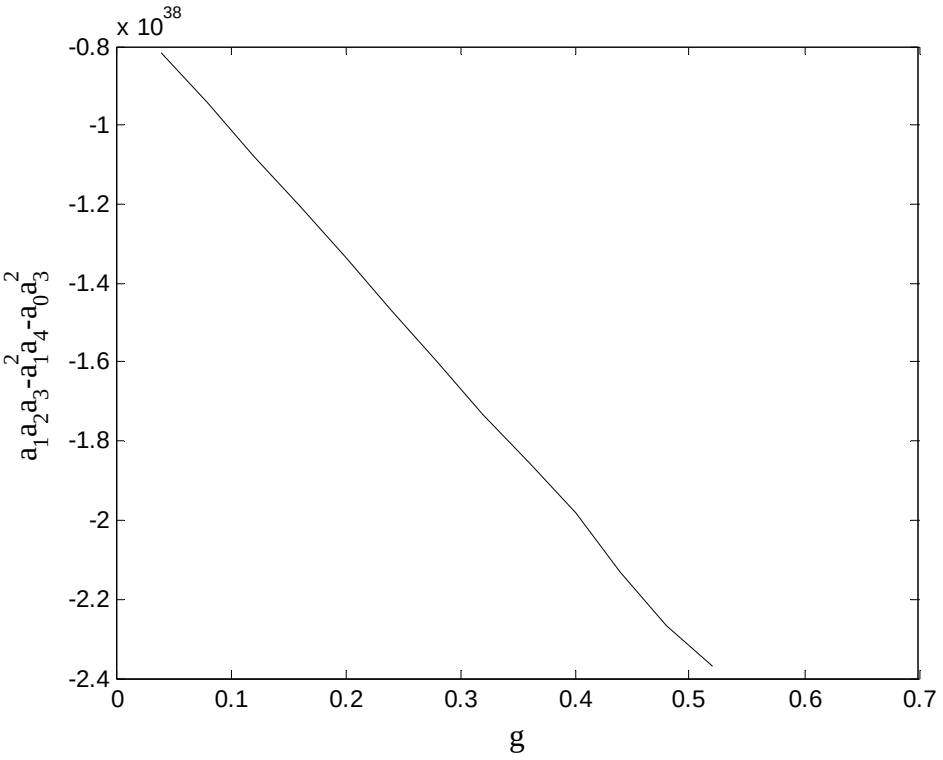

Figure 5.3: Graph showing the variation of the coefficient $(a_1a_2a_3 - a_1^2a_4 - a_0a_3^2)$ with g

Real part of eigen values is plotted as a function of g in Figure 5.4. Real part of eigen values are found to be positive for every g value which show that the solutions are Routh Hurwitz unstable.

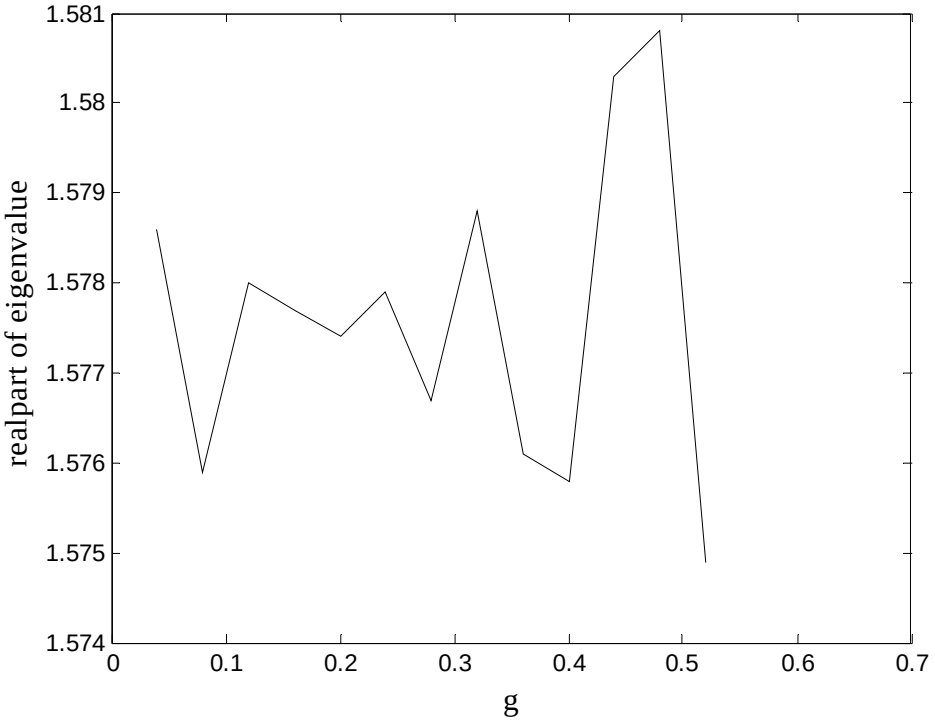

Figure 5.4: Graph showing the variation of real part of eigen value with g

5.3.3 NUMERICAL ANALYSIS

Equations (5.1) and (5.2) are integrated numerically using Runge Kutta fourth order method for different g values. Figure 5.5 shows the intensity time series plots for the laser at different g values. For g=0.08 the output intensity is found to be stable (5.5a). As the g value is increased to 0.5 we can see oscillations of constant amplitude which remains in that state for higher g values (5.5b).

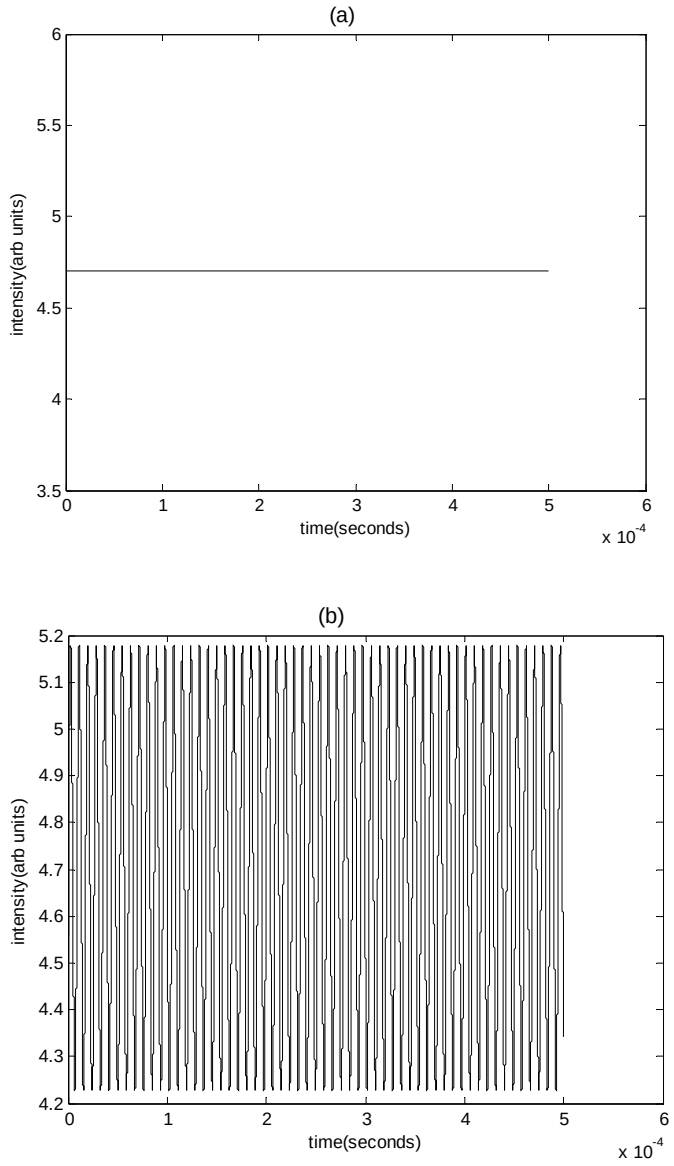

Figure 5.5: Intensity time series plot for the laser at g=0.08 (a) and at g=0.5 (b)

Figure 5.6 shows the corresponding phase space plots where the total output intensity is plotted against total gain for various g values. For g=0.08, the phase trajectory is a single spot which implies that the laser is operating in the stable mode for this g value. (5.6a). At g=0.5, the phase trajectory evolves as a clear limit cycle (5.6b).

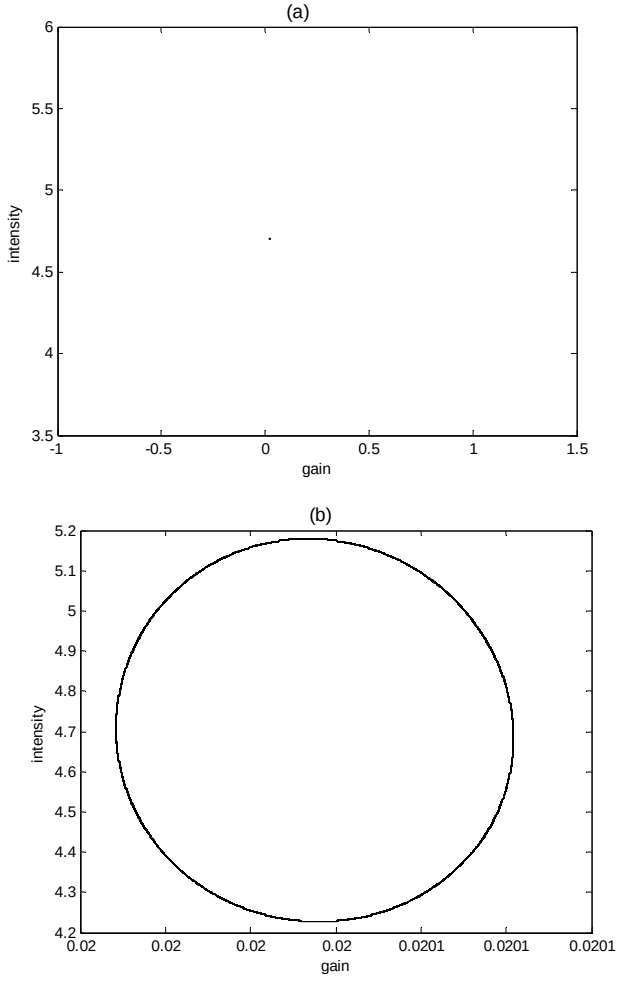

Figure 5. 6: Phase space plots for the laser at g=0.08 (a) and at g=0.5 (b)

The Hopf bifurcation phenomena is evident from the bifurcation diagram where the maxima and minima of total output intensity is plotted against the control parameter (Fig 5.7)

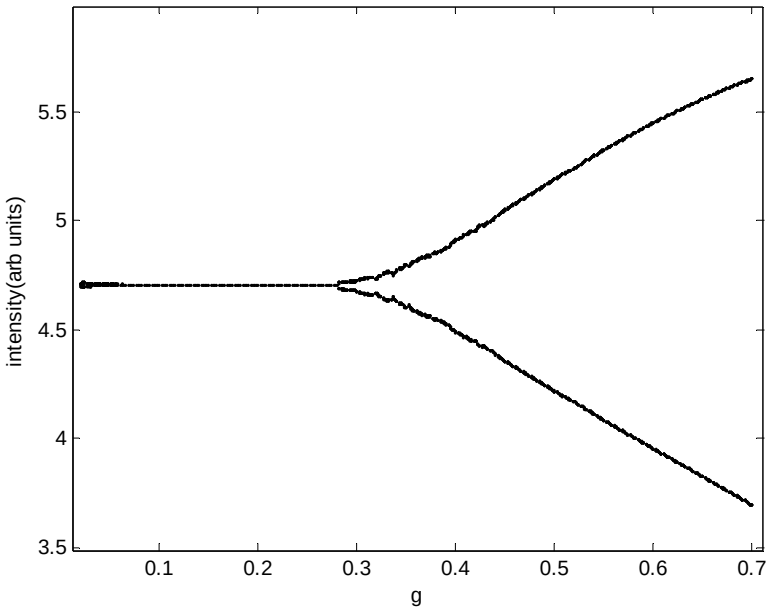

Figure 5.7: Bifurcation diagram where the maxima and minima of total output intensity is plotted as a function of the control parameter g.

We have also studied the exchange of energy between the two modes. For this the intensity in the X polarized mode is plotted against that in the Y polarized mode. Figure 5.8 shows the plots for different values of g. In the stable region for g=0.08, it is a single spot indicating that there is no exchange of energy between the modes. (5.8a). For g=0.28 and g=0.32 it is a straight line which implies that a linear relationship exists between the energy of two modes in this region. (5.8b and 5.8c). It also shows that the total energy of two modes remain a constant in this region. As the g value is

increased it changes into a closed loop (corresponding to the limit cycle region) indicating a periodic exchange of energy between the two modes. (5.8d and 5.8e)

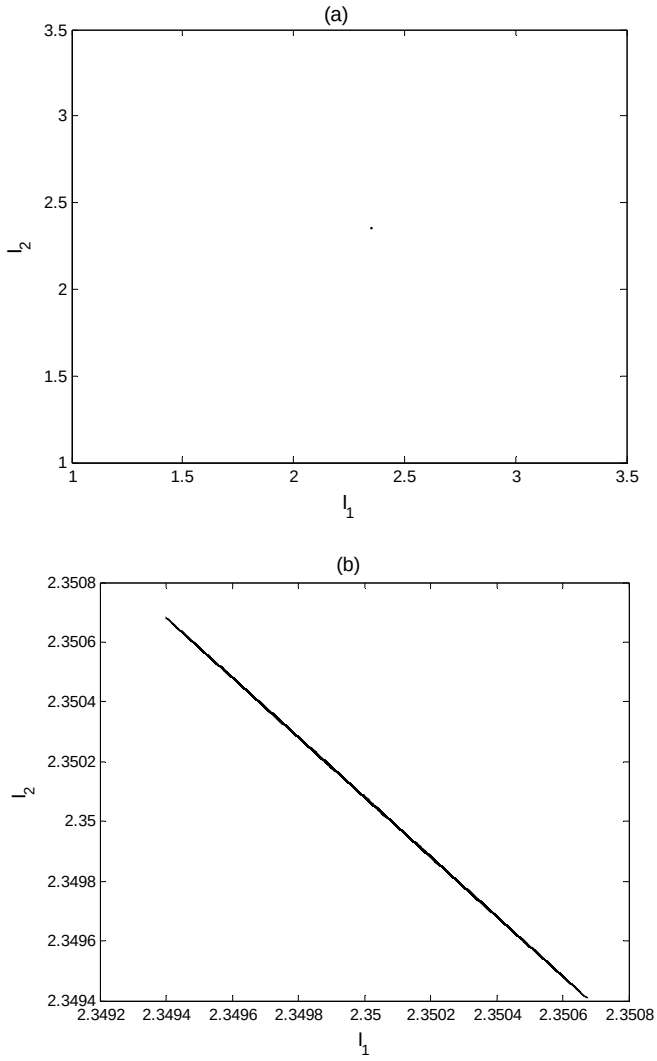

Figure 5.8: Intensity of X polarized mode plotted against that in the Y polarized mode for g=0.08 (a); g=0.28 (b)

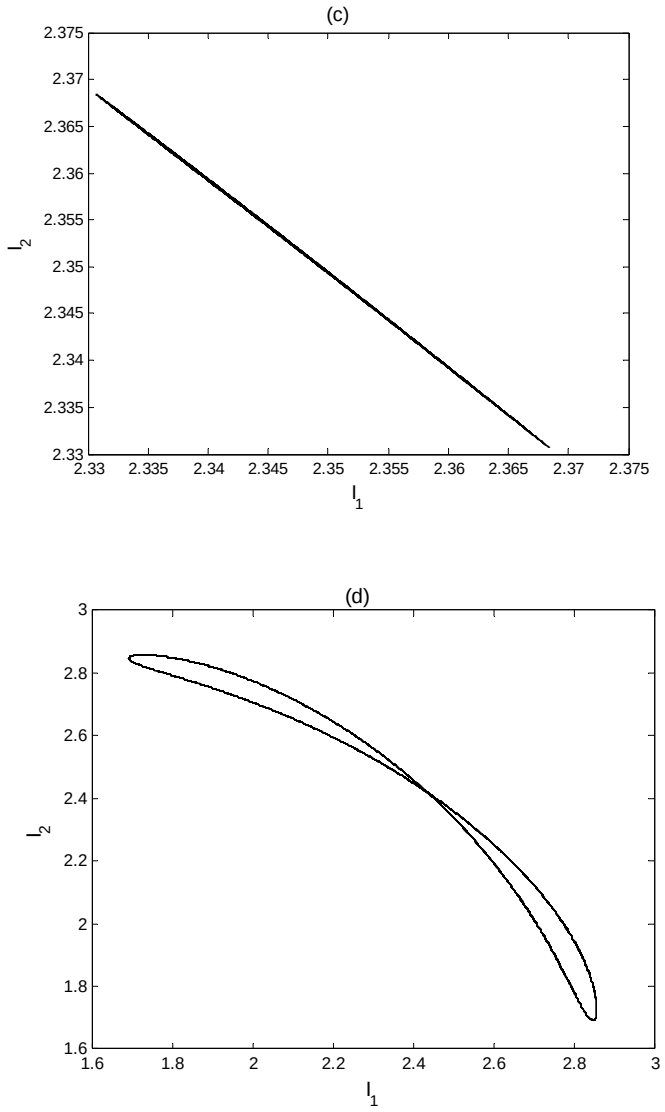

Figure 5.8: Intensity of X polarized mode plotted against that in the Y polarized mode for g=0.32 (c); g=0.4 (d)

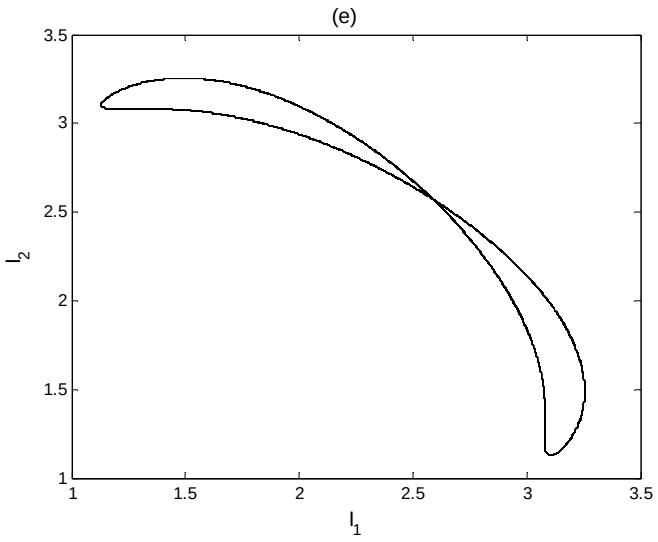

Figure 5.8: Intensity of X polarized mode plotted against that in the Y polarized mode for g=0.5 (e).

5.4 CONCLUSIONS

Nonlinear dynamics of Nd: YAG laser with intracavity KTP crystal operating with two parallel polarized modes is studied. System equilibrium points were found out analytically. It was found that the system possesses three equilibrium points. The stability of each of them was investigated using Routh Hurwitz criteria and also verified by calculating the eigen values of the Jacobian. One of the equilibrium points loses stability at a particular value of the control parameter (g=0.28) and evolves as a limit cycle- the phenomenon called Hopf bifurcation. The other two equilibrium points remain unstable through out the entire region of g value. This is different from the case where reverse period doubling route from chaos to stability was found for laser oscillating with two orthogonally polarized modes.

Occurrence of Hopf bifurcation in the output dynamics is investigated numerically also.

Energy sharing between the two longitudinal modes is studied as a function of the control parameter. Polarization of the cavity modes is found to have great influence on the nature of energy transfer between the modes.

REFERENCES

[1] T.Baer, J.Opt.Soc.Am.B. **3** (1986) 1175

[2] C.Bracikowaski and Rajarshi Roy, CHAOS **1** (1991) 49

[3] C.Bracikowski and Rajarshi Roy, Phys.Rev.A. **43** (1991) 6455

[4] M.Oka and S.Kubota, Opt.Lett. **13 (**1988) 805

[5] Thomas Kuruvilla and V.M.nandakumaran., CHAOS **9** (1999) 208

[6] C. Czeranowsky, V. M. Baev, G. Huber, P. A. Khandokhin, Ya. I. Khanin, I. V. Koryukin and E. Yu. Shirokov, Radiophysics and Quantum electronics, **47** (2004) 723

[7] M.R.Parvathi , Bindu.M.Krishna , S.Rajesh, M.P.John and V.M.Nandakumaran, Chaos Solitons and Fractals, doi: 10.1016/j.chaos.2009.01.013

[8] Elman Mohammed-Oglu Shahverdiev, Phys. Rev.E. **60** (1999) 3905

[9] Ming-kai Nan,Xiang-quan Shi,Kim-fung Tsang and Chak-nam Wong,Communications and Control Symposium 2000 IEEE: 457-460

[10] Apratim Mitra and Somdatta Sinha, Proc f the National Conference on Nonlinear Systems and Dynamics 2006.

[11] Katsuhiko Ogata. Modern Control Engineering. New Delhi: Prentice Hall of India Private Limited(1991).

CHAPTER 6

DELAY INDUCED MULTISTABILITY IN PARALLEL POLARIZED Nd:YAG LASER

In this chapter the effect of a delayed optoelectronic feedback on the dynamics of a two mode intracavity doubled Nd:YAG laser operating in the limit cycle region is investigated numerically. Both positive and negative delay feedbacks are studied separately. Bifurcation diagrams, time series plots, phase portraits, power spectra and intensity peak series plots are used to study laser dynamics. Periodic, quasiperiodic and chaotic dynamics regimes are identified in the output. Existence of chaotic region is confirmed with a positive Lyapunov exponent and a fractional correlation dimension. It is also found that the laser exhibits hysteresis and multistability for certain delay times.

6.1 INTRODUCTION

Laser chaos and synchronization of chaotic lasers [1-4] have been studied extensively as they have found applications in areas like secure communication. Privacy and security of communication systems can be enhanced utilizing the synchronization property of chaotic semiconductor lasers [5]. Recently chaotic multimode Nd:YAG lasers are found to be ideal candidates for multichannel communication [6-8]. Influence of a feedback has been studied widely in various dynamical systems especially in lasers. Introduction of a feedback is found to be the origin of chaos in many laser systems. In 1970 Paoli and Ripper studied the effect of an optoelectronic feedback on the dynamics of a self-pulsing GaAs junction laser [9]. In 1986, Arecchi et. al observed self-pulsing and deterministic chaos in a single-mode, homogeneous-line CO_2 laser under a negative feedback [10]. They also made a theoretical model which gave results in good agreement with the experimental ones. Later a successive transition from Hopf bifurcation to Shilnikov chaos and then to a regular spiking were also observed in CO_2 laser with feedback with increase of the control parameter [11]. Introduction of an optoelectronic feedback to a high speed self pulsing semiconductor laser was found to be an effective means for generating picosecond optical pulses [12]. In 1988, Chang-Hee Lee et al devised a method for generating optical pulses with repetition rates of several gigahertz and pulsewidth of the order of picoseconds by applying a negative optoelectronic feedback to a diode laser [13]. Gregory et.al reported the observation of a quasiperiodic route to chaos in coherence collapse of a single mode semiconductor laser subjected to an optical feedback [14].

Systems with delayed feedback exhibit a rich variety of dynamical phenomena because of their high dimensionality. A lot of studies have been

done to investigate delay feedback induced instabilities in various dynamical systems. Various instabilities in a semiconductor laser operating with a delayed optoelectronic feedback were studied by Giacomelli et.al [15]. Delay feedback has found applications such as suppression of relaxation oscillations [16], generation of stable oscillations [9], generation of low and high dimensional chaos [17, 18] and stabilization of unstable orbits [19]. Spectral bistability, sub harmonic generation, self-pulsing and chaos have been observed in a stable semiconductor laser with a delayed optoelectronic feedback [20]. A quasiperiodic route to chaos was achieved in quantum well lasers under a delayed optoelectronic feedback [21]. Chaotic pulsing and a quasiperiodic route to chaos in a semiconductor laser with delayed positive optoelectronic feedback were investigated by Liu et.al [22]. Almost similar dynamics was exhibited by the laser under delayed negative optoelectronic feedback [23].The effect of positive and negative delayed optoelectronic feedback on the dynamics of a directly modulated semiconductor laser operating in the optimum range of nonlinear gain reduction factor has been studied [24]. It was found that a negative delayed optoelectronic feedback is more effective in producing chaotic output keeping the nonlinear gain reduction factor in the practical value range.

An important dynamical behavior exhibited by laser systems is multistability. Multistability means coexistence of several attractors for a given set of parameters. Multistable systems are highly sensitive to perturbations because of the complex relationship between their attractors. The asymptotic state of the system is determined by its initial conditions. Multistability has been reported in lasers [25-31], electronic circuits [32], Duffing oscillators [33] and biological systems [34-39]. An interesting phenomenon associated with multistability is hysteresis. Hysteresis

represents the history dependence of the system i.e in order to predict the state of the system at some instant in time one must be aware of the history of the input or the state of the system for a given input. Hysteresis along with multistability has been reported in laser systems [40-44]. The coexistence of two distinct states is referred to as bistability of the laser. A positive optoelectronic feed back along with a strong current modulation is found to suppress hystreresis and bistability in directly modulated semiconductor lasers [45].

The phenomenon of bistability has some promising technological applications too. Materials displaying intrinsic optical bistability are technologically important as they have applications related to optical data switching and data manipulation [46]. Bistable magnetic behavior of amorphous wires is the key factor for the development of magneto-elastic sensors, magnetic switches and magnetic field detectors [47].All-optical transistor operation is a prominent application of double optical bistability observed in CW nonlinear transmission characteristics of chalcogenide fibre bragg gratings [48]. Bistable behavior of optically addressed ferro electric liquid- crystal spatial light modulators finds applications in neurocomputing [49].

Bistability and hysteresis are found to be the important mechanisms that control cell differentiation and cell cycle progression in many biological systems. A system that toggles between two discrete and alternate stable steady states is known as a bistable system. Cell cycle regulatory circuits in South African clawed frogs Xenopus laevis and in Saccharomyces cerevisiae (a species of budding yeast) , mitogen- activated protein kinase cascades in animal cells [50-53] are biological examples of bistable systems.

Works by Jonathan et al revealed that hysteresis is exhibited by the molecular control system in Xenopus laevis egg extracts as a result of some biological positive feedback loop [50]. This in turn causes the synthesis and degradation of cyclin which is an important protein that controls the cell cycle progression. It is also found that multistability is the basic mechanism for memory storage and pattern recognition in artificial and living neural networks [34, 54]. Recently Dubnau and Losick studied heterogeneity in bacteria populations emerging from bistability [55]. Thus multistability and associated hysteresis effects have numerous applications in biology. While studying these biological systems sometimes it seems to be difficult to change the parameters and the environmental conditions that control the system. Here comes the importance of laser systems. Availability of good and fast computational tools and easily accessible control parameters make the lasers good candidates as model systems to study these phenomena.

6.2 LASER MODEL

We perform our studies on a diode pumped Nd:YAG laser operating with two parallel polarized modes. The Hopf bifurcation phenomenon exhibited by this laser is discussed in [56]. The rate equation model and the laser dynamics are discussed in detail in chapter 3. The system can be modeled by the rate equations for the intensity I_k and gain G_k for the k^{th} longitudinal mode [57]

$$\tau_c \frac{dI_k}{dt} = \left(G_k - \alpha - g\varepsilon I_k - 2\varepsilon \sum_{j \neq k} \mu_{jk} I_j \right) I_k \qquad (6.1)$$

$$\tau_f \frac{dG_k}{dt} = \gamma - \left(1 + I_k + \beta \sum_{j \neq k} I_j \right) G_k \qquad (6.2)$$

The modes chosen are having parallel polarization. Therefore we take μ_{jk} =g.

The parameter values used in numerical simulation are given in table 3.1 in chapter 3.

We choose the control parameter as g=0.4 such that the laser is operating in the limit cycle region. Here the feedback is introduced by modulating the term γ which is related to the pumping of semiconductor laser. Output of the Nd:YAG laser which is an optical signal is converted into an electronic signal using a photodiode. This electronic signal is added to the injection current of the semiconductor laser which provides the pumping with an appropriate delay to modulate the pumping rate. Then γ will be modified as

$$\gamma = \gamma_b + K\sum_k I_k(t-\tau) \qquad (6.3)$$

Where K is the feedback strength and τ is the delay time and $\sum_k I_k$ is the total output intensity in all modes.

6.3 NUMERICAL RESULTS AND DISCUSSION

In this section we present the results of our numerical studies on the effect of positive and negative delayed optoelectronic feedback on the dynamics of Nd:YAG laser. We choose the control parameter as g=0.4 such that the laser is operating in the limit cycle region.

6.3.1 DYNAMICS UNDER DELAYED POSITIVE FEEDBACK

The feedback fraction is kept at a low value of 0.001 and the delay is increased in small steps. Figure 6.1 is the bifurcation diagram showing the variation of laser output intensity with delay time.

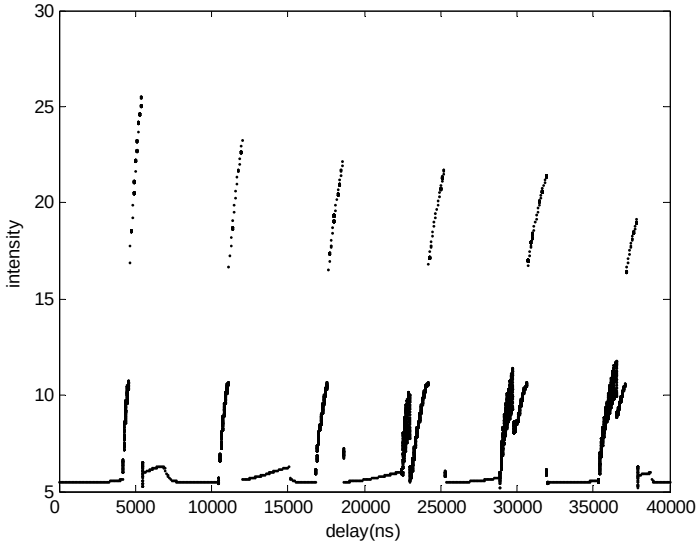

Figure 6.1: Bifurcation diagram for the laser under delayed positive feedback with a feedback fraction of K=0.001

Output intensity remains periodic for delay upto 20000ns. As the delay is increased further there is appearance of chaotic windows. It should be noted that the chaotic windows appear in regular intervals of feedback delay time. We have also drawn bifurcation diagrams for K=0.002, 0.003 and 0.004. The laser is found to exhibit rich dynamical behavior at K=0.002 which we have studied in detail. Bifurcation diagram for K=0.002 is shown in figure 6.2.

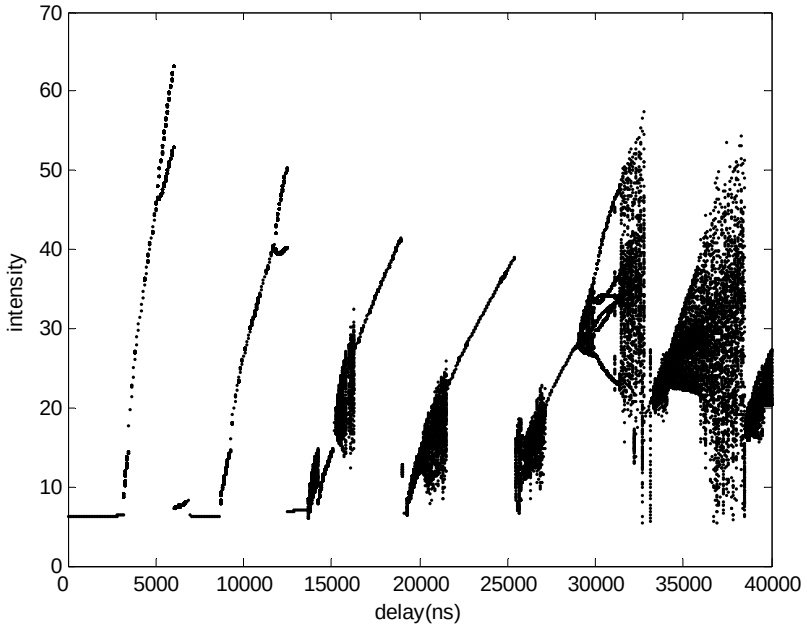

Figure 6.2: Bifurcation diagram for the laser under delayed positive feedback with a feedback fraction of K=0.002

We can identify various regions in the output as the delay time is increased. Output is a limit cycle for delay up to 3000ns and changes into two frequency quasiperiodic state at higher delay times. The output remains in the quasiperiodic state from 3000ns-3500ns. As the delay is increased we can see period one and period two regions. (3500ns-6375ns). Period doubling repeats for delays from 6375ns to 12500 ns. As the delay is increased further chaotic windows appear in the output in a regular manner. Corresponding to a delay of 30000 ns, there is a region which resembles period doubling route to chaos. Chaotic windows appear also for delays above 31100ns but with a higher peak intensity value. Figure 6.3 shows the intensity time series plots for different delay times. Figure 6.4 show the corresponding phase space plots.

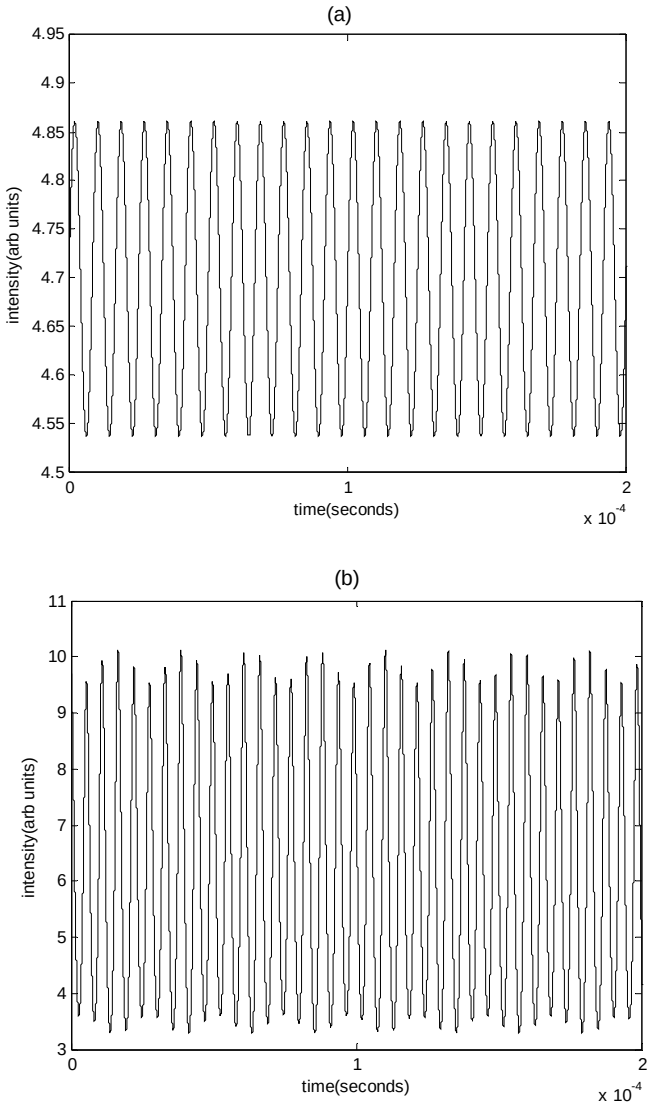

Figure 6.3: Intensity time series plots for the laser for a delay of a) 2950ns (limit cycle) b) 3250 ns (two frequency quasiperiodic)

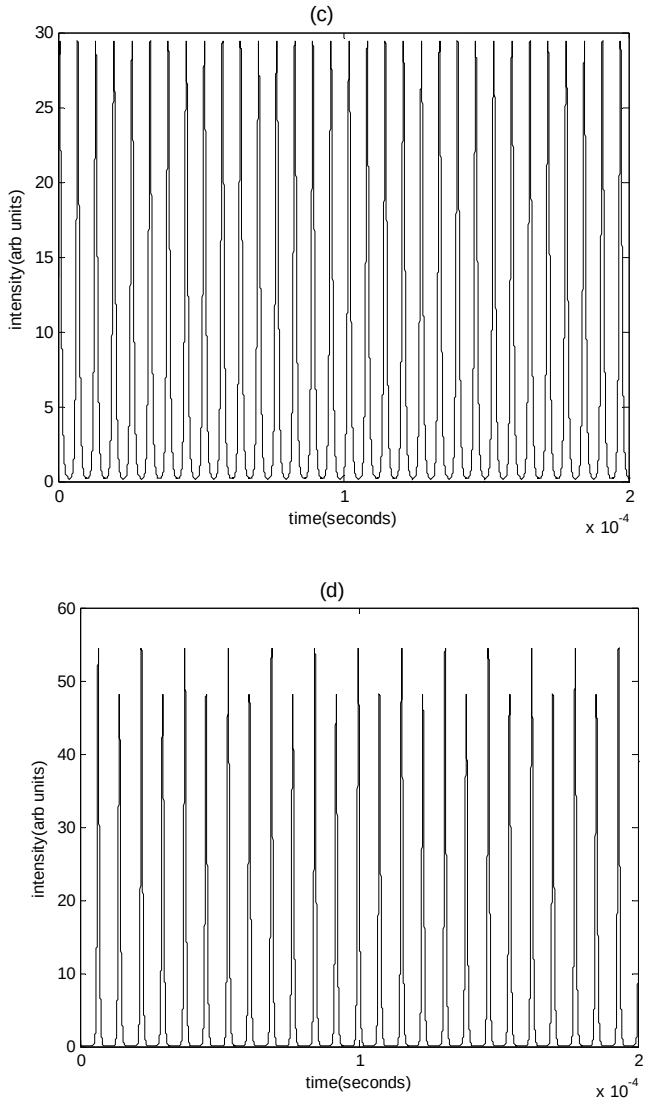

Figure 6.3: Intensity time series plots for the laser for a delay of c) 4000ns (period one) d) 5500 ns (period two)

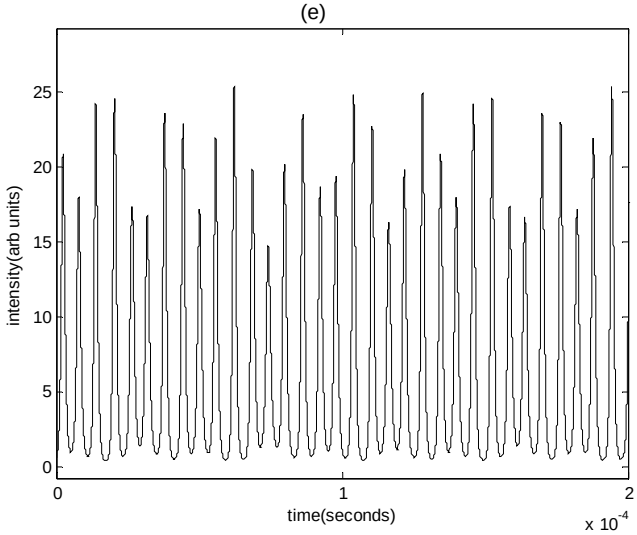

Figure 6.3: Intensity time series plots for the laser for a delay of e) 15700 ns (chaotic)

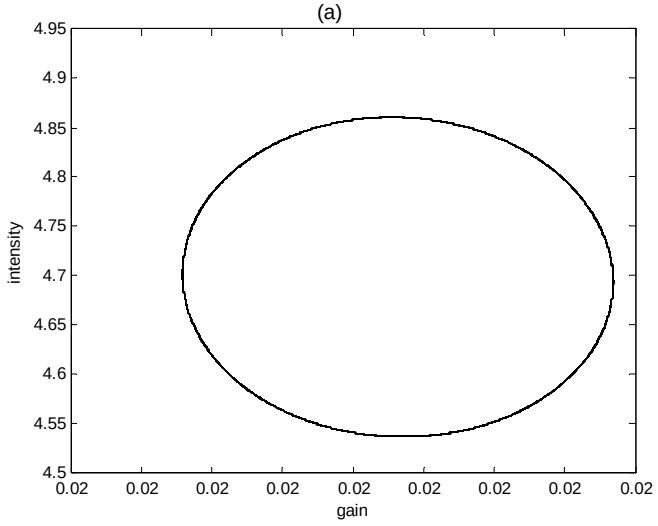

Figure 6.4: Phase space plots for the laser for a delay of a) 2950 ns (limit cycle)

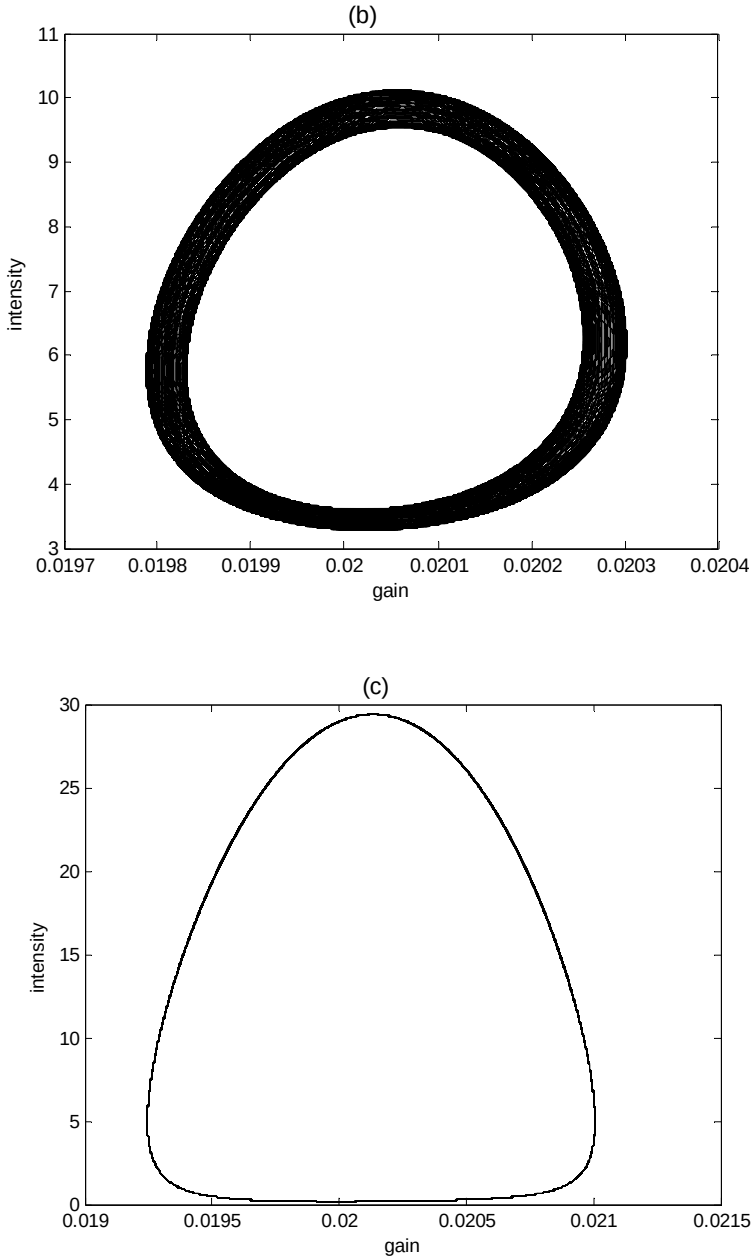

Figure 6.4: Phase space plots for the laser for a delay of b) 3250 ns (two frequency quasiperiodic) c) 4000 ns (period one)

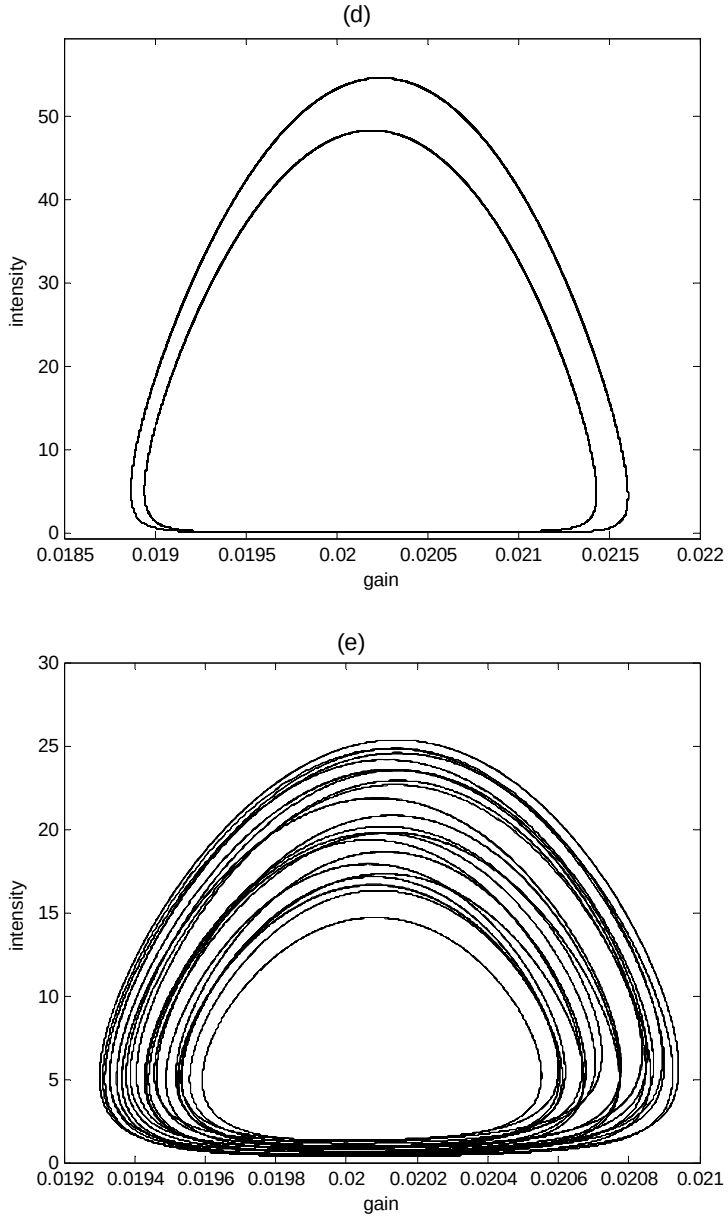

Figure 6.4: Phase space plots for the laser for a delay of d) 5500 ns (period two) e) 15700ns (chaotic)

Power spectra are used to characterize various dynamical regimes. Figure 6.5 shows the power spectra of different pulsing states.

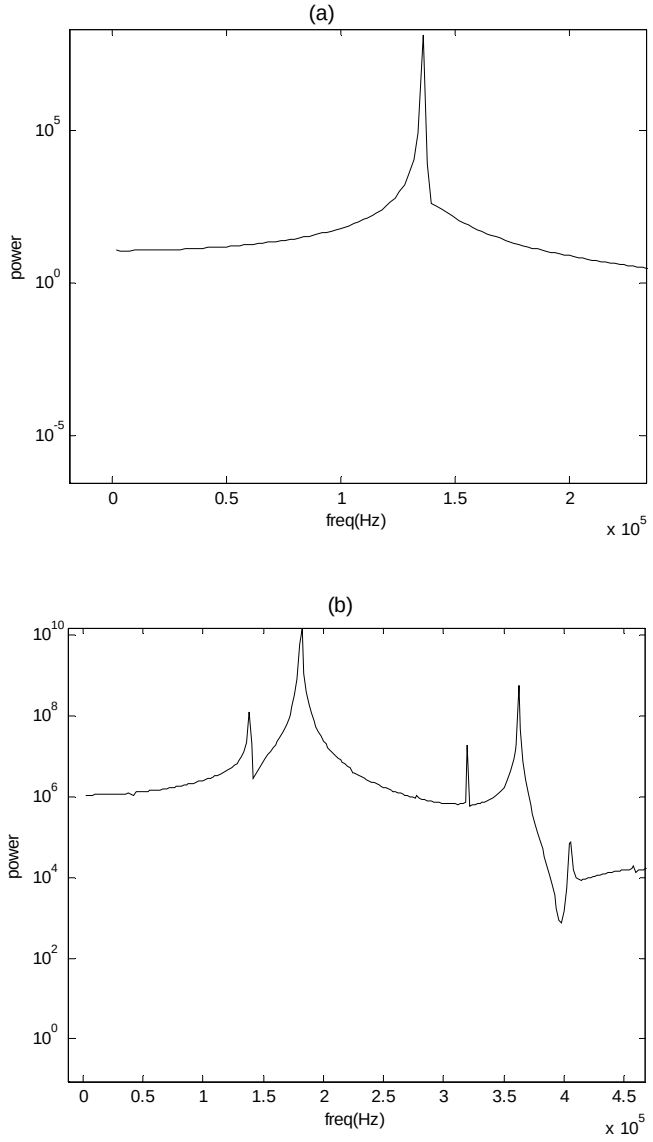

Figure 6.5: Power spectra of different pulsing states a) limit cycle at 2950 ns b) two frequency quasiperiodic at 3250 ns

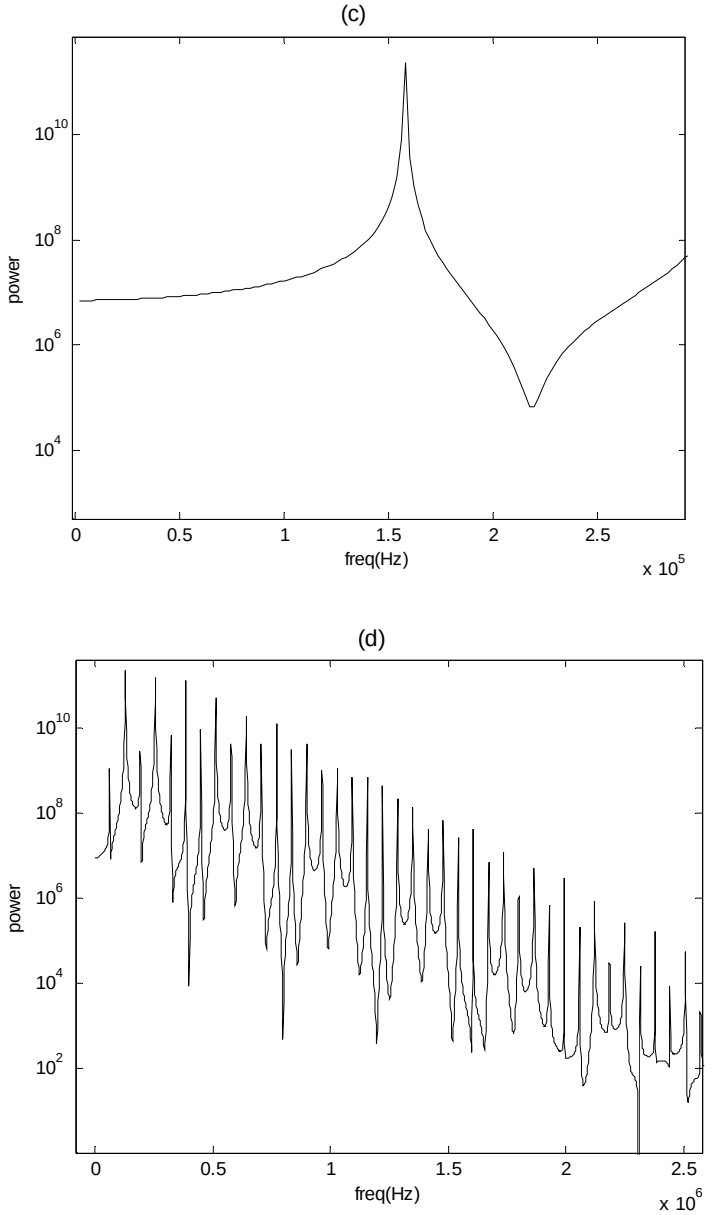

Figure 6.5: Power spectra of different pulsing states c) period one at 4000 ns d) period two at 5500 ns

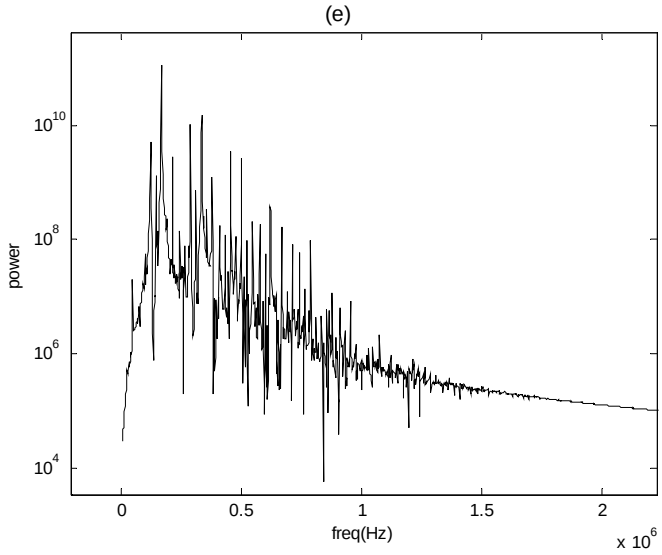

Figure 6.5: Power spectra of different pulsing states e) chaotic at 15700 ns

At τ= 2950 ns, where the laser is operating in the limit cycle region, the power spectra shows a single peak at the fundamental pulsing frequency f_1= $1.38\times10^5 Hz$. When the delay time is increased to 3250ns the laser enters two frequency quasiperiodic state where the pulsing intensity is modulated at a certain frequency f_2= $3.2\times10^5 Hz$. This frequency is found to be close to the inverse of delay time. The appearance of two incommensurate frequencies is a clear indication of quasiperiodicity. As the delay is again increased we can see period doubling. The power spectrum for the period one region shows a peak at frequency $1.52\times10^5 Hz$ which is different from the peak obtained for the limit cycle region. The difference in amplitude is clearly shown in the power spectra also. The laser output becomes chaotic as the delay is further increased where the power spectra is found to be broadened. Existence of chaotic region is verified with a positive Lyapunov exponent of 2.5237×10^{-2} for 5ns and a fractional correlation dimension of 1.89015.

We also define a peak series which is obtained by taking peak values in the intensity time series. Figure 6.6 shows the phase portraits of peak intensities I (n+1) versus I (n) for various delay times.

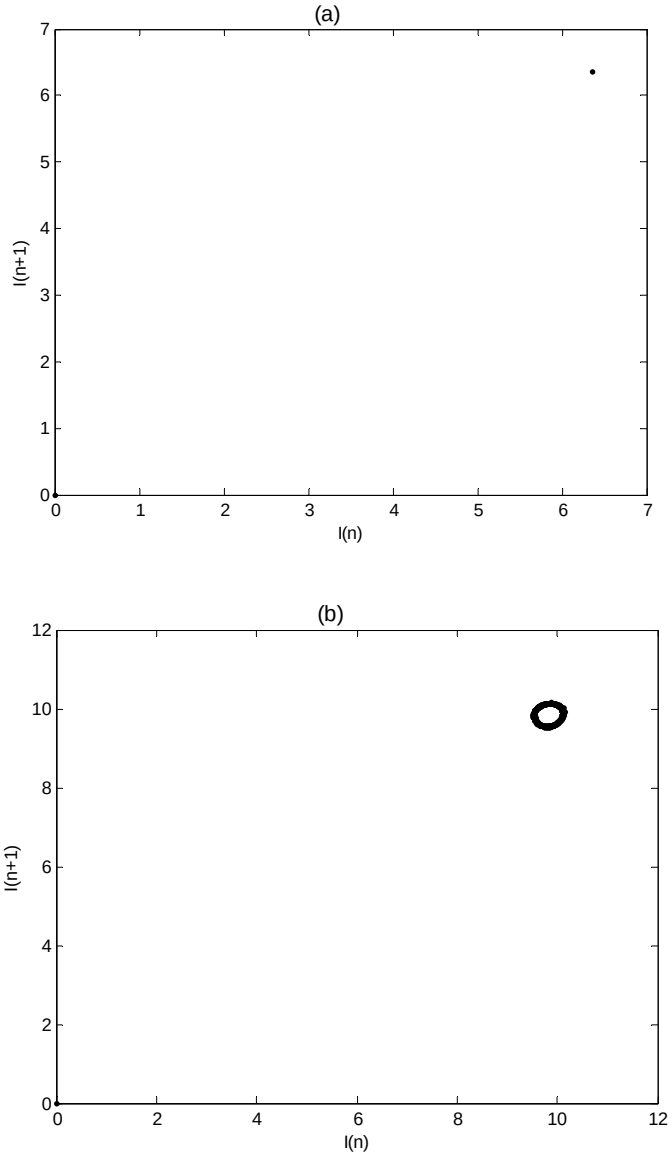

Figure 6.6: Phase portrait of peak intensities I(n+1) versus I(n) at different delay times. a) limit cycle at 2950 ns b) two frequency quasiperiodic at 3250 ns

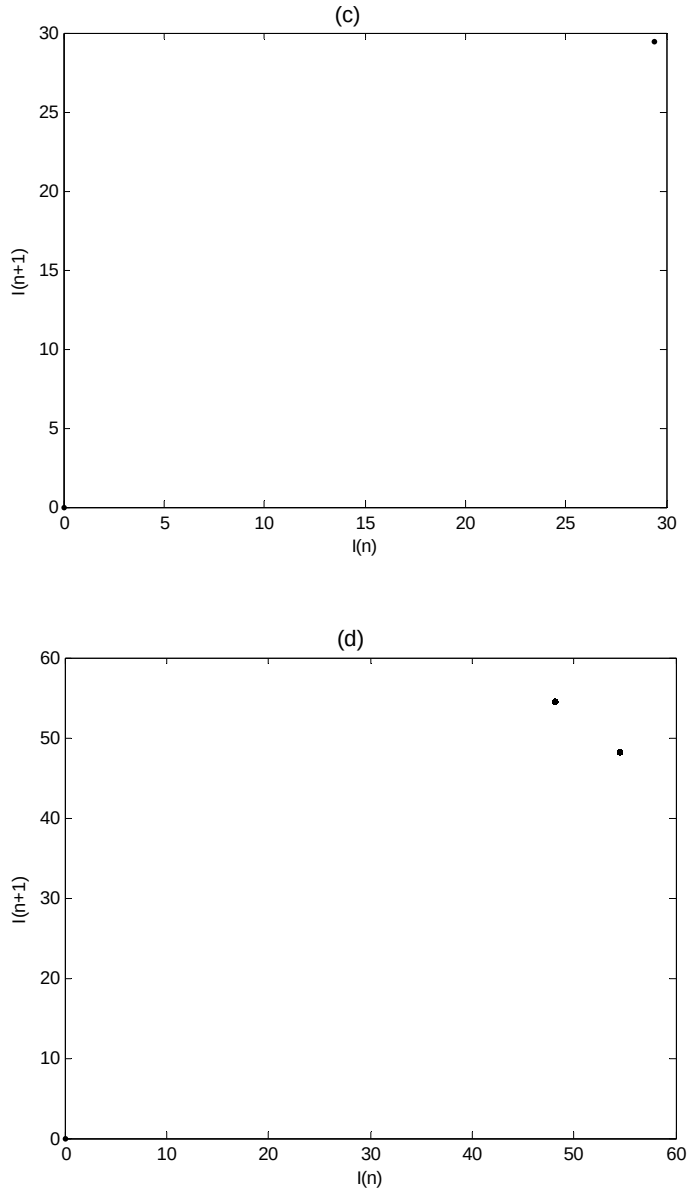

Figure 6.6: Phase portrait of peak intensities I(n+1) versus I(n) at different delay times c) period one at 4000 ns d) period two at 5500 ns

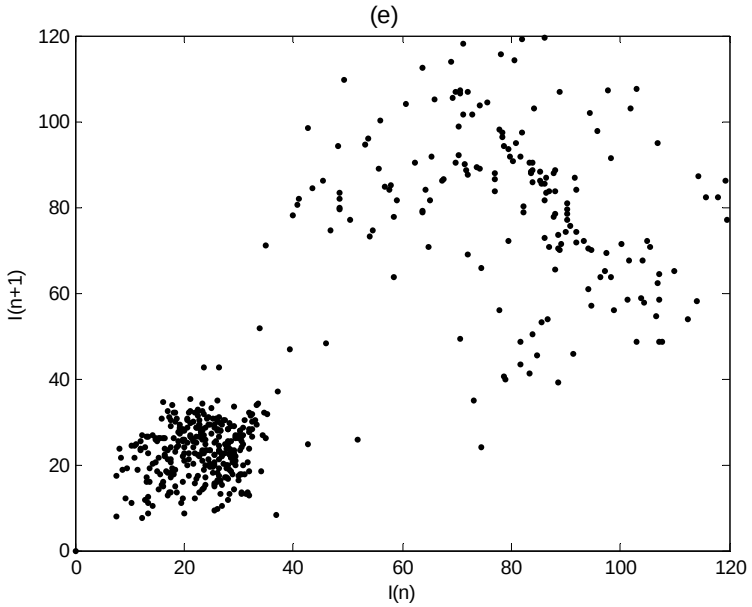

Figure 6.6: Phase portrait of peak intensities I(n+1) versus I(n) at different delay times. e) chaotic at 15700 ns

When the laser is operating in the limit cycle region the phase portrait is a single spot. For quasiperiodic region it appears as a clear circle. For the period one region also it is a single spot, but appears in a different region of the phase space. There are two dots in the phase portrait corresponding to period two region. Finally when the laser is in the chaotic state the phase portrait spreads over a wide range.

6.3.1.1 HYSTERESIS AND BISTABILITY

This laser is found to exhibit hysteresis and multistability for certain delay times under delayed positive feedback. To study the hysteresis effect clearly the bifurcation diagram is drawn by continuous time approach. Initial

conditions are given only in the beginning of the simulation. All the parameters are fixed and the delay is increased in small steps.

We can identify two regions in the bifurcation diagram where the laser shows hysteresis. The first hysteresis loop occurs for delay from 5500ns to 8000ns. Figure 6.7 shows the bifurcation diagram corresponding to this region.

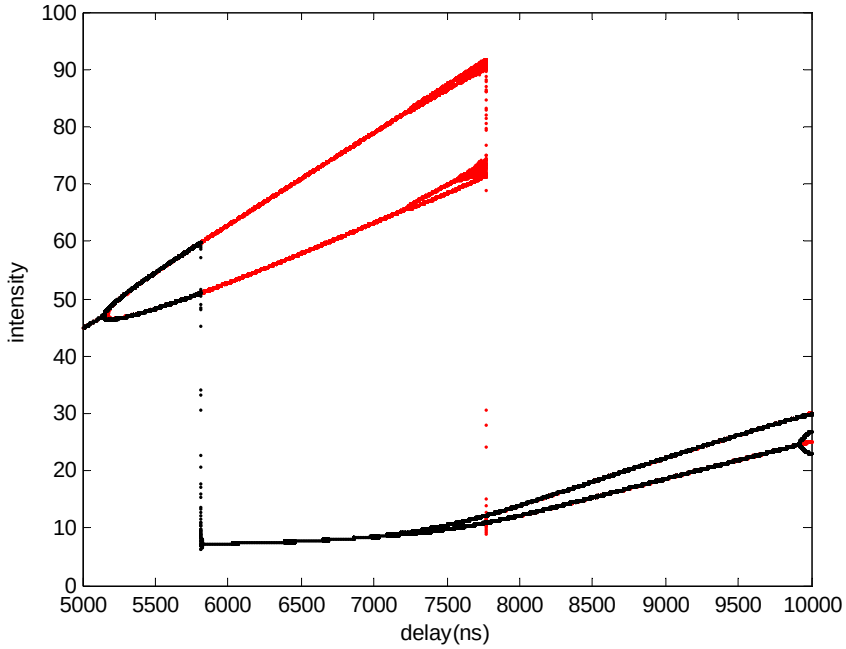

Figure 6.7: Bifurcation diagram showing the first hysteresis exhibited by the laser under delayed positive feedback with a feedback fraction of K=0.002

Delay is increased in small steps starting from 5000ns to 10000ns. Path followed by the laser output while increasing the delay is shown in red color in the diagram. The portion in black denotes the same for decreasing delay value. The output laser intensity shows period doubling as the delay is

reached 5145ns and remains in the period two region for higher delay times. But as the delay is decreased, the output intensity follows a different path as seen (in black color) thus forming a hysteresis loop. Formation of hysteresis loop indicates that there are two stable solutions for the laser for any value of delay between 5500ns and 8000ns. Figure 6.8a and 6.8b show the intensity time series of two different optical pulses obtained for the same delay time of 6500ns. Figure 6.8a corresponds to the output which is obtained while increasing the delay from 5500ns to 8000ns. It clearly shows period two oscillations. Figure 6.8b is the intensity time series obtained while decreasing the delay. It is also periodic with the peak at a lower value. Thus it is evident that laser exhibits bistable behavior for a delay ranging from 5500ns to 8000ns. Figure 6.9a and 6.9b give the corresponding power spectra.

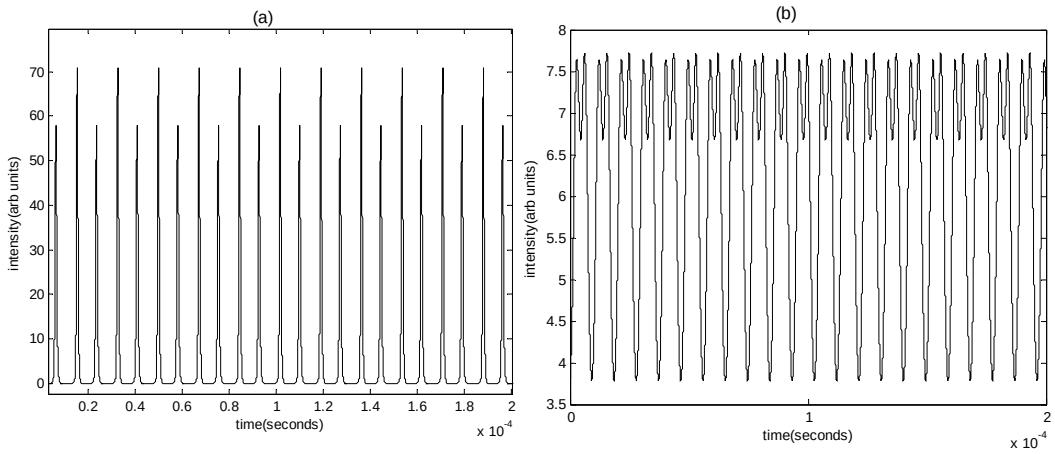

Figure 6.8: Intensity time series plots for the laser for a delay of 6500ns corresponding to (a) increasing delay and (b) decreasing delay

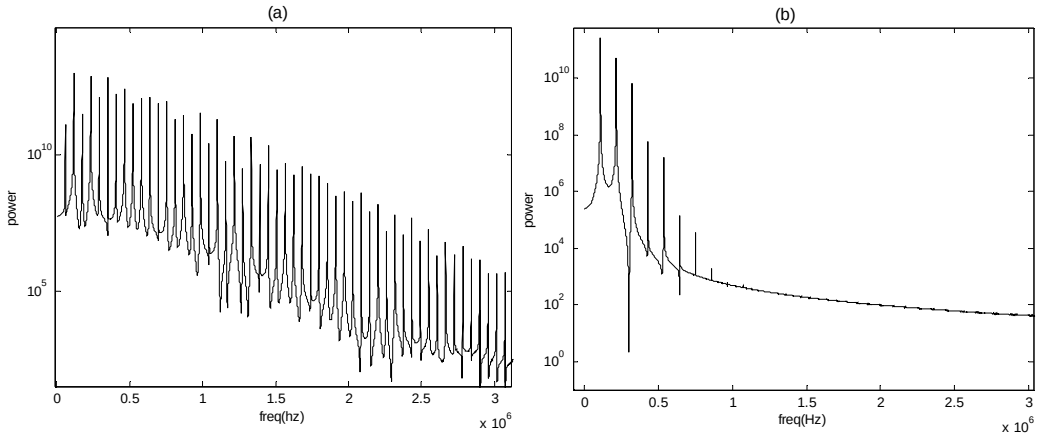

Figure 6.9: Power spectra for the laser for a delay of 6500ns corresponding to (a) increasing delay and (b) decreasing delay

The second hysteresis loop occurs for delay between 12000ns to 14500ns. The bifurcation diagram is drawn as in the previous case for delay starting from 11000ns to 16000ns and is shown in figure 6.10.

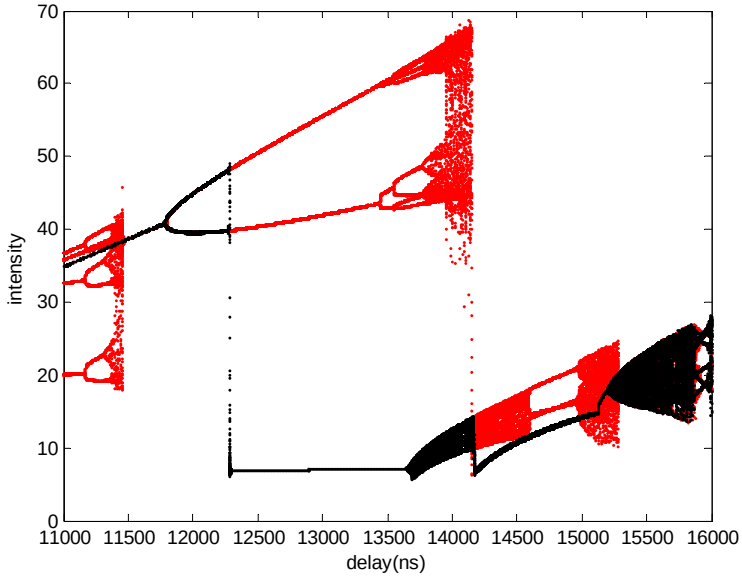

Figure 6.10: Bifurcation diagram showing the second hysteresis exhibited by the laser under delayed positive feedback with a feedback fraction of K=0.002

The laser exhibits period doubling route to chaos as the delay is increased (as shown in red color). But it follows an entirely different path as the delay is decreased as is evident from the portion of the bifurcation diagram shown in black. We can identify two delay times where the laser shows bistable behavior. One at a delay of 13000ns and the other at14000ns. Figure 6.11a shows the intensity time series plots for the laser obtained for a delay of 13000ns while the delay is increased from 12000ns to 14500ns. There are period two oscillations in the output. Period one oscillation shown in figure 6.11b corresponds to the same delay of 13000ns which is obtained while

decreasing the delay. The pulses are found to have a lower peak value. Corresponding power spectra are given in figure 6.12. Thus there is a clear indication of laser bistability for a delay of 13000ns.

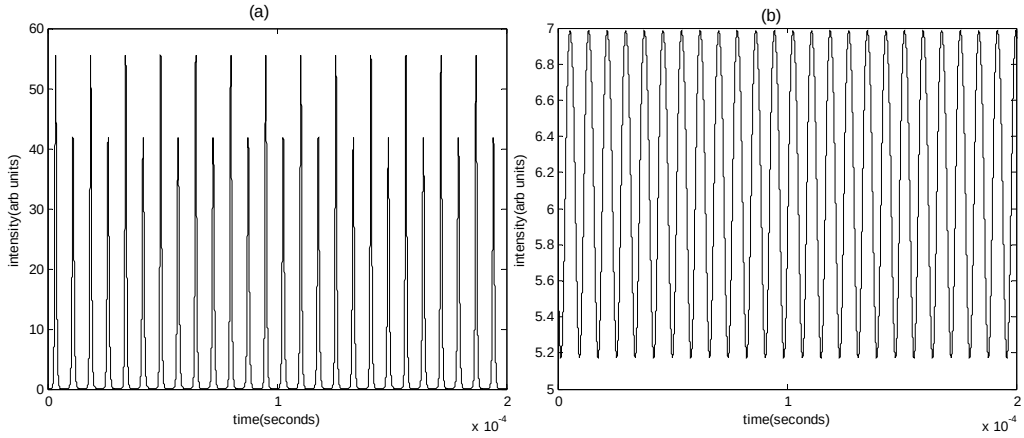

Figure 6.11: Intensity time series plots for the laser for a delay of 13000ns corresponding to (a) increasing delay and (b) decreasing delay

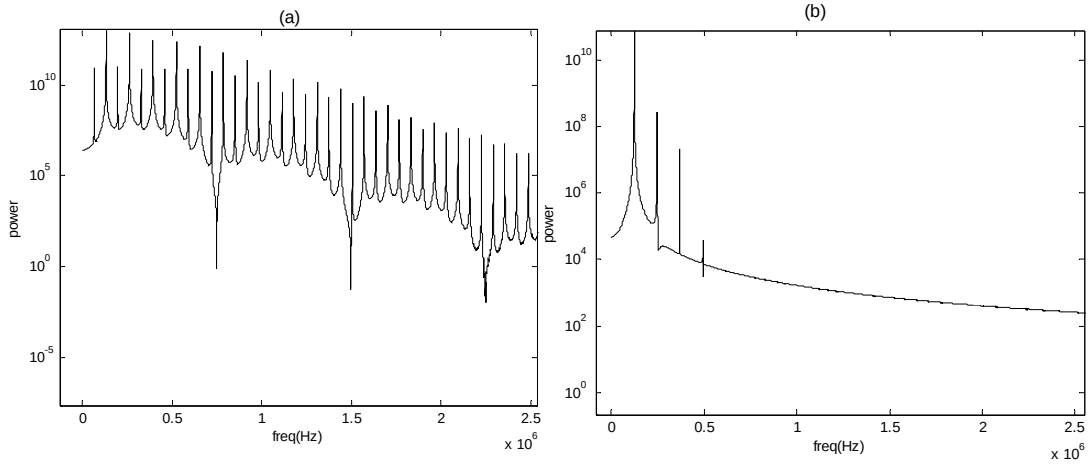

Figure 6.12: Power spectra for the laser for a delay of 13000ns corresponding to (a) increasing delay and (b) decreasing delay

For a delay of 14000 ns we find the two coexisting states to be chaotic and quasiperiodic. Figure 6.13a shows the chaotic time series corresponding to

the delay of 14000ns which is obtained while increasing the delay. As the delay is decreased we get a quasiperiodic state corresponding to the same delay. Figure 6.13b is the time series for the quasiperiodic state. Figure 6.14 shows the power spectra for the chaotic (6.14a) and the quasiperiodic (6.14b) state.

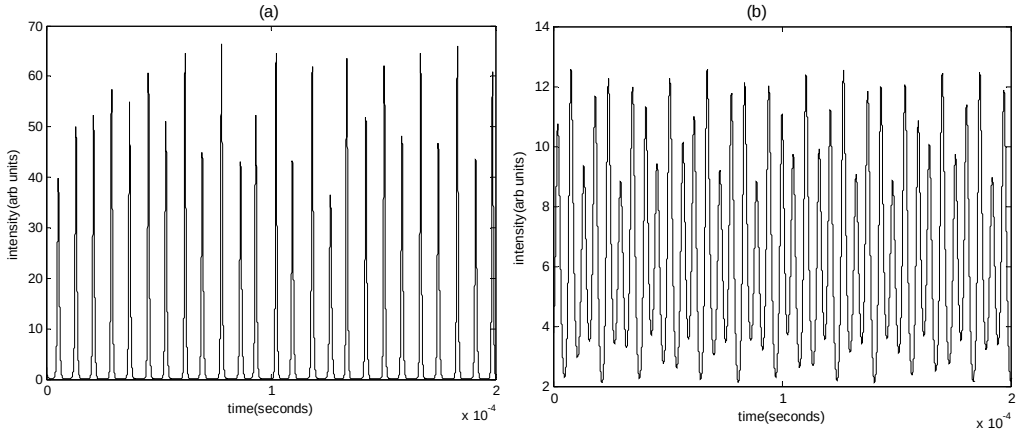

Figure 6.13: Intensity time series plots for the laser for a delay of 14000ns corresponding to (a) increasing delay and (b) decreasing delay.

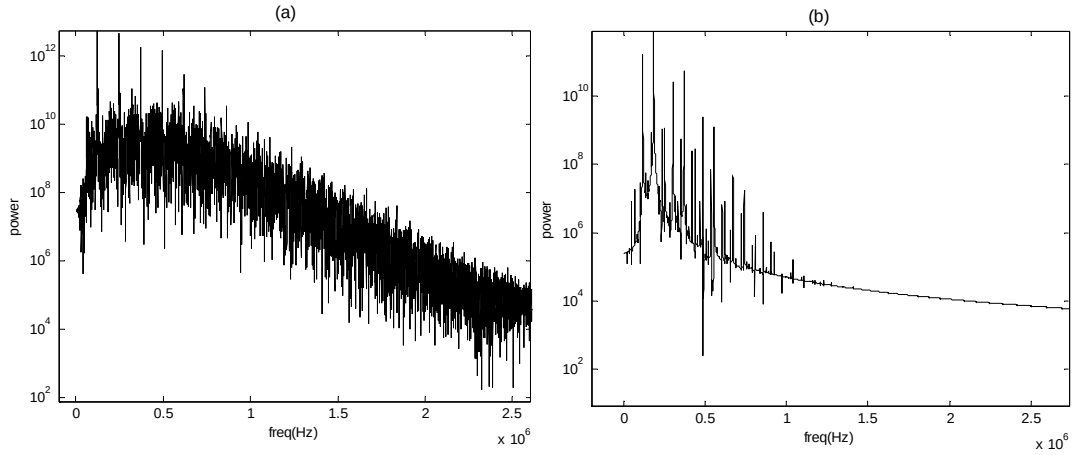

Figure 6.14: Power spectra for the laser for a delay of 14000ns corresponding to (a) increasing delay and (b) decreasing delay

The laser dynamics at a feedback fraction of K=0.002 can be summarized in the following tables.

Delay (ns)	Dynamics
0-3000	Limit cycle
3000-3500	Two frequency quasiperiodic
3500-6375	Period one and period two
6375-12500	Repetition of period doubling
12500-30000	Appearance of chaotic windows in regular fashion
Above 30000	A region which resembles period doubling and again appearance of chaotic windows with higher peak intensity values.

Table 6.1: Summary of the laser dynamics for K=0.002

Range of delay values where the system shows hysteresis effect (ns)	States coexisting in the region
5000-8000	Two, periodic states
12000-14500	a) Period two and period one oscillations at 13000 ns b) Chaotic and quasiperiodic states at 14000 ns

Table 6.2: Hysteresis and bistability exhibited by the laser for K=0.002

Figure 6.15 and 6.16 give the bifurcation diagrams for feedback fractions K=0.003 and 0.004 respectively. The dynamics becomes more complex at higher feedback fractions. As the feedback fraction is increased, chaos occurs in the laser output at smaller delay values. Also there is an overall increase in the laser output intensity as the feedback fraction is increased.

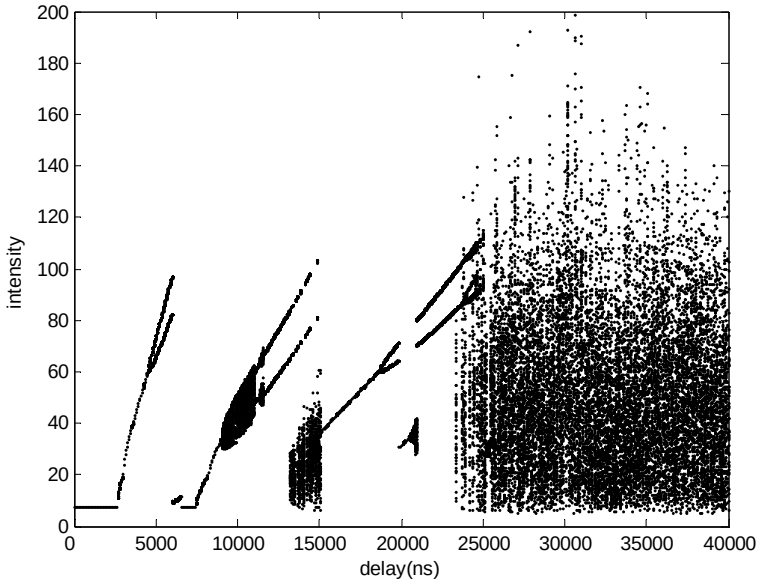

Figure 6.15: Bifurcation diagram for the laser under delayed positive feedback with a feedback fraction of K=0.003

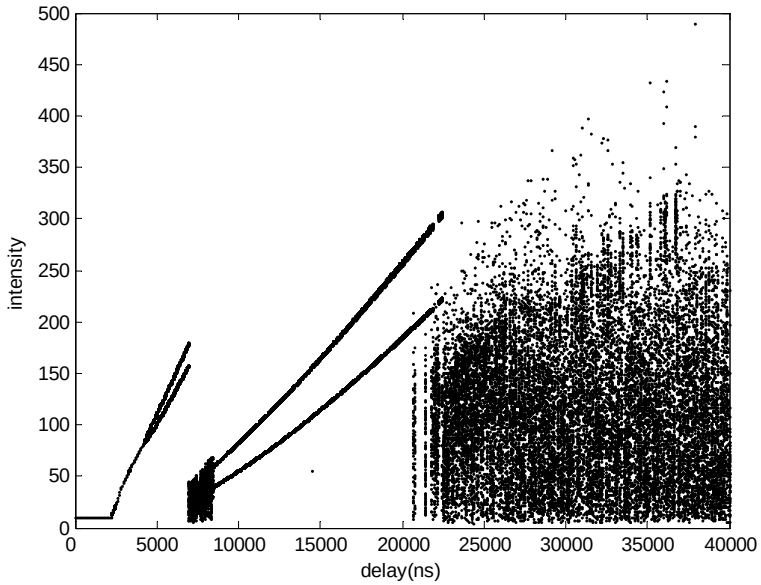

Figure 6.16: Bifurcation diagram for the laser under delayed positive feedback with a feedback fraction of K=0.004

6.3.2 DYNAMICS UNDER DELAYED NEGATIVE FEEDBACK

We have also investigated the system dynamics under a negative delay feedback. The feedback fraction is kept at a low value of K=0.001 and the delay time is increased. Figure 6.17 below is the bifurcation diagram showing the variation of laser output intensity with delay time.

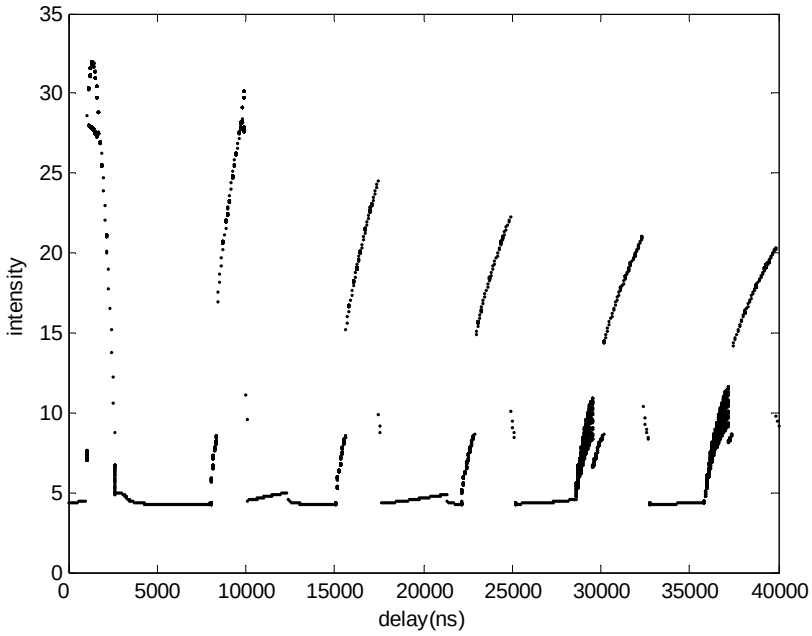

Figure 6.17: Bifurcation diagram for the laser under delayed negative feedback with a feedback fraction of K=0.001

The dynamics is found to be somewhat similar to that with positive feedback. We can see periodic regions and then the appearance of chaotic windows at higher delays. We have also drawn bifurcation diagrams at higher feedback fractions. Figure 6.18 gives the dynamics for a feedback fraction of K=0.002.

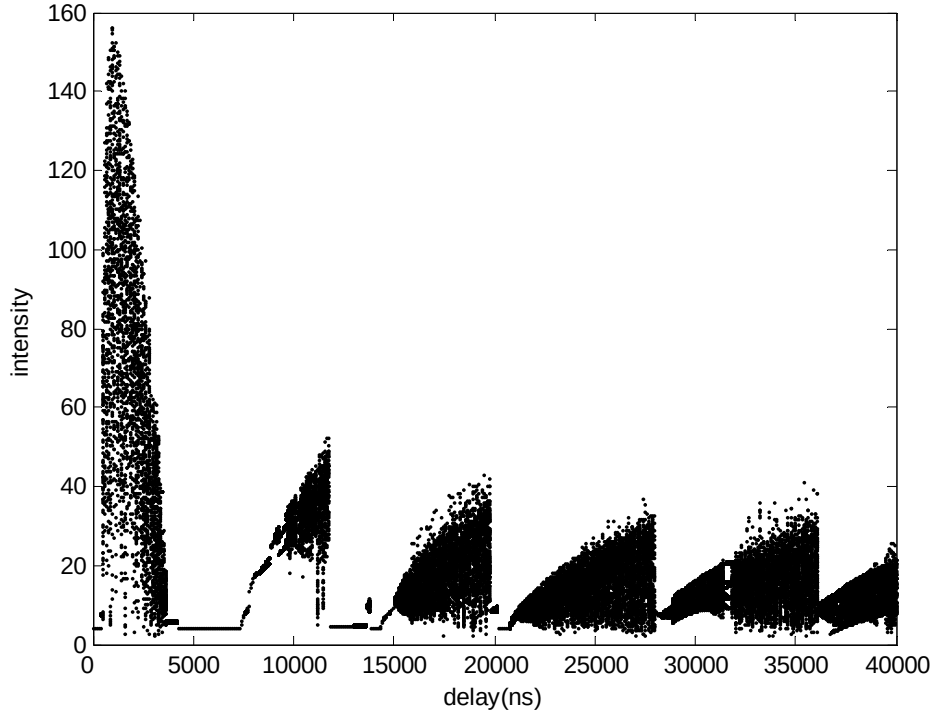

Figure 6.18: Bifurcation diagram for the laser under delayed negative feedback with a feedback fraction of K=0.002.

For very small delay times the output is stable. Then there is a sudden jump into the chaotic state for delay as low as 400 ns. Portion of the bifurcation diagram showing this jump is given in figure 6.19. Periodic and chaotic regions are repeated as the delay is increased. The frequency with which the chaotic region appears increases as the delay is increased. Also we can see a decrease in the peak intensity value of the chaotic region with increase in delay. A close examination of the bifurcation diagram reveals that the laser exhibits hysteresis and bistability for delay between 7250ns and 8000ns. The hysteresis loop corresponding to this region is shown in figure 6.20.

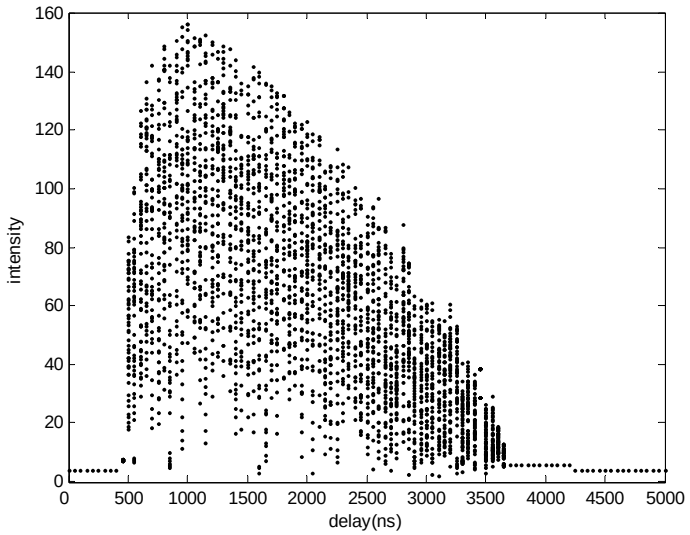

Figure 6.19: Bifurcation diagram showing the jump into chaotic state in the laser output intensity under delayed negative feedback for K=0.002

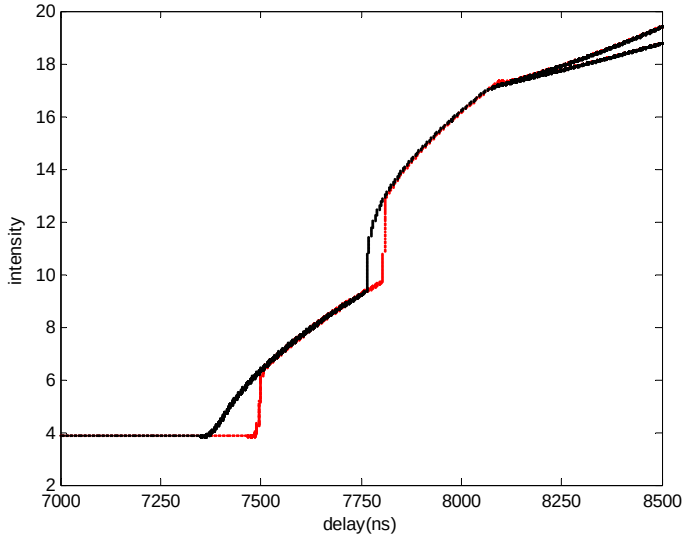

Figure 6.20: Hysteresis exhibited by the laser under delayed negative feedback for a feedback fraction of K=0.002.

Laser dynamics is studied under higher feedback fractions of K=0.003 and K=0.004. At higher feedback fractions not much interesting behavior is exhibited by the laser except for a sudden jump into the chaotic state at smaller delays. The output remains chaotic at higher delay times. As the feedback fraction is increased, the peak intensity value of the initial chaotic jump also increases. The bifurcation diagrams are given in figures 6.21 and 6.22.

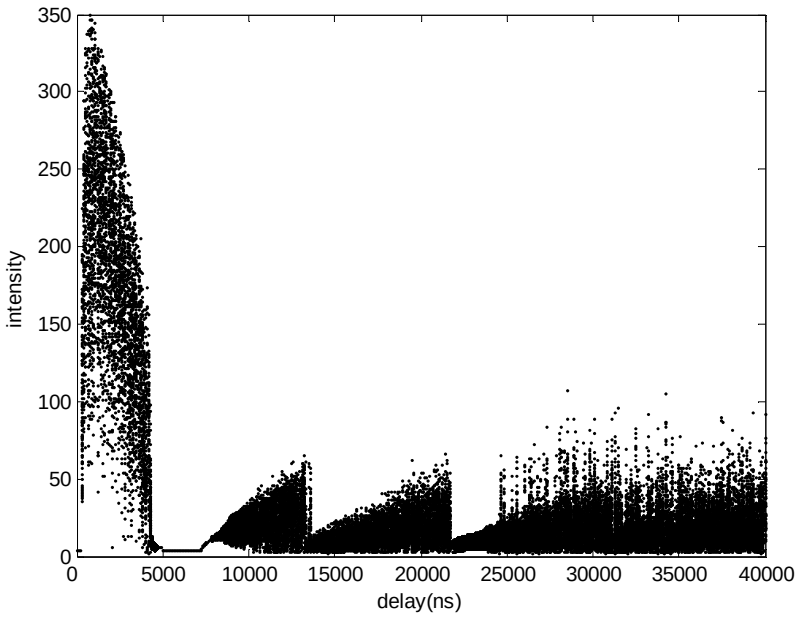

Figure 6.21: Bifurcation diagram for the laser under delayed negative feedback with a feedback fraction of K=0.003.

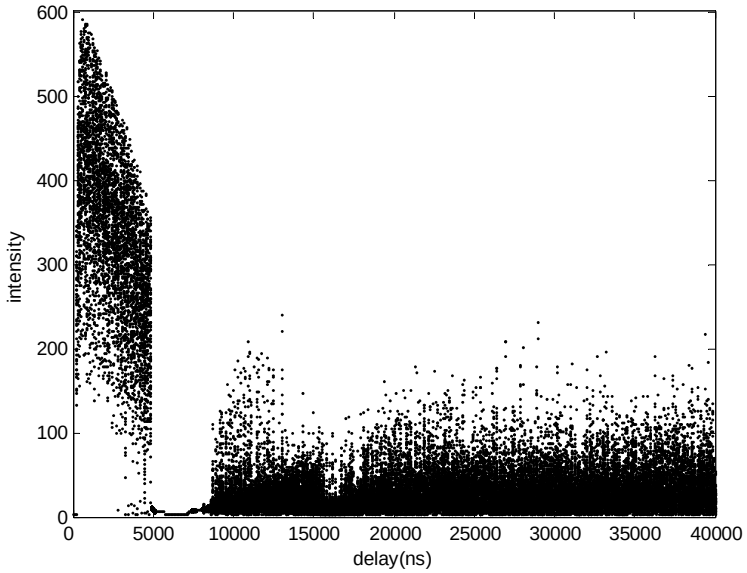

Figure 6.22: Bifurcation diagram for the laser under delayed negative feedback with a feedback fraction of K=0.004.

6.4 CONCLUSIONS

Dynamics of Nd:YAG laser operating in the limit cycle region under a delayed positive and negative optoelectronic feedback is studied numerically. The laser is having two modes with parallel polarization. A detailed analysis of the laser dynamics is carried out using bifurcation diagrams, time series plots, phase space plots, power spectra and intensity peak series plots. It is found that under positive feedback and for low values of delay the laser is in the limit cycle region with the fundamental pulsing intensity at 1.38×10^5 Hz. As the delay is increased laser enters a two frequency quasiperiodic state where the fundamental pulsing intensity is modulated at a frequency of 3.2×10^5 Hz. This frequency is found to be close to the inverse of the delay time. Laser shows period one and period two oscillations following the quasiperiodic state. There is a repetition of period doubling as the delay is

increased further. At higher delays there is chaos. Existence of chaotic region is verified with a positive lyapunov exponent and a fractional correlation dimension. The path followed by Nd:YAG laser under a delayed positive optoelectronic feedback is found to be different from semiconductor laser where a quasiperiodic route to chaos is seen. We have identified two regions in the bifurcation diagram where the laser exhibits hysteresis and bistability. For a delay ranging from 5500ns to 8000ns there is a coexistence of two different periodic regions with different amplitudes. The most interesting finding is the coexistence of chaotic and quasiperiodic states in between the delay times from 12000ns to 14500ns. Coexistence of regular pulsing and quasiperiodic pulsing states were observed experimentally in a distributed feedback semiconductor laser under delayed optoelectronic feedback [58]. To the best of our knowledge coexistence of chaotic and quasiperiodic states has not yet been reported in any other laser systems. Chaotic windows appear in the output in a regular manner at higher delay times. As the feedback fraction is increased, chaos occurs in the output for smaller delay times along with an overall increase in the output intensity.

With negative feedback the output intensity undergoes a sudden jump into the chaotic state at smaller delays. Laser exhibits hysteresis and bistability for a feedback fraction of K=0.002. Periodic and chaotic regions occur alternately at higher delays. It should be noted that as the delay is increased, chaotic regions appear more frequently with smaller and smaller intensity peak value. As the feedback fraction is increased, the peak intensity value of the initial chaotic jump increases and the output remains chaotic at higher delays.

REFERENCES

[1] R.Roy and K.S.Thornburg Jr., Phys.Rev.Lett.**72** (1994) 2009

[2] V.Bindu and V.M.Nandakumaran, Phys.Lett.A. **277** (2000) 345

[3] Thomas Kuruvilla and V.M.Nandakumaran, Pramana **54** (2000) 393

[4] M.R.Parvathi,Bindu M.Krishna, S.Rajesh, M.P.John and V.M.Nandakumaran, Phys.Lett.A. **373** (2008) 96

[5] V.Bindu and V.M.Nandakumaran. J. Opt. A. Pure& Appl. Opt. **4** (2002) 115

[6] Zhou Yun, Wu Liang and Zhu Shi-Qun, Chinese Phys. **14** (2005) 2196

[7] R.M.Lopez-Gutierrez, C.Cruz-Hernadez, C.Posadas- Castillo and E.E.Garcia- Guerrero, PROCEEDINGS OF WORLD ACADEMY OF SCIENCE, ENGINERING AND TECHNOLOGY, **30** (2008) 1032

[8] Liang Wu and Shiqun Zhu, Phys.Lett.A. **308** (2003) 157

[9] T.L.Paoli and J.E.Ripper, J.Quan.Elec. QE **6** (1970) 335

[10] F.T.Arecchi, W.Gadomski and R.Meucci, Phys.Rev.A. **34** (1986) 1617

[11] F.T.Arecchi, R.Meucci and W.Gadomski, Phys.Rev.Lett. **58** (1987) 2205

[12] K.Y.Lau and A.Yariv, Appl.Phys.Lett. **45** (1984) 124

[13] Chang-Hee Lee, Sang-Yung Shin and Soo-Young Lee, Optics Lett. **13** (1988) 464

[14] Gregory.C.Dente, Peter.S.Durkin, Kimberley .A.Wilson and Charles. E.Moeller, IEEE J.Quan. Elec. **24** (1988) 2441.

[15] G.Giacomelli, M.Calzavara and F.T.Arecchi, Optics Comm. **74** (1989) 97

[16] H.Statz, G.A.de Mars, D.T. Wilson and C.L.Tang. J.Appl.Phys. **36** (1965) 1515

[17] K.Ikeda and K.Matsumoto, Physica D. **29** (1987) 223

[18] M.Wegener and C.Klingshirn, Phys.Rev.A. **35** (1987) 4247

[19] W.Lu and R.G.Harison, Optics.Comm. **109** (1994) 457

[20] Chang-Hee Lee and Sang-Yung Shin, Appl. Phys.Lett. **62** (1993) 922

[21] C.Juang, C.C.Huang, T.M.Hwang, J.Juang and W.W.Lin, Optics.Comm. **192** (2001) 77

[22] S.Tang and J.M..Liu, IEEE .J. Quan.Elec.**37** (2001) 329

[23] Fan-yi Lin and Jia-Ming Liu, IEEE J.Quan.Elec. **39 (**2003) 562

[24] Bindu M.Krishna, Mamu P.John and V.M.Nandakumaran, Pramana **71** (2008) 1259

[25] F.T.Arecchi, R.Meucci , G.Puccioni and J.Tredicce, Phys.Rev.Lett. **49** (1982) 1217

[26] E.Brun, B.Derighette, D.Meier , R.Holzner and M.Raveni, J.Opt.Soc.Am.B. **2** (1985)156

[27] J.R.Tredicce, F.T.Arecchi, G.P.Puccioni, A.Poggi and W.Gadomski, Phys.Rev.A. **34** (1986) 2073

[28] H.G.Solari, E.Eschenazi, R.Glimore and J.T.Tredicce, Opt.Comm. **64** (1987) 49

[29] I.I.Matorin, A.S.Pikovski and Ya I Khanin, Sov. J. Quan. Elec. **14** (1984) 1401

[30] Kawaguchi.H, IEEE. J. Quan.Elec.**23** (1987) 1429

[31] J P Goedgebuer, A.Fischer and H.Porter, IEEE. J.Quan.Elec. **26** (1996) 242

[32] J.Maurer and A.Libchaber, J.Phys.France Lett. **41** (1980) 515

[33] F.T.Arecchi, R.Badii and A.Politi, Phys.Rev.A. **32** (1985) 402

[34] J.Foss, A.Longtin , B.Mensour and J.Milton, Phys.Rev.Lett. **76** (1996) 708

[35] P.Cordo, J.T.Inglis, S.Verschueren, J.J.Collins, D.M.Merfeld,

S.Rosenblum, S.Buckley and F.Moss, Nature **383** (1996) 769

[36] Jennifer Foss and John Milton, The Journal of Neurophysiology **84** (2000) 975

[37] S. Morfu, B.Nofiele and P.Marquie, Phys.Lett.A. **367** (2007) 192

[38] Angeli D, Ferrell JE Jr and Sontag ED, Proc. Natl.Acad.Sci USA 2004 17; 101(7):1822-7.

[39] Younghae Do and Ying-Chen Lai, CHAOS **18** (2008) 043107

[40] I.B.Schwartz and T.Erneux, SIAM J.Appl.Math. **54** (1994) 1083

[41] Kh G. Gafurov and D.P.Krindach, Sov. J. Quan.Elec. **15** (1985) 408

[42] Calvani.R and Caponi.R, Opt. Comm. **11**(1988) 388

[43] M.J.Adams , P.E.Barnsley and J.Chen, Electronics Letters **28**(1992)395

[44] Chris J.Born, Matthew Hill, Marc Sorel and Siyuan Yu, Conference on Lasers and Electro-Optics (CLEO) Baltimore, Maryland, May 22, 2005

[45] S.Rajesh and V.M.Nandakumaran, Physica D. **213** (2006) 113

[46] Daniel R., Gamelin, Stefan R.Luthi and Hans U.Gudel, J.Phys.Chem.B. **104** (2000) 11045

[47] Vazquez, M., Gomez-Polo, C., Chen, D.-X. and Hernando, A., IEEE Transactions on Magenetics **30** (1994) 907

[48] Y.Yosia and Shum Ping, Physica B:Condensed Matter **394** (2007) 293

[49] M. Killinger, J. L. de Bougrenet de la Tocnaye, P. Cambon, R. C. Chittick, and W. A. Crossland, Applied Optics **31** (1992) 3930

[50] Wei Sha, Jonathan Moore, Katherine Chen, Antonio D.Lassaletta, Chung-Seon Yi, John J.Tyson and Jill C.Sible, Proc.Natl.Acad.Sci USA 100 (2003) 975

[51] Nicholas T. Ingolia and Andrew W.Murray, Current Biology **17**

(2007) 668

[52] Upinder S.Bhalla, Prahlad T.Ram and Ravi Iyengar, Science **297** (2002) 1018

[53] Christoph P.Bagowski, Jaya Besser, Christian R.Frey and James E.Ferrell, Jr, Current Biology **13** (2003) 315

[54] R.Thomas and M.Kaufman, CHAOS **11** (2001) 170

[55] Dubnau D. and R.Losick, Mol.Microbiol **61** (2006) 564

[56] M.R.Parvathi, Bindu M.Krishna, S.Rajesh, M.P.John and V.M.Nandakumaran, Chaos, Solitons and Fractals, doi: 10.1016/j.chaos.2009.01.013

[57] C.Bracikowaski and Rajarshi Roy, CHAOS **1** (1991) 49

[58] Guang-Qiong Xia, Sze-Chun Chan and Jia Ming Liu, OPTICS EXPRESS **15** (2007) 572

CHAPTER 7

SUMMARY AND CONCLUSIONS

In this chapter we summarize our work presenting the results we have obtained. A brief description of some possible works in this direction is also given.

7.1 SUMMARY AND CONCLUSIONS

In this thesis we have presented some aspects of the nonlinear dynamics of Nd:YAG lasers including synchronization, Hopf bifurcation, chaos control and delay induced multistability. We have chosen diode pumped Nd:YAG laser with intracavity KTP crystal operating with two mode and three mode output as our model system. Different types of orientation for the laser cavity modes were considered to carry out the studies. For laser operating with two mode output we have chosen the modes as having parallel polarization and perpendicular polarization. For laser having three mode output, we have chosen them as two modes polarized parallel to each other while the third mode polarized orthogonal to them.

The effect of various coupling schemes on the dynamics of two chaotic multi mode Nd:YAG lasers was studied. We employed external electronic coupling in which the pumping of each laser is modulated according to the output intensity of the other. Two chaotic multimode Nd:YAG lasers were coupled unidirectionally and bidirectionally using direct and difference coupling schemes. It was found that bidirectional direct coupling can induce complete synchronization between the lasers operating in two mode output. In addition there is control of chaos and amplification in output intensity for both the lasers. The lasers were found to be chaotic for the entire range of coupling strength with bidirectional difference coupling. The outputs of the lasers were neither amplified nor synchronized under this scheme. Under unidirectional direct coupling, phase synchronization between the lasers were observed at higher coupling strength. There was also amplification in the output intensity of second laser under this type of coupling. Unidirectional

difference coupling can only give amplification without leading to any type of synchronization between the lasers.

For lasers operating with three mode output bidirectional difference coupling gave better quality synchronization as compared to unidirectional difference coupling, but the coupling strength needed for synchronization was higher. Chaos control can be obtained with bidirectional direct coupling, while unidirectional direct coupling is not effective in controlling chaos or synchronizing the lasers. Our studies indicate that there is a strong dependence of the system dynamics and type of synchronization exhibited on the coupling strategies chosen and on the inherent properties of the system.

Hopf bifurcation phenomenon exhibited by Nd:YAG laser operating with two parallel polarized modes was studied analytically and numerically. The system fixed points were found out analytically. It was found that although the system has nine sets of equilibrium points, only three of them are having real valued solutions. The stability analysis of these three fixed points was carried out based on two criteria. First we found out the Routh Hurwitz stability conditions for our system and checked the variation of the Routh Hurwitz coefficients with increasing control parameter value. It was found that one equilibrium point loses stability at a particular value of the control parameter and evolves as a limit cycle thereafter. This is the phenomenon called Hopf bifurcation. The limit cycle thus formed was found to be stable for higher g values. The other two solutions remain unstable for the entire range of g values. To confirm the stability analysis we also calculated the eigen values of the Jacobian for our model system. For the fixed point which exhibited Hopf bifurcation, the real part of the eigen values changed from negative to positive at the critical value of the control parameter. Such a

change in the eigen value clearly indicates the loss of stability of the fixed point. Occurrence of Hopf bifurcation phenomenon was also verified numerically using time series plots, phase space plots and bifurcation diagram. Influence of the control parameter on the energy exchange between the two modes was also studied.

Application of a delayed optoelectronic feedback to the laser operating in the limit cycle region was found to generate some interesting dynamics in the output. The feedback was introduced by modulating the pump power of the semiconductor laser. The output optical signal of the Nd:YAG laser was converted into an electronic signal using a photodiode which in turn was added to the injection current of the semiconductor laser with appropriate delay to modulate the pumping rate. Effect of both positive and negative feedback were studied. Bifurcation diagrams, time series plots, phase space plots, power spectra and intensity peak series plots were used for a detailed analysis of the laser dynamics. Periodic, quasiperiodic and chaotic regions were identified in the laser output for various delay times under positive feedback and at a smaller feedback fraction. Laser was found to exhibit multistability and hysteresis for certain delay times. There was also coexistence of chaotic and quasiperiodic regions in the laser output. The laser dynamics becomes more complex at higher feedback fractions. Chaos appears in the output for smaller delay values. There is an overall increase in the output intensity as the feedback fraction is increased.

With negative feedback, a sudden jump into the chaotic region was exhibited by the laser output at smaller delays. Periodic and chaotic regions occurred alternately at higher delays. At higher feedback fractions also the laser

exhibits sudden jump into the chaotic state. The output remained in the chaotic state as the delay is increased.

7.2 FUTURE PROSPECTS

In future we would like to study the effect of delay on the dynamics of coupled lasers. Different types of synchronization such as anticipatory, lag, phase and complete synchronization have been reported in various dynamical systems under the introduction of a delay either in the coupling or in the feedback. Similar studies can be done for coupled chaotic multimode Nd:YAG lasers. Projective synchronization is another interesting phenomena observed in delay coupled systems. The existence of such a phenomenon in coupled Nd:YAG lasers can also be checked. We have observed the phenomenon called Hopf bifurcation in parallel polarized Nd:YAG laser. We can extend the work to a system of two coupled limit cycle oscillators. Coupled limit cycle oscillators are reported to exhibit a transition from antiphase oscillations to inphase oscillations in the output laser intensity. There is a possibility for such a phenomena to be observed in our system too.

List of papers published/ presented/ communicated:

International Journals

1. **M.R.Parvathi**, Bindu M.Krishna, S.Rajesh, M.P.John and V.M.Nandakumaran, **Synchronization and control of chaos in coupled chaotic multimode Nd:YAG lasers**, Physics Letters A **373,** 96 (2008)

2. **M.R.Parvathi**, Bindu M.Krishna, S.Rajesh, M.P.John and V.M.Nandakumaran, **Hopf bifurcation in parallel polarized Nd:YAG laser.** doi: 10.1016/j.chaos.2009.01.013

3. **M.R.Parvathi**, S.Rajesh, Bindu M.Krishna, M.P.John and V.M.Nandakumaran, **Delay induced multistability in parallel polarized Nd:YAG lasers**.(Communicated to CHAOS)

Conferences

1. **M.R.Parvathi**, M.P.John and V.M.Nandakumaran, **Numerical study of chaotic behavior in a two mode intracavity doubled Nd:YAG laser**, Photonics 2006, Dec 13-16, 2006, University of Hyderabad, Hyderabad

2. **M.R.Parvathi**, M.P.John and V.M.Nandakumaran, **Nonlinear dynamics of a two mode intracavity doubled Nd:YAG laser**, National Conference on recent trends in Optoelectronics and Laser technology, NCOL 2007**,** April 9-11**,** 2007, University of Kerala, Thiruvananthapuram

3. **Parvathi.M.R,** Bindu M.Krishna and V.M.Nandakumaran, **Transition from phase to complete synchronization in coupled chaotic multimode Nd:YAG lasers with a parameter mismatch**, National Laser Symposium, NLS 2007**,** Dec 17-20, 2007, Indore

4. **Parvathi.M.R**, Bindu M.Krishna, M.P.John and V.M.Nandakumaran, **Synchronization and control of chaos in coupled chaotic multimode Nd:YAG lasers,** National Conference

on Nonlinear Systems and Dynamics, NCNSD 2008**,** Jan 3-5 2008, PRL, Ahmedabad

5. **Parvathi.M.R**, Bindu M.Krishna, M.P.John and V.M.Nandakumaran, **Hopf bifurcation and phase transition in Nd:YAG lasers**, Recent Developments in Nonlinear Dynamics, RDND 2008**,** Feb 13-16, 2008**,** Bharatidasan University, Tiruchirappally

6. **Parvathi.M.R**, Bindu M.Krishna, S.Rajesh and V.M.Nandakumaran, **Effect of delay feedback on the dynamics of Nd:YAG laser**, Photonics 2008**,** Dec 13-17, 2008 **,**IIT Delhi**,** Delhi

7. **Parvathi.M.R**, Bindu M.Krishna, S.Rajesh, Manu P.John and V.M.Nandakumaran, **Dynamics of Nd: YAG laser under delayed optoelectronic feedback**, NLS 2008**,** Jan 7-10, 2009, LASTEC**,** Delhi